

**Metabolic Engineering of *Saccharomyces cerevisiae* using  
antisense hammerhead ribozymes**

vorgelegt von

Diplom-Biochemikerin

Sonia Carolina Vilches Gonzalez

Von der Fakultät III für Prozesswissenschaften

der Technischen Universität Berlin

zur Erlangung des akademischen Grades

Doktor der Naturwissenschaften

-Dr. rer. nat.-

genehmigte Dissertation

Vorsitzender: Prof. Dr. rer.nat. Roland Lauster

Berichter: Prof. Dipl.-Ing. Dr. Ulf Stahl

Berichter: Prof. Dipl.-Ing. Dr. Diethard Mattanovich

Tag der wissenschaftlichen Aussprache: 22.03.2004

Berlin 2004

D 83

## **Acknowledgements**

This thesis was developed at the Microbiology and Genetic Institute of the Technical University Berlin and financial support by Daimler Chrysler –Karl Benz Foundation (October 1999-november 2001) and Nafög (April 2002-2004) Grants.

I want to especially thank Professor Ulf Stahl for accepting and helping me to perform this work and for trusting in this overseas student. Deeply thanks Dr. Udo Schmidt for his help, understanding, interesting discussion, and learning.

I would like to thank Doris Rindermann and Tanja Hartkopf for their friendly support and care, and Dirk Müller especially for his patiently help and conversations. My best regards to lab 406 team; Karola Lehmann, Oliver Goldenberg, Maria Bernardez, Nicole Abdallah, Stefan Junge, Cornelia Luban and Melanie Beutel.

Thanks Dr. Engelke for kindly providing the pRS423 RPR vectors.

I am grateful to Sonja Leberecht, Rosslin Bensmann and to all members of the Department Microbiology and Genetics, Technical University of Berlin.

## Contents

<b>1</b>	<b>Metabolic engineering of <i>Saccharomyces cerevisiae</i> using antisense hammerhead ribozymes</b>	<b>9</b>
1.1	Introduction	9
1.2	General features of hammerhead ribozymes	10
1.2.1	History	10
1.2.2	Secondary structure	11
1.2.3	Mechanisms and catalysis	13
1.2.4	Design of efficient hammerhead ribozymes	18
1.2.5	Selection of the target sites	20
1.3.1	Development of vectors	26
1.3.2	Expression Vectors	26
1.3.3	Co-localization	28
1.4	Metabolic engineering	29
1.5	Concluding remarks	31
<b>2</b>	<b>Subject description</b>	<b>32</b>
2.1	Aim of this thesis	34
<b>3</b>	<b>Material and Methods</b>	<b>38</b>
3.1	Materials	38
3.1.1	Equipment	38
3.1.2	Enzymes, chemicals and kits	38
3.1.3	Strains	39
3.1.4	Plasmids	39
3.1.5	Oligonucleotides	40
3.1.6	Media, buffers and solutions	41
3.1.7	Cultivation conditions	42
3.2	DNA and RNA isolation	43
3.2.1	Isolation of plasmid DNA from <i>E.coli</i> strains	43
3.2.2	Isolation of genomic DNA from <i>S. cerevisiae</i> strains	43
3.2.3	Isolation of plasmid DNA from <i>S. cerevisiae</i>	43
3.2.4	Isolation of RNA from <i>S. cerevisiae</i>	43
3.2.5	Isolation of DNA from Agarose gels	44
3.2.6	Isolation of labelled RNA from PAA gels	44
3.3	DNA <i>in vitro</i> recombination methods: Restriction, dephosphorylation, and ligation	44
3.4	General PCR Method	44
3.5	Gel Electrophoreses	45
3.6	Northern blot analyses	45
3.7	Transformation methods	46
3.7.1	Transformation of <i>E.coli</i>	46
3.7.2	Transformation of <i>S. cerevisiae</i>	46
3.8	Radioactive labelling of DNA	46
3.9	Ribozyme cleavage activity	47
3.9.1	<i>In vitro</i> transcription reaction by T7 polymerase	47
3.9.2	<i>In vitro trans</i> -cleavage reaction	47
3.9.3	Primer extension	47
3.10	Ribozyme DNA construction	48
3.11	Sequence analysis of DNA	48

3.12	Protein analyses and Glycerol determination.....	48
3.12.1	Isolation of total protein from <i>S. cerevisiae</i> .....	48
3.12.2	Activity and protein concentration.....	48
3.12.3	Glycerol determination.....	49
3.13	Tetrad analysis.....	49
4	Results.....	50
4.1	Selection of the hammerhead target sites.....	50
4.2	Designing and cloning of hammerhead ribozymes.....	52
4.3	Cloning of the ribozyme DNAs into vectors of the pIIIEx423 series.....	53
4.4	<i>pgk1</i> -knock-out strain.....	55
4.5	Delivery of hammerhead ribozymes.....	59
4.6	Detection of cleavage activity.....	61
4.6.1	<i>In vitro</i> assays.....	61
4.6.2	<i>In vivo</i> assays.....	65
4.7	Ribozyme expression.....	75
4.8	Improving the co-localization of ribozyme and target RNA.....	77
4.9	Determining <i>in vivo</i> catalytic activity using primer extension.....	80
4.10	Regulated ribozyme delivery.....	82
5	Discussion.....	83
5.1	Selection of sites for ribozyme design.....	83
5.2	Use of pIIIEx423 RPR for ribozyme delivery and its influence on the metabolism.....	86
5.3	High interaction of target and ribozymes (one-plasmid system).....	88
5.4	High degree of compartmentalization (two-plasmid system).....	89
5.5	Enhancement on the glycerol production by ribozyme co-localization signals.....	90
5.6	High target gene expression.....	91
5.7	Differential expression of transcripts.....	91
5.8	PGK1 and glycolysis.....	93
5.9	No evidence for cleavage products.....	94
5.10	Intracellular Ribozyme applications.....	96
6	Summary and future prospects.....	99
7	Zusammenfassung und Ausblick.....	101
8	References.....	104
9	Appendix.....	111

## List of abbreviations

A	Adenine
aa	Amino acid
AP	Alkaline Phosphatase
APS	Ammonium persulfate
bp	Basepair(s)
c	Crick strand
C	Cytosine
dATP	Deoxyadenosine triphosphate
DNA	Deoxyribonucleic acid
dNTP's	Deoxynucleotide triphosphate set
DTT	Dithiothreitol
EDTA	Ethylendiamine-tetra-acetic acid
Fig.	Figure
i.e.	Id est
G	Guanine
g	Gram
H	Not G (A, C orT)
IPTG	Isopropyl- $\beta$ -D-thiogalactopyranoside
K	1000
KDa	Kilo Dalton
l	Liter
min	Minute(s)
MW	Molecular weight
mRNA	Messenger RNA
ORF	Open reading frame
PAGE	Polyacrylamide gel electrophoresis
PCR	Polymerase chain reaction
PGK1	Phosphoglycerate kinase
PMSF	Phenylmethylsulfonyl fluoride
Pu	Purine
Py	Pyrimidine
RNA	Ribonucleic acid
Rz	Ribozyme

rpm	Rotation per minute
sec	Second(s)
SDS	Sodium dodecyl sulfate
T	Thymine
Tab.	Table
TEMED	Tetramethylethylenediamine
Tris	Tris(hydroxymethyl)aminomethane
tsp	Transcription start point
U	Unit
w	Watson strand
w/v	Weight per volume
wt	Wild type
v/v	Volume per volume
X-Gal	5-Bromo-4-chloro-3-indolyl-galactopyranoside

## List of figures

- Figure 1: Minimal consensus structure for a *trans*-hammerhead ribozyme. N represents any nucleotide; H represents any nucleotide except G. R is purine and Y is pyrimidine. .... 12
- Figure 2: Hammerhead ribozyme schematic crystal view (Scott et al., 1996). The RNA backbone is colored in blue. The nucleotides of the catalytic pocket are shown in green, and the magnesium cations in yellow highlighted by van der Waals spheres. The cleavage site is indicated by the red portion of the RNA backbone. .... 14
- Figure 3: Schematic representation of possible mechanisms for the  $Mg^{2+}$ -catalyzed cleavage reaction of hammerhead ribozymes. (A). One-metal-hydroxide-ion model. (B) Two-metal-ion model (Hammann & Tabler, 1999). .... 15
- Figure 4: Mechanism of association, cleavage, and dissociation by *trans*-acting hammerhead ribozymes. The hammerhead ribozymes are able to cleave another target molecule immediately after the first reaction and the cleavage products might be degraded by RNases. .... 16
- Figure 5: Schematic representation of a metabolic network illustrating the fluxes JA, JB and JC around the intermediate I, that is the precursor of metabolite B and C. .... 30
- Figure 6: Schematic representation of the glycolytic pathway. Genes of products which are involved in this cellular process are given next to the arrows. In the glycerol flux, dihydroxyacetone-phosphate (DHAP) is detoxified by its reduction to glycerol-3-phosphate (Glycerol-3-P) and subsequent dephosphorylation to glycerol. Abbreviations: *FBA*: Fructose-1,6-bisphosphate aldolase gene, *TPI*: Triose phosphate isomerase gene, *GPDH*: Glyceraldehyde-3-phosphate dehydrogenase gene, *PGK1*: Phosphoglycerate kinase gene, *PGM*: Phosphoglycerate mutase gene, *PYK*: Pyruvate kinase gene, *PDC*: Pyruvate decarboxylase gene, *ADH*: Alcohol dehydrogenase gene, GA3P: Glyceraldehyde-3-phosphate, 1,3-BPG: 1,3-Bisphosphoglycerate, 3-PG: 3-Phosphoglycerate, 2-PG: 2-Phosphoglycerate. .... 33
- Figure 7: Secondary structure of three different regions of the *PGK1* mRNA selected by "RNA draw". The green arrows mark the GUC triplets selected to design *trans*-acting hammerheads for *PGK1* mRNA cleavage. .... 51
- Figure 8: DNA sequence of the Watson and Crick strand (w and c, respectively) of the three cloned *trans*-acting ribozyme genes. The constructs contain the conserved sequence of the hammerhead ribozyme (bold type), the complementary flanks of the targets and the *EcoRI* overhangs for cloning (underlined). .... 52
- Figure 9: Schematic representation of the insertion site used for cloning of hammerhead ribozymes in the *RPR1* leader RNA designed by Good and Engelke (1994). Thus, the hammerhead ribozyme encoding sequences were inserted into single *EcoRI* site of pIIIEx423 RPR. .... 53
- Figure 10: Checking the correct insertion of the ribozyme DNAs by restriction-analysis with *BamHI/EcoRI* and separation on a 2.5% agarose gel. Digestion of plasmids pIIIEx423 RPR without ribozyme DNA (lane 1), Rz1, Rz5, and Rz9 (lanes 2, 3, and 4, respectively). The right arrow shows the bands corresponding to the *BamHI/EcoRI* fragments carrying the correct insertion of the ribozyme expression cassette of about 440 bp. .... 54
- Figure 11: PCR analysis of the correct integration of the kan cassette in kanamycin resistant diploid CEY transformants.  $\lambda$  DNA /*HindIII* marker (lane 1); amplified DNA of a Kan resistant transformant using *pgk1-4* and G1 (lane 2), *pgk1-3* and G2 (lane 4), *pgk1-5* and G2 (lane 6), and *pgk1-3* and *pgk1-4* (lane 8); amplified DNA of the wild-type strain

CEY using <i>pgk1-4</i> and G1 (lane 3), <i>pgk1-3</i> and G2 (lane 5), <i>pgk1-5</i> and G2 (lane 7), and <i>pgk1-3</i> and <i>pgk1-4</i> (lane 9) as a control.....	56
Figure 12: Growth characteristics of different spore-isolates from tetrads of the diploid strain CEY <i>PGK1/pgk1::KanMX</i> . The haploid <i>pgk1</i> knock-out strains are known to grow only on media with non-fermentable carbon sources like ethanol and/or glycerol (YEGE), but cannot grow on glucose medium (YE). The spore isolates carrying the Kan resistance cassette grow on YEGE plates with Geneticin 418 (G418), but are unable to grow on glucose containing media. ....	57
Figure 13: PCR analysis of correct integration of the kan cassette in kanamycin resistant diploid transformants and haploid spore isolates using <i>pgk1-3</i> and <i>pgk1-4</i> . $\lambda$ DNA/ <i>HindIII</i> (lane 1); diploid wild-type CEY (lane 2); diploid Kan transformant (lane 3); haploid spore a1 with $\Delta$ <i>pgk1</i> phenotype (lane 4); haploid spore a2 with <i>PGK1</i> phenotype (lane 5) and haploid spore a3 with $\Delta$ <i>pgk1</i> phenotype (lane 6). ....	58
Figure 14: Ribozyme-delivery strategy. This schematic model presents the three systems used for ribozyme expression in yeast cells for determining cellular factors involved in cleavage activity. ....	60
Figure 15: Cleavage of the <i>PGK1</i> target by hammerhead ribozymes. The <i>PGK1</i> RNA fragment was internally labelled with [ $\alpha^{32}$ P] UTP and incubated with each of the individual ribozyme cassettes to cleave the selected sites. ....	62
Figure 16: Cleavage activity detection. A. DNA sequence of both strands (w and c) of the two cloned trans-acting ribozyme genes designed with longer flanks. The constructs contain the conserved sequence of the hammerhead ribozyme (bold type), the complementary flanks of the targets and the <i>EcoRI</i> overhangs for cloning (underlined). B. Cleavage reaction of the <i>in vitro</i> <i>PGK1</i> small transcript internally labelled with [ $\alpha^{35}$ S] UTP. The <i>PGK1</i> transcript was incubated with each of the individual ribozyme cassettes to cleave the selected sites. Cleavage reactions were started by adding magnesium and performed at 37°C for 60 min. ....	64
Figure 17: Growth rates of <i>S. cerevisiae</i> strains on minimal media containing glucose as the sole carbon source (YNB). ....	67
Figure 18: <i>PGK1</i> expression analyses by Northern blotting. The transformants and wt strains were grown on YEDP at 30 °C and total RNA was isolated, blotted and hybridized with the <i>PGK1</i> probes. The <i>S. cerevisiae</i> actine was used as internal control for balanced RNA loading. ....	69
Figure 19: Analyses of the <i>Pgk1</i> activity. A. Schematic representation of the glycolytic pathway part used to determine the <i>Pgk1</i> activity. B, C, D. Specific phosphoglycerate kinase activities of transformant strains. For enzyme activity assays, free extracts were obtained from log phase cells grown on minimal medium (YNB). ....	72
Figure 20: Glycerol amounts in transformed strains after anaerobic growth in minimal medium. Glycerol yields were expressed in relation to biomass (as dry weight). The strains were grown under anaerobic conditions on minimal medium with glucose for 24h (starting up OD <sub>600</sub> = 0.1-0.15), to the early stationary phase, and collected for glycerol and dry weight analysis. A. Comparison of glycerol production in Simple system transformants and the influence of longer flanks. B. Glycerol production from Rz1 8/7 transformants in all three systems. ....	74
Figure 21: Ribozyme expression analysis. A. vector map of pIIEx423 RPR used for ribozyme expression. B. Ribozyme expression of the different systems using Northern blot analysis. Total RNAs were isolated, blotted and hybridized with the <i>RPR1</i> probes. The <i>S. cerevisiae</i> 25/26 S and 18 S RNAs were used as internal control for equivalent RNA loading. The wild-type strain, a two-plasmid system control strain ( $\Delta$ <i>pgk1</i> transformed with pRS416 <i>PGK1</i> used as expression control) and the transformants were grown at 30 °C in minimal medium. ....	76



Figure 22: Schematic representation of the construction of the cassettes used for testing ribozyme target co-localization with the <i>PGK1</i> 3'UTR.....	78
Figure 23: Glycerol production following introduction of the <i>PGK1</i> 3'UTR into the ribozyme expression cassettes.....	79
Figure 24: Primer extension analysis of the <i>in vitro</i> and <i>in vivo</i> ribozyme cleavage activity. A. Detection by primer extension of ribozyme mediated cleavage by RZ1 8/7 on the <i>in vitro</i> <i>PGK1</i> transcript fragment; pgk1-8 was used as nested primer. B. poly (A)+ mRNA isolated from Simple system transformants were analyzed by primer extension. ....	81
Figure 25: Schematic representation for the construction of regulated expression vectors. A. Design of pYEX-BX-RZ plasmid. B. Design of pYEX-BX RPR1 ribozymes plasmids.	82

## List of tables

Table 1: Approaches carried out <i>in vivo</i> to study antisense and trans-acting ribozymes to mediate gene suppression in <i>Saccharomyces cerevisiae</i> .....	23
Table 2: Characteristic of glycolytic gene products.....	35

# **1 Metabolic engineering of *Saccharomyces cerevisiae* using antisense hammerhead ribozymes**

## **1.1 Introduction**

In the last few years the development of new strategies for delivering ribozymes has been followed with interest. The use of ribozyme technology has enormous potential in research and biotechnology due to the advantages of ribozymes over other genetic approaches. In mammalian cells this technique has been used successfully and its application in cancer treatment as well as gene-therapy appears to be a new goal in pharmaceutical research. However, in *Saccharomyces cerevisiae* only few reports showed that a catalytic active RNA is able to reduce the gene expression.

The strategy to improve the yield of a yeast metabolic product by down-regulation of the expression of a specific gene by cleaving its mRNA using antisense-ribozymes is promising. In contrast to direct mutational modification or disruption of a gene, this technique allows the temporary limited manipulation of genes essential for vitality and/or viability of the organism. Moreover, when using a regulatory system for ribozyme delivery, it should be possible to reduce gene expression at a specific optimal stage in the fermentation process. This chapter is focused on the description of the small catalytic RNA, the hammerhead ribozyme as a *trans*-acting factor to reduce gene expression, as well as considerations and requirements to have high efficient catalysis in yeast cells.

## 1.2 General features of hammerhead ribozymes

### 1.2.1 History

Ribozymes (RNA enzymes) are RNA molecules with catalytic activity. The first naturally occurring ribozyme activity was detected in the self-splicing group I intron of *Tetrahymena thermophila*, located in the nuclear gene for the large ribosome RNA. The intron has an autocatalytic unit. This unit makes a self-excision and the flanking exons are ligated to form a mature RNA. Shortly afterwards, the RNase P enzyme was purified from *Escherichia coli* in which the 400 nucleotide RNA component of RNase P was shown to cleave its substrate (pre-tRNA) in the absence of the protein subunit. The catalytic RNAs were divided into six main groups: (1) Ribozymes derived from self-splicing *Tetrahymena* group I introns, (2) RNA component of RNase P, (3) RNAs of the hepatitis & virus, (4) RNAs transcripts of the mitochondrial DNA plasmid of *Neurospora*, (5) Hairpin ribozymes, and (6) Hammerhead ribozymes (Gaughan & Whitehead, 1999). In addition, structural and chemical analyses strongly suggest that the ribosomal RNA is a ribozyme and the RNA components of the spliceosome appear to have catalytic activity (Takagi et al., 2001).

The hammerhead ribozyme is the smallest catalytic RNA motif observed so far and also the simplest in terms of structure and requirements. It was originally detected in RNA molecules of several plant viroids and viruses, such as tobacco ringspot virus (TRSV), avocado sunblotch virus (ASBV) and in satellite RNAs. Approximately 16 hammerhead motifs are known in the plus and minus strands of these plant pathogens and three other motifs are found in the satellite 2 RNAs from salamanders *Triturus vulgyris*, *Ambystoma talpoideum* and *Amphiuma tridactylum* (Tanner, 1999). These RNAs can mediate self-cleavage in the course of their replicative cycle. This process requires highly specific intramolecular cleavage of concatemeric RNAs, which result from a rolling cycle replication mechanism and leads to monomeric units (Amarzguigui & Prydz, 1998; Eckstein et al.,

2001). A sequence of only ~50 nucleotides was found to be the minimum requirement for self-cleavage.

### **1.2.2 Secondary structure**

The molecular structure of the hammerhead ribozyme is probably the most studied of all ribozymes. The name hammerhead was given based on the secondary structure of the self-cleaving model, which was reminiscent of the head of a hammerhead shark for its Australian discoverers (Haselhoff & Gerlach, 1988). The model consists of three putative stems (I, II, and III) two of which are flanking the susceptible phosphodiester bond, and two single-stranded loop regions which are highly conserved among different self-cleaving RNAs and participate in catalysis. A GUC triplet in stem III sequence immediately preceding the phosphodiester bond is also highly conserved (Tanner, 1999). Haselhoff and Gerlach determined the first hammerhead ribozyme consensus nucleotide sequence by analyzing the minimum number of nucleotides required for cleavage (Haselhoff & Gerlach, 1988). They identified non-conserved nucleotides in stem I and III that determined specific binding to RNAs. Furthermore, the catalytic core appears to have two stretches of highly conserved sequence: 5'-CUGANGA and 5'GAAG. These sequences are highly sensitive to any change in terms of catalytic activity.

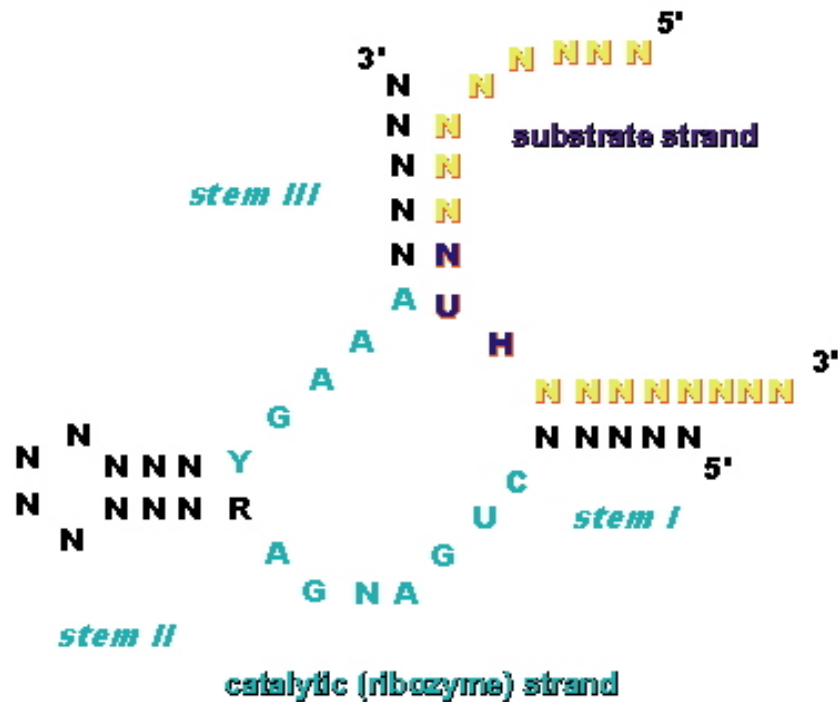


Figure 1: Minimal consensus structure for a *trans*-hammerhead ribozyme. N represents any nucleotide; H represents any nucleotide except G. R is purine and Y is pyrimidine.

*In vivo*, the cleavage in self-cleaving RNAs occurs in *cis*; however, the hammerhead ribozyme can be divided into two separate RNA components that hybridize via helices I and III (See fig. 1). Thus, the cleavage reaction proceeds in *trans*. In a *trans*-cleavage reaction, the RNA to be cleaved is called the target or substrate, and the catalytic active RNA, enzyme is the ribozyme.

### 1.2.3 Mechanisms and catalysis

Many experiments have been performed to determine the mechanisms of cleavage and the role of divalent cations on catalysis. Naturally, the hammerhead ribozyme catalyzes the endonucleolytic cleavage of RNA via a mechanism that involves nucleophilic attack by a 2'-OH group on the phosphorus of the neighboring phosphodiester bond, generating 5'-OH and 2', 3' -cyclic phosphate termini. This reaction seems to be accompanied by an inversion of the configuration of the phosphorus atom suggesting a direct in-line attack with development of a pentacoordinate transition state. Hammerhead ribozymes have a basic requirement for divalent metal ions, such as  $Mg^{2+}$ . In 1996 Scott and collaborators captured the structure of a catalytic intermediate (Fig. 2). The RNA structure was crystallized in the presence and absence of  $Mg^{2+}$ . The ribozyme could cleave itself when  $Mg^{2+}$  was added showing conformational changes placed around the active site (Scott et al., 1996).

The role of  $Mg^{2+}$  in the molecular mechanism of ribozyme catalysis has been widely investigated; however the number of  $Mg^{2+}$  ions involved in such an event is unknown. Until now two theories have been developed.

A single-metal-ion mechanism was suggested (Fig. 3). Analyzing the differences in the rates of cleavage observed in the presence of metal ions, as well as the relationship at certain pH between the  $\Delta pK_a$  values of the corresponding metal ions in water, support the idea that  $Mg^{2+}$  acts as a general base catalyst (Takagi et al., 2001).

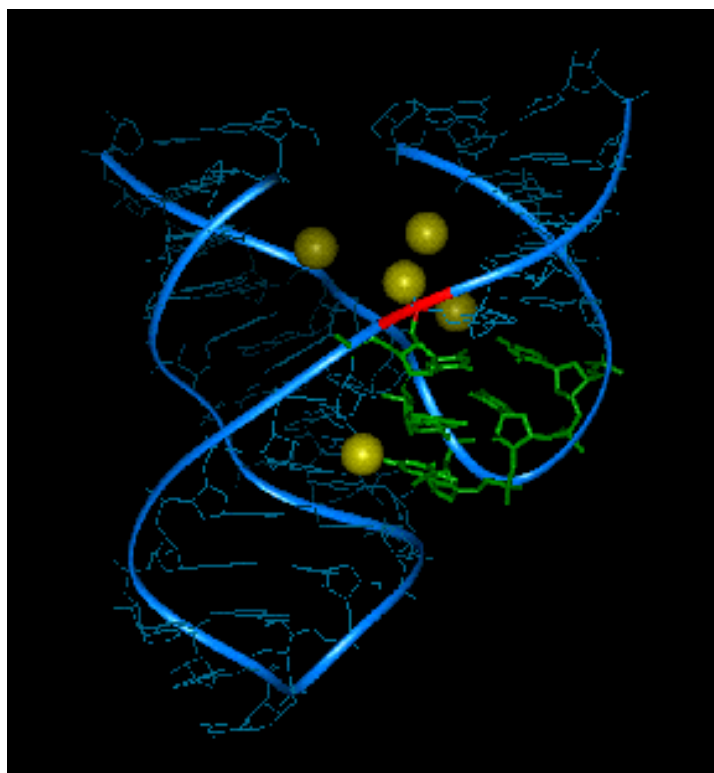


Figure 2: Hammerhead ribozyme schematic crystal view (Scott et al., 1996). The RNA backbone is colored in blue. The nucleotides of the catalytic pocket are shown in green, and the magnesium cations in yellow highlighted by van der Waals spheres. The cleavage site is indicated by the red portion of the RNA backbone.

However, a double-metal-ion mechanism is also described, in which one-metal-ion coordinates to the 2'-oxygen, and the other acts as Lewis acid by binding to the 5' oxygen on the leaving group, see fig. 3 (Vaish et al., 1998). This theory might also explain reactions catalyzed by hammerhead ribozymes. The existence of such a mechanism can be supported by cleavage experiments where  $\text{Mg}^{2+}$  ions showed to play different roles on catalysis (Lott et al., 1998).

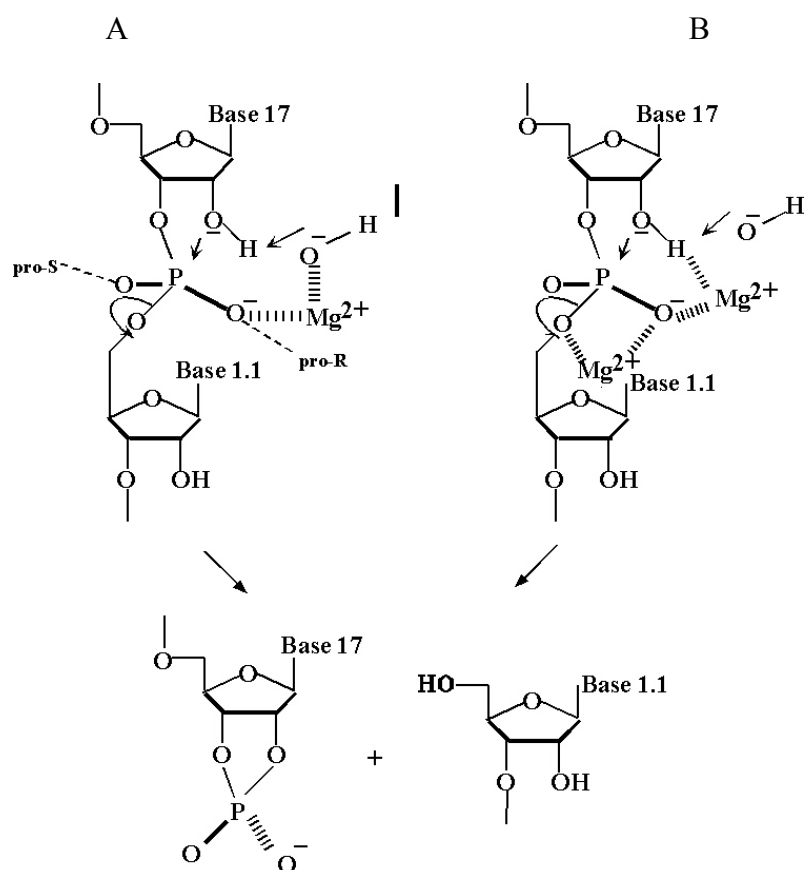


Figure 3: Schematic representation of possible mechanisms for the Mg<sup>2+</sup>-catalyzed cleavage reaction of hammerhead ribozymes. (A). One-metal-hydroxide-ion model. (B) Two-metal-ion model (Hammann & Tabler, 1999).

Furthermore, under extreme conditions the hammerhead ribozyme can also use monovalent cations for catalysis (Curtis & Bartel, 2001). These findings indicate that the hammerhead ribozyme catalysis might operate via a variety of cleavage mechanisms. Bounded metal-ions could act as either Lewis acids or bases depending on the conditions of reaction. However, the mechanistic details still seem to be under debate (reviewed by Blount & Uhlenbeck, 2002; Takagi et al., 2001; Tanner, 1999).



The mechanism of a hammerhead ribozyme-catalyzed reaction can be divided in three steps: substrate interaction, cleavage and dissociation. Therefore, it is possible to analyze the steady-state kinetic of this reaction with a standard Michaelis-Menten model, establishing the individual constants for  $K_m$  and  $k_{cat}$  for the reaction (Fig. 4).

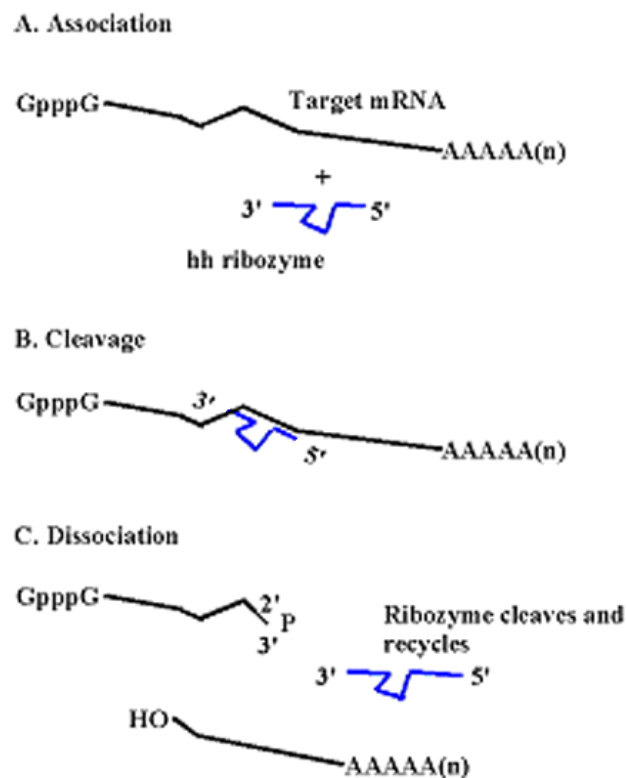
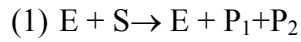


Figure 4: Mechanism of association, cleavage, and dissociation by *trans*-acting hammerhead ribozymes. The hammerhead ribozymes are able to cleave another target molecule immediately after the first reaction and the cleavage products might be degraded by RNases.

In this system binding and release of substrate and product follow the kinetics expected for formation and dissociation of standard Watson-Crick duplexes in the stem regions (McKay & Wedekind, 1999). Based on this model it was demonstrated that the association rate of ribozyme for the reaction with long substrates (mRNAs) may be slowed or suppressed due to the presence of secondary structures in the target RNA that may hamper the association step. The cleavage rate reflects the velocity of the phosphodiester bond cleavage and depends on salt concentration, pH and temperature. The turnover conditions can be single or multiple depending on the substrates and ribozymes concentrations. Single turnover is characterized by the excess number of ribozymes over long mRNA substrate (reviewed by Muotri et al., 1999). Multiple turnover takes place in excess of substrate (short oligonucleotides) over the ribozyme; a hammerhead ribozyme molecule can catalyze the cleavage of several RNA molecules. The reaction rate for single turnover is slower in several orders of magnitude than multiple turnover rates.

#### 1.2.4 Design of efficient hammerhead ribozymes

The hammerhead ribozymes can be engineered to cleave any target RNA; however, during design some structural properties need to be considered such as: (i) the lengths of the arms at the complementary regions, (ii) the structure of the RNA in the target region, and (iii) the nucleotides surrounding the phosphodiester bond at the cleavage site. Sequence modifications can affect the turnover and the stability of the hammerhead ribozyme as well as the possible bindings of cellular proteins, which could also have an important influence on the *in vivo* catalytic reaction (Rossi, 1999).

The only requirement for the target is the presence of a three-nucleotide motif NUH, where N is any nucleotide and H is any nucleotide but G. Different triplet-flanking sequence combinations can be designed. However, the resulting variants can differ drastically when the kinetic of the cleavage reactions are tested. Therefore, most researchers rely on GUC, since this motif is found most frequently among the natural hammerheads and has high catalytic rate (Amarzguioui & Prydz, 1998).

Many concepts can be used in order to design the length of the antisense arms. It is now known that five to eight nucleotides on either side are the minimum sequences required to perform a good and specific process (Amarzguioui & Prydz, 1998). Lieber and Strauss (1995) have determined that the most active ribozymes *in vitro* had a consecutive complementary stretch with a substrate of only 15 nt, i.e. 7 and 8 nt on either arm. They implemented a new strategy for selection of accessible cleavage sites in target RNAs by using a library of random sequences that flank the unique sequence of a hammerhead. The *in vivo* analysis of the ribozymes variants showed that the strongest inhibition effect is close to 99% when the shortest stretch complementarities (7 and 8 nt on either side) are used.

When multiple turnovers are desired, i.e. one molecule will cleave several substrate RNA molecules, the lengths of the arms directly influence the association and dissociation steps. Obviously, there is a size window for the antisense flanks of a ribozyme where association and dissociation simultaneously proceed well (Hammann & Tabler, 1999).

Analyzing the minimal length for the binding of helix I and helix III in order to achieve the optimal *in vitro* cleavage rate, it was also demonstrated that asymmetric hammerhead ribozymes cleaved more rapidly than symmetric hammerheads. The enhancement on the cleavage rate when one of the helices is relatively weak, i.e. one complementary flank is shorter than the other, is consistent with a pre-equilibrium between active and inactive conformations of the ribozyme-substrate complex. Hence, it was observed that a relatively short helix I of about 5 bp accompanied by a helix III of 10 bp are required for fast *in vitro* cleavage rates (Hendry & McCall, 1996).

Asymmetric hammerhead ribozymes have also been constructed with a short helix I where only three nucleotides are required, in combination with a long helix III. This new version of a hammerhead ribozyme is divided into two functional domains, the 3' domain responsible for hybridization and the second 5' domain responsible for catalysis. The localization of the catalytic domain at the 5' end facilitates the construction of a hammerhead ribozyme variant by a simple PCR step (Hammann & Tabler, 1999).

### 1.2.5 Selection of the target sites

A good choice of an appropriate ribozyme target site is one of the most critical steps in hammerhead design. The tertiary and secondary structures of RNAs as well as the association to RNA-binding proteins *in vivo* can have a negative effect on the catalytic activity. Therefore, many approaches have been directed to identify a possible target through the prediction of the secondary structure of the target RNAs. The most common RNA folding program is MFOLD based on the algorithm developed by Zuker. This program predicts a selection of several structures for one RNA sequence, which might differ significantly from each other with respect to the fold, although they differ only slightly in free energy (Zuker, 1994).

The rules for target selection through computer programs have been analyzed. The ideal optimal location of a target must consider: (i) the target sequences embedded within a long base-paired stem (double stranded region) have to be avoided, (ii) the sites should fall within a loop that is not smaller than four nucleotides, (iii) one or preferably both of the 5' and 3' ends of the antisense segment should fall within a single stranded rather than a stem region, (iv) target sequences within the first several hundred nucleotides of a large RNA molecule are favored (more details below), and (v) short antisense segments with 7-12 nucleotides for each arm of a hammerhead ribozyme, as well as 12-23 nucleotides for an antisense oligo give best results (Jiagang & Lemke, 1998).

The selection of target sequences located at the 5' end is supported by different approaches. The regions surrounding the translation-initiation site and splice-sites have been targeted so far. In these regions, the RNA may be more accessible to hybridization by

ribozymes due to the need for relatively open structures for binding of the translation machinery and spliceosomes respectively. On the contrary, the downstream coding region has been considered less efficient for binding ribozymes since the moving translation machinery may displace slow-cleaving ribozymes before cleavage can occur (Amarzguioui & Prydz, 1998).

Computer programs predict secondary structures but they are not able to select the most accessible sites in the targets. Hence other approaches must be considered.

Experimentally, the use of random ribozymes libraries is the most straight-forward approach to target identification and is the best option to find the most efficient ribozymes against any target. However, practical difficulties arise because ribozymes are present in such small amounts in the cell that the detection of the cleavage products is a very laborious procedure. Therefore, the cloning and sequence analysis of the reverse transcription-polymerase reaction (RT-PCR) products are necessary (Lieber & Strauss, 1995). All the tested cleavage sites were predicted as taking place in single stranded regions by computer programs. This suggests that the ribozymes should be targeted to predicted single stranded regions only.

Enzyme as well as chemical assays have been used for *in vitro* detection of the targets. The principle of these assays is that regions accessible for hybridization with oligonucleotides should also be accessible to ribozymes. The transcripts are incubated with RNase H and decadeoxyoligonucleotides and the RNase H cleaves the sites accessible for hybridization (due to the ability of RNase H to cleave RNA strands only in RNA/DNA hybrids). The sites can be identified by the size of the labeled cleavage product (Birikh et al., 1997). For human

transcripts, this technical approach was shown to be better for selection of active target sites than the use of ribozymes designed by computer programs.

Nevertheless, the *in vivo* situation is different because many proteins bind the RNA and can either mask the potential targets and/or influence the structure of the RNA in its non-complex form. Heterogeneous ribonuclear proteins (hnRNPs) and small nuclear ribonuclear proteins (snRNPs) in the nucleus and the translational machinery in the cytoplasm as well might sequester the RNA transcripts in a form that hampers the accessibility of ribozymes to their respective targets.

Referring to the method mentioned above, another strategy has been developed in order to take advantage of the RNA in its native, protein-associated state. Therefore, the native RNAs in cellular extracts associated with the proteins should be the best substrates for selection of the sites, which can hybridize with oligonucleotides. The use of cell extracts prepared from cells which are expressing the RNA of interest is the most important component in this system. The outcome of this approach was in accordance with results obtained *in vivo* (Castanotto et al., 1999).

Furthermore, the consensus sequence AUGUC, placed at the start codon is frequently found in a considerably number of yeast genes. Experimental approaches showed that this GUC triplet is contained in an accessible region and therefore can be used for designing *trans*-acting hammerhead ribozymes in *S. cerevisiae* (Ferbeyre et al., 1995).

### 1.3 Delivering ribozyme in yeast

Although the regulation of gene expression in animals and plant using antisense ribozymes is widely reported, there are only a few reports where hammerhead ribozymes were used to influence gene expression in *S. cerevisiae* (Table 1). That might be ascribed to the efficiency of homologous recombination in *S. cerevisiae* that permits replacement, disruption or altering of the sequence at any chromosomal site. However, the enormous advantages obtained through application of *trans*-acting ribozymes in gene therapy of mammalian cells and the alteration of traits in plants have recently suggested the creation of simple *in vivo* models to evaluate these technologies appropriately (Arndt & Atkins, 2001).

Table 1: Approaches carried out *in vivo* to study antisense and trans-acting ribozymes to mediate gene suppression in *Saccharomyces cerevisiae*.

Target gene	Antisense/Ribozyme	Reference
CAT	5' Antisense, nonaribozyme; <i>cis</i> - and <i>trans</i> -hammerhead ribozymes	Atkins & Gerlach (1994)
ADE1	<i>Cis</i> - and <i>trans</i> -hammerhead ribozymes	Ferbeyre et al.(1995)
ADE1	<i>Trans</i> -hammerhead ribozymes expressed under control of galactose-inducible promoter	Ferbeyre et al. (1996)
U3 RNA	<i>Trans</i> -hammerhead ribozyme designed Snorbozyme (Small nucleolar RNA:ribozymes)	Samarsky et al. (1999)
Hepatitis B viral X mRNA (X-lacZ fusion gene)	<i>Cis</i> -hammerhead ribozymes	Yim et al.(2000)



Despite all the experiments carried out until now, the *trans*-cleavage *in vivo* has been difficult to be measured. There is no evidence so far that a *trans*-catalytic reaction proceeded to complete turnover *in vivo*.

Ferbeyre and co-workers described the effect of *cis*- and *trans*-acting hammerhead ribozymes on *ADE1* gene expression. The *cis*- and *trans*-acting ribozymes were directed against the previously tested target site for this gene which was insensitive to antisense RNAs (Ferbeyre et al., 1995). The ribozymes and mutant ribozymes (no catalytic activity) were transcribed under control of the *GAL1* promoter from episomal expression plasmids. The *cis*-acting ribozymes were able to cleave the RNA resulting in the expected phenotype of reduction on the *ADE1* expression; however, *trans*-acting ribozymes did not show any effect on the *ADE1* expression. They concluded that the catalytic activity *in vivo* could easily be 10-100-fold slower than *in vitro*; the secondary structure *in vivo* is complex and binds proteins, and the ribozymes must diffuse to the site of action. The *trans*-cleavage activity would not be as successful in rapidly growing yeast cells as in mammalian cells due to their markedly faster cell cycle and faster RNA metabolism. These problems were eliminated in further studies by arresting yeast cells in the G1-phase of the cell cycle. In those cells, *trans*-cleavage by hammerhead ribozymes on *ADE1* mRNA was observed (Ferbeyre et al., 1996).

In order to explain the lack of *trans*-cleavage activity in yeast, further analyses suggested that *S. cerevisiae* cells have an immanent inhibition-activity, that affects hammerhead ribozymes mediated *trans*-cleavage. Yeast splicing extracts added to an *in vitro* cleavage reaction inhibited the cleavage activity; this observation has not been found in mammalian extracts (Castanotto et al., 1998). However, whether this activity also influences the *in vivo trans*-cleavage activity is not clear until now.

The reduction of the expression level in the presence of ribozymes has been difficult to point out if the reduction is due to a cleavage activity rather than an antisense mechanism. In a more recent communication, it was reported that hammerhead ribozymes induce a translational suppression rather than cleavage activity in *S. cerevisiae*, although the cleavage of the target was detected by primer extension assays. Inactive variants of hammerhead ribozymes directed against the same target were found to suppress the expression *in vivo* (Yim et al., 2000).

The information reveals that the key requirements to be considered in order to have an efficient cleavage activity involve:

1. Unlimited intracellular concentration of ribozymes which requires a robust transcription rate or good metabolic stability of the ribozymes.
2. High degree of co-localization of the ribozyme in the same compartment(s) as the target molecule.
3. Highly productive ribozyme-target interaction, i.e. good accessibility to the relevant RNA sequences of the catalytic and substrate molecules.

Effective *trans*-acting ribozymes have been described that allow near perfect cleavage *in vivo* when these critical facts were considered (Samarsky et al., 1999). Small nucleolar RNAs were used as both catalytic and target molecules. In this approach, hammerhead ribozymes were localized to the yeast nucleolus by using the U3 small nucleolar RNA as a carrier. The hybrid molecules cleave the U3 RNA with a nearly 100% efficiency *in vivo*. These results pointed out that the use of *trans*-acting hammerhead ribozymes is a feasible strategy to reduce the gene expression *in vivo* when stability, co-localization and accessibility of the relevant regions in the cleavage reaction is ensured.

### 1.3.1 Development of vectors

Hammerhead ribozymes can be expressed endogenously from expression vectors containing the ribozymes gene. The selection of an appropriate cassette for intracellular gene expression is an important step in obtaining active ribozymes in the cell. Following the requirements mentioned above, the use of (i) promoters for high level expression, (ii) specific termination sequences, and (iii) sequences to increase the stability of the transcript or to facilitate selection of the transformants in cases of stable expression must be considered (Amarzguioui & Prydz, 1998).

### 1.3.2 Expression Vectors

Strong promoters to drive ribozymes expression such as pol II and pol III promoters have been tested. For pol II promoters, the addition of a 5'cap and a 3'poly (a) tail should increase the stability and should influence the cytoplasmic localization. However, this implies the need for very long upstream and downstream sequences in order to have a high level of transcription. The short ribozyme sequence is embedded between long untranslated regions which might influence the formation of the catalytic active structure. Expressing ribozymes from pol III cassettes leads to high intracellular levels of the ribozymes. This expression can localize the ribozymes either in the nucleus or in the cytoplasm, depending on the pol III system used. Good and Engelke (1994) have created a special system, to promote the accumulation of transcripts under the control of intragenic promoters for *SUP4* tRNA and RNase P (RPR1) genes on episomal plasmid derived from the Sikorski and Hieter pRS vector series (Sikorski & Hieter, 1989). The *SUP4* tRNA gene intragenic promoter was tested to

express an RNA consisting of the full tRNA primary transcript attached to the ribozymes. Normally in yeast, dimeric tRNA genes have their promoter in a coding region of the first gene in the pair. This first construct does not have the sequences needed for processing the tRNA and remains bonded to the following RNA. This leads to a stabilizing effect preventing a 5'-3' exonucleolytic attack. Such an approach has been used with enormous success in mammalian cells (Castanotto et al., 1999, Amarzguioui & Prydz, 1998). The second intragenic promoter analyzed was the promoter of RNase P RNA gene. Ribozymes were fused to the leader of this promoter. The corresponding RNAs were not recognized by the RNase P maturation process resulting in a high and stable accumulation of the transcripts. A high degree of ribozyme expression could be observed depending on the copy number of the plasmid used and the RNA expressed (Good & Engelke, 1994).

In a further analysis, a comparison was made between a novel system that was constructed from regulatory elements present in the pol I promoter and the enhancer/ termination of rDNA with the pol II-and pol III-dependent system to express hammerhead ribozymes (Blancafort et al., 1997). The pol I vector contained the ribosomal promoter, the enhancer/termination region of the ribosomal RNA transcription and the yeast *URA3* gene. The pol II plasmid was constructed by inserting the hammerhead ribozyme gene between the inducible galactose promoter and the *ADH1* terminator. The pol III plasmid pIIIEx426 was chosen from the Good and Engelke plasmid series (described above) and a hammerhead ribozyme sequence was inserted between the *RPR1* promoter and the terminator. The pol III system gave the highest RNA expression levels while expression with the pol I system was only detectable when some modifications were made in order to extend the distance between promoter and enhancer. Thus, the RNA expression of pol I reached a level similar to the level of the pol II expression. Moreover, the expression obtained with the pol I system depends on the composition of the medium and the growth rate. Both factors regulate the number of active transcription units.

### **1.3.3 Co-localization**

It is well known that the co-localization of ribozymes with the target RNA improves the efficiency of the hammerhead catalysis. However, it is not clear yet which are the mechanisms that control the transport of RNAs from the transcription site to the translation site. It has been described that some nuclear transcripts are processed and delivered along specific routes and the transcripts are distributed in specific positions on the nucleus (Brodsky, A. S. & Silver, P. A., 2000). Co-localization strategies could take advantage of various post-transcriptional processing events that take place in the nucleus of the cell. Beach et al. (1999) described that the 3' untranslated regions of some RNAs may carry signals that are responsible for their localization in the cell. These signals can be used to direct ribozymes to specific locations. Samarski and co-workers (1999) used the small nucleolar RNA as carrier of ribozymes to the yeast nucleolus. The hammerhead ribozymes were delivered as hybrid molecules to the expected sub-cellular target location place. The cleavage activity observed has been the most efficient result reported up to now. This can be beneficial for decreasing the expression of some nucleolus associated RNAs.

## 1.4 Metabolic engineering

For several centuries *S. cerevisiae* has been used in the production of food and alcoholic beverages, and today it is also used in different processes within the pharmaceutical industry. *S. cerevisiae* is classified as a GRAS organism, i.e. generally regarded as a safe organism, is non-pathogenic and can be added in consumable products. Genetic modifications by recombinant DNA technology in *S. cerevisiae* have enabled the manipulation of a given pathway of interest in order to facilitate the production of a particular metabolite.

Metabolic engineering has been defined as improvements to the cellular properties achieved from the interplay of theoretical analysis relying on biochemical information and application of genetic engineering. The analytical side deals with the analysis of the cells in order to identify the most promising targets. Genetic engineering of cells basically consists of genetic modifications that are made for producing a certain cell construct. The synthesis part of the metabolic engineering must consider the limiting factors of the analytical part. These factors depend on the complexity of the cellular metabolism. It is possible that metabolite levels may interact with gene expression or the gene expression might determine the metabolite levels via enzyme concentrations. In cases where many modifications are made, each modification implies unexpected changes in the cellular metabolism (Ostergaard et al., 2000).

The applications of metabolic engineering in *S. cerevisiae* are divided in four categories; (i) extension of substrate range, (ii) improvements of productivity and yield, (iii) elimination of by-products, and (iv) improvements of cellular properties and extension of product range including heterologous protein production.

In the area of yield and productivity improvement, the pathway analysis often describes the application of metabolic flux analysis and metabolic control analysis. The concept of metabolite balancing can be explained using a simple pathway where a product A is converted to product B with the formation of a by-product C (Fig. 5). The overall yield of product from the substrate is given by the ratio of the fluxes  $J_B$  and  $J_A$ , and the productivity is given by the flux  $J_B$ .

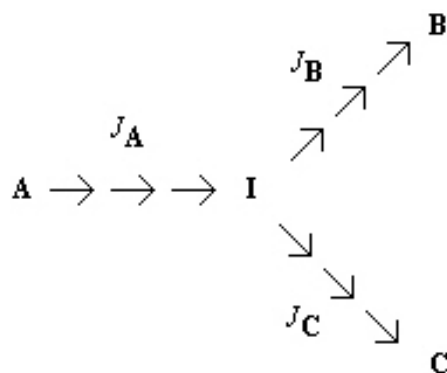


Figure 5: Schematic representation of a metabolic network illustrating the fluxes  $J_A$ ,  $J_B$  and  $J_C$  around the intermediate I, that is the precursor of metabolite B and C.

The intermediate I does not accumulate in the cell and the flux into this metabolite will therefore equal the flux out of the metabolite pool. The fluxes are constrained as  $(J_A = J_B + J_C)$ , and one flux can be calculated when the others are measured (Ostergaard et al., 2000). Therefore, in order to improve the productivity of one product, B for example, it is clear that the other flux must be reduced or eliminated. However the formation of C could play an important role in the metabolism, and its elimination will be lethal or lead to auxotrophy. Here the use of *trans*-acting hammerhead ribozymes might be a promising strategy in metabolic engineering. Using this technique, it should be possible to induce an increment of a specific

metabolite by reducing the expression of a specific gene without disturbing or destroying the viability (and/or vitality) of the organism. This is an important advantage over other approaches such as the use of antisense nucleic acids or gene disruption which may affect the viability of the cells. Therefore, the *trans*-acting ribozyme technology will enable the identification of enzymes that exert flux control in a given metabolic pathway as well as possibly contributing to information about regulation of different fluxes in “sensitive” routes.

### 1.5 Concluding remarks

The hammerhead ribozyme belongs to the most attractive tools for reducing gene expression. Its simple structure and design, as well as its specific properties and broad application range, makes this small catalytic RNA useful for studying cellular pathways in different systems. It has not been clear until now which is the intermolecular mechanism that mediates the cleavage reaction. However, the catalytic process mediated by hammerhead ribozymes has been widely used. The design of ribozymes and the selection of appropriate targets have been the aim of many investigations during the last few years. The elaboration of model systems for simple ribozyme delivery to have an efficient reduction of the gene expression is important to establish the prerequisites needed for the ribozyme cleavage activity. For investigating metabolic pathways in *S. cerevisiae*, the ribozyme technology is promising when it is applied to the manipulation of target genes that are essential for vitality or viability. However, the data published until now reveals the absence of information about the factors involved in catalytic activity *in vivo*. Moreover, many vectors for ribozyme expression in yeast have been described but were successful only in a few cases. The localization and expression levels of ribozyme are important factors to be considered.



## 2 Subject description

The importance of glycerol for synthesis of many products ranging from cosmetics to lubricants has attracted increasing attention during the last few years. The annual production of ca. 600,000 tons is mainly recovered as a by-product of soap manufacturing or it is produced from propylene. However, glycerol can also be produced by microbial fermentation and the investigation into this route has been pursued at mostly in yeast cells (Overkamp et al., 2002). Glycerol is involved in carbon metabolism of *Saccharomyces cerevisiae* in different ways. It can be utilized as a sole carbon source under aerobic conditions and it is formed as a major by-product when *S. cerevisiae* ferments sugar to ethanol via a redox-neutral process. Glycerol is formed by the reduction of dihydroxyacetone phosphate (DHAP) to glycerol-3-phosphate, concomitant with a NADH oxidation by NAD<sup>+</sup>-dependent 3-phosphate dehydrogenase. Then glycerol-3-phosphate is dephosphorylated to glycerol by glycerol-3-phosphatase (Fig. 6). The synthesis of glycerol seems to play an important role in maintaining the cytosolic redox state under anaerobic and glucose repression conditions as well as functioning as osmolite for enabling yeast to grow in high osmolarity (Overkamp et al., 2002; Cronwright et al., 2002; Nevoigt & Stahl, 1997).

Furthermore, glycerol-3-phosphate, the intermediate in the glycerol formation pathway, is a key metabolite for the synthesis of lipids; therefore, the optimization of its production is an interesting biotechnological goal. The development of strains that produce larger-than-normal amounts of glycerol-3-phosphate has received major attention (Nevoigt & Stahl, 1997).

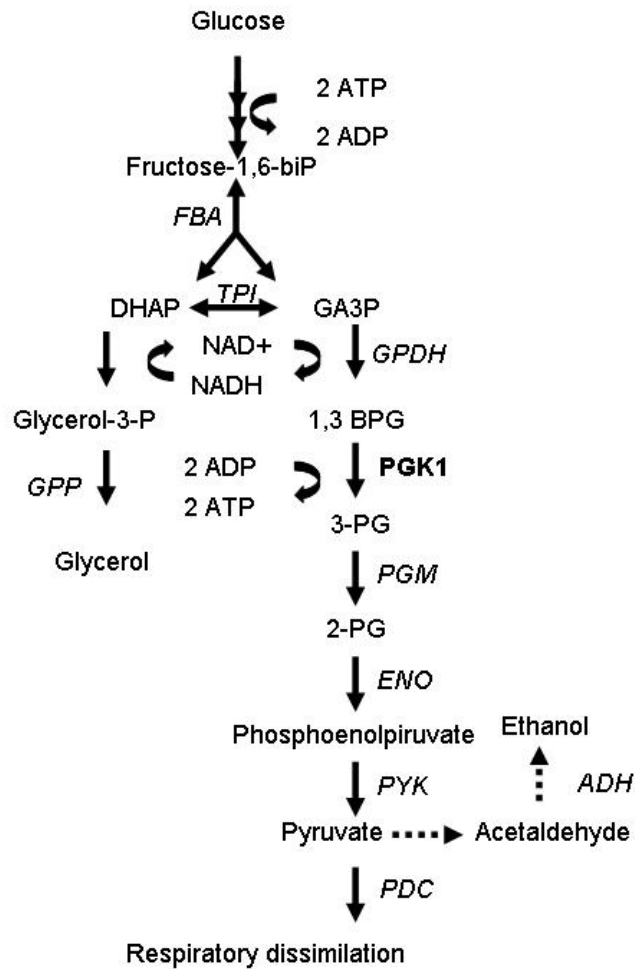


Figure 6: Schematic representation of the glycolytic pathway. Genes of products which are involved in this cellular process are given next to the arrows. In the glycerol flux, dihydroxyacetone-phosphate (DHAP) is detoxified by its reduction to glycerol-3-phosphate (Glycerol-3-P) and subsequent dephosphorylation to glycerol. Abbreviations: *FBA*: Fructose-1,6-bisphosphate aldolase gene, *TPI*: Triose phosphate isomerase gene, *GPDH*: Glyceraldehyde-3-phosphate dehydrogenase gene, *PGK1*: Phosphoglycerate kinase gene, *PGM*: Phosphoglycerate mutase gene, *PYK*: Pyruvate kinase gene, *PDC*: Pyruvate decarboxylase gene, *ADH*: Alcohol dehydrogenase gene, GA3P: Glyceraldehyde-3-phosphate, 1,3-BPG: 1,3-Biphosphoglycerate, 3-PG: 3-Phopshoglycerate, 2-PG: 2-Phosphoglycerate.

## 2.1 Aim of this thesis

The aim of this thesis is to apply hammerhead ribozymes in *S. cerevisiae* to reduce the expression of a gene encoding glycolytic enzyme in order to influence the metabolic pathway of glycerol. This creates an influence on the glycolytic fluxes which ideally should lead to a decrease in the ethanol production and improve the glycerol-3-phosphate yield.

The glycolytic gene chosen as target for effective *trans*-acting hammerhead ribozyme application should have the following characteristics:

- i) No available isoenzymes. This is important since a reduction on the gene expression might be by-passed with enzymes and no effect could be observed.
- ii) Known knock-out and over-expressed phenotype. The knowledge of both types can be an aid in determining the real influence on the glycolysis.
- iii) High copy number and slow turnover transcript. Thus, the detection of the cleavage products will be enhanced and the ribozyme activity can be confirmed.

The information for glycolytic genes available as targets is listed below (Table 2). This was obtained from the *Saccharomyces* Genome Database published in the internet (<http://genome-www4.stanford.edu/Saccharomyces/SGD/>) and RNA decay data was obtained from Precision and functional specificity in RNA-decay available at the web site: <http://www-genome.stanford.edu/turnover/index.shtml>).

Table 2: Characteristic of glycolytic gene products.

Enzyme	Associated gene	null mutant	mRNA copies/cell <sup>a</sup>	mRNA half life (min)
Triose phosphate isomerase	<i>TPI1</i>	inviable	n.a.	32
Glyceraldehyde-3- phosphate dehydrogenase	<i>TDH1</i> <i>TDH2</i> <i>TDH3</i>	viable viable viable	425 <sup>TDH2/TDH3</sup>	55 49 59
Phosphoglycerate kinase	<i>PGK1</i>	inviable in glucose media	139	70; 40 <sup>b</sup>
Phosphoglycerate mutase	<i>GPM1</i> <i>GPM2</i> <i>GPM3</i>	inviable viable viable	168	67 71 11.
Enolase	<i>ENO1</i> <i>ENO2</i> ERR1 (homolog)	viable inviable unknown	229	39 51
Pyruvate kinase	<i>PYK1</i> <i>PYK2</i>	inviable viable	69	67 <sup>b</sup>

a. Published by Velculescu et al., 1997.

b. Published by Moore et al., 1991.

n.a. not available.

The phosphoglycerate kinase 1 gene (*PGK1*) seems to be adequate as a target; its transcript has high stability and slow turnover. Hence, it should provide abundant substrate for detecting ribozyme-mediated cleavage. Furthermore, its knock-out phenotype is known, i.e. *pgk1* knock-out is inviable in media with glucose as carbon source. This strain can only grow on non-fermentative carbon sources and no isozymes have been identified. Thus, alterations on the *PGK1* gene expression directly affect the glycolysis and there is no other enzyme involved in this metabolic process that can fulfil the role of *PGK1*. Only one copy of the *PGK1* gene is found in the haploid cell. The primary sequence, open reading frame and information about the flanking regions are available (Hitzeman et al., 1982; Holland & Holland, 1978). The *PGK1* promoter yields a high level of expression and is regulated in response to a carbon source. It is highly expressed in glucose but less well expressed in yeast cells grown in carbon sources such as pyruvate and acetate. It has furthermore been employed in yeast expression vectors for high expression of heterologous genes (Holland & Holland, 1978; Piper et al., 1988a; Piper et al., 1988b; Chambers et al., 1989).

Phosphoglycerate kinase (*Pgk1*) catalyses a reversible reaction, by transferring a phosphoryl group of 1,3-diphosphoglycerate to ADP to give 3-phosphoglycerate and ATP (Fig. 6). Ciriacy and Breitenbach (1979) showed that a block of the glycolytic pathway at the level of *PGK1* induces an accumulation of dihydroxyacetone-phosphate (DHAP). DHAP is an important intermediate for glycerol production and revealed a positive influence on the glycerol flux.

Reduction in the *PGK1* expression should induce an increment of the production of glycerol-3-phosphate (G-3-P). Thus the subject of this work is the **design of a model system to decrease the expression of the *PGK1* gene encoding the phosphoglycerate kinase of the glycolytic pathway by *trans*-acting hammerhead ribozymes, in order to get an increment of the G-3-P production and to observe the effects on the glycolytic pathway.**

This project is a new approach in the study of the ribozyme expression in yeast to identify the factors to be considered for the creation of a system to deliver ribozymes in yeast. Moreover, the improvement of the glycerol-3-phosphate yield is biotechnologically important for industrial purposes in the phospholipids synthesis market.

A *trans*-ribozyme activity in yeast has only been documented in a few cases. It is well known that an efficient *trans*-cleavage reaction depends on an unlimited intracellular concentration of the ribozyme, as well as a high degree of co-localization and efficient interaction of the ribozyme with the target molecule. Therefore, this project starts with the identification of possible targets on the *PGK1* RNA by computer programs that might be useful for designing asymmetrical hammerhead ribozymes. Constructed *PGK1*/ribozyme expressing plasmids containing a pol III promoter should lead to a high concentration of the ribozyme and co-localization with its target mRNA. The ribozyme delivery is tested through three different systems and a *pgk1* knock-out strain is created. The cleavage activity is investigated *in vitro* and *in vivo*. *In vitro* activity of the ribozymes is tested by cleavage reaction and *in vivo* activity is determined by northern blot and primer extension. The influence on the *PGK1* expression is analyzed by measurements on the *PGK1* activity and glycerol production.

### 3 Material and Methods

#### 3.1 Materials

##### 3.1.1 Equipment

Autoclave	1651; Fedegari, Italia
Balances	Type 1907 and 2462; Sartorius, Goettingen
Centrifuges	Sorvall RC-5B; Dupont, Bad Homburg; Microrapid; Hettich, Tuttlingen
Clean bench	uvub 1200 Uniflow
Electrophoresis chambers	Bio-Rad
Geiger-Mueller counter	Bertold LB 1210 C; Wildbald
Incubators	Biometra OV1; Biometra, Goettingen
Micromanipulator	MSM System, Singer instruments
Microscope	Leitz, Wetzlar
PCR equipment	T Gradient Whatman; Biometra, Goettingen
Photographic equipment	Olympus OM-2 with 50 mm objective; Dunco, Berlin; INTAS
Pipetting equipment	P10, P20, P200, P 1000; Abimed
Power suppliers	Phero-Stab 500; Biotec Fischer, Reiskirchen
Rotors	GSA, SS34; Dupont, Bad Homburg
Spectrophotometer	Uvikon 860; Kontron Instruments
Transilluminator	INTAS; Goettingen
Vacuum equipment	Rotary Slide pump; Heraeus, Hanau Cooler; Uni-Equip, Matinsried Centrifuge Speed-Vac; Savant, Hickville
UV Crosslinker	UV Stratalinker™ 1800; Stratagene, La Jolla, USA
Water baths	Grant LTD; Thermomix 1460 Braun, Melsungen “thermed” 5001; GFL, Burgwedel
X-ray cassettes	Kodak X-Omatic with intensifying screen; Kodak, Berlin

##### 3.1.2 Enzymes, chemicals and kits

Manufacturer, Location	Product (s)
Amersham, Buchler	Hybond N+ membranes, Multiprime DNA-Labelling Kit
BIOMOL, Hamburg	Ampiciline, IPTG, X-Gal, Phenol
Boehringer, Mannheim	dNTP's, DTT, λDNA size marker, restriction enzymes
Qiagen, Duesseldorf	Qiagen midi/maxi plasmid preparation kit, Oligotex mRNA kit
Fluka, Neu-Ulm	APS, Cellulose, Urea
Fuji, Japan	X-ray films NewRX
Greiner, Nuertingen	Eppendorf tubes, pipettes tips, petri dishes
ICN Biomedicals Inc., Ohio	Lytic enzyme, Glyceraldehyde phosphate dehydrogenase
Kodak, Berlin	X-ray development solution
MBI Fermentas, St.Leon-Rot	<i>Taq</i> polymerase, RNA ladder low range, M-MuL V Reverse Transcriptase
Merck, Darmstadt	Acetic acid, ethidium bromide, HCl, KCl, β-

Millipore, Eschborn	mercaptoethanol, MgCl <sub>2</sub> , MgSO <sub>4</sub> ·7H <sub>2</sub> O, NaCl, potassium acetate, Rnase A, sodium acetate, ZnCl <sub>2</sub> , PEG 4000
New England Biolabs,	Microdialysis membranes (0,025µm)
Schwalbach	Restriction enzymes
Oxoid, Hampshire	Peptone
Pharmacia, Freiburg	Agarose NA, restriction enzymes
Promega	pGEM-T and pGEM-T Easy kit
Roth, Karlsruhe	Isopropanol
Serva, Heidelberg	Glucose, EDTA, SDS, TEMED, MOPS, Agar-Agar
Sigma Deisenhofen	Tris, Triton X-100, 3-Phosphoglycerate, ATP, β-Glucuronidase
Stratagene	Restriction enzymes

Most all the chemicals used in this study were listed above otherwise were obtained from Merck, Serva, Sigma, Pharmacia with analytical grade or even better quality.

### 3.1.3 Strains

<i>Escherichia coli</i> NM522	supE thi-1 Δ( <i>lac-proAB</i> ) Δ( <i>mcrB-hsdSM</i> )5 (rK <sup>-</sup> mK <sup>+</sup> ) [F' <i>proABZ</i> ΔM15] supplied by Amersham Pharmacia Biotech Europe, Freiburg.
<i>Saccharomyces cerevisiae</i> CEY 1118-6B	<i>MAT</i> α, <i>his3Δ1</i> , <i>leu2Δ0</i> , <i>lys2Δ0</i> , <i>ura3Δ1</i>
<i>Saccharomyces cerevisiae</i> CEY 1123-6D	<i>MAT</i> α, <i>his3Δ1</i> , <i>trp1Δ63</i> , <i>ura3Δ1</i>
<i>Saccharomyces cerevisiae</i> diploid strain CEY	This strain was obtained by crossing the spore clones CEY 1118-6B and CEY 1123-6D which were kindly provided by Charles B. Epstein (University of Texas, SWMC at Dallas, TX, USA)

### 3.1.4 Plasmids

pGEM-T	Linear plasmid containing <i>E.coli</i> lac Z gene (Promega)
pGEM-T Easy	Linear plasmid containing <i>E.coli</i> lac Z gene (Promega)
pRS416	Low copy yeast shuttle vector derivative from pRS vectors series created by Sikorski and Hieter (Sikorski & Hieter, 1989) containing CEN6/ARS and URA3 gene (Stratagene, La Jolla, CA, USA)
pIIIEx423 RPR	High copy yeast shuttle vector developed by Good and Engelke (Good & Engelke, 1994) derivative from Sikorski and Hieter plasmid vectors, containing 2µ ori, His3 gene, RPR1 intragenic promoter and RPR1 poly (T) terminator. This vector was kindly provided by D.R. Engelke (University of Michigan, Ann Arbor, MI, USA)
pUG6	Derivative from pFA6-kanMX4 containing the <i>loxP</i> - <i>kanMX-loP</i> disruption cassette (Gueldener et al., 1996)



### 3.1.5 Oligonucleotides

All the oligonucleotides used in this study were synthesized by Metabion (Berlin).

Oligonucleotides	Sequence <u>For <i>PGK1</i> disruption</u>
KO5	5'-GTT GCT GCT TTG CCA ACC ATC AAG TAC GTT TTG GAA CAC C-3'
KO3	5'-CTT CTT AGC GAC AGT GGC AGT GTC ACC ACC ACC AAT GAT GGC ATA GGC CAC TAG TGG ATC TG-3'
	<u>For <i>PGK1</i> cloning and checking of <i>PGK1</i> disruption</u>
Pgk1-3	5'-CAT TTG CAT TGA ACG TCA TTA CAC-3'
Pgk1-4	5'-CAA GTG GGA TGA GCT TGG AGC-3'
Pgk1-5	5'-CAT CAC AGC AGT CAA TG-3'
3'UTR stp	5'-CGG AAT TCC GGC TTT CTT ATC CGA AAA GAA ATA A-3'
3'UTR ter	5'-CAT CCG CTC GAG CGG TCC AAG CTT ACA CAA CAC-3'
G1	5'-ACT GGC AAA GCT TCA CC-3'
G2	5'-TCA CTC GCA TCA ACC CA-3'
	<u>For probes generation via PCR</u>
Pgk1-6	5'-CAG TGT TTT CCA AAA CCT TCT TG -3'
Pgk1-7	5'-CAT CAA GTA CGT TTT GGA ACA CC-3'
Actin-1a	5'-GAT AAC AGA TCT GGT ATG TGT AAA GCC-3'
Actin-1e	5'-CAC TCA AGA TCT TCA TCA AGT AGT C-3'
	<u>For probe generation via polynucleotide kinase reaction</u>
Pgk1-0	5'-CAT TTT TCA TCT ATT AAT AG-3'
	<u>For probes generation via PCR used in <i>PGK1 in vitro</i> transcription</u>
Pgk1-8	5'-AGT GAG AAG CCA AGA CAA CGT -3'
Pgk1-9	5'-ACC TTC TTC TTC GAT GTG GTA -3'
Pgk1 tsp	5'-TAA TAC GAC TCA CTA TAG GGA GAA GTA ATT ATC TAC TTT TTA C-3'
	<u>For cloning of Hammerhead ribozymes</u>
Rz 1 8/7 w GUC	5'-AAT TAG ATA AAC TGA TGA GTC CGT GAG GAC GAA ACA TTG TTG-3'
Rz1 8/7 c GUC	5'-AAT TCA ACA ATG TTT CGT CCT CAC GGA CTC

Rz 5 w GUC	ATC AGT TTA TCT-3' 5'-AAT TTC CAA TGG CTG ATG AGT CCG TGA GGA CGA AAC GTT GAA G-3'
Rz 5 c GUC	5'-AAT TCT TCA ACG TTT CGT CCT CAC GGA CTC ATC AGC CAT TGG A-3'
Rz 9 w GUC	5'-AAT TAA GCC TTC TGA TGA GTC CGT GAG GAC GAA ACA GCG GCG-3'
Rz 9 c GUC	5'-AAT TCG CCG CTG TTT CGT CCT CAC GGA CTC ATC AGA AGG CTT-3'
Rz 1 11//10 w GUC	5'-AAT TTG AAG ATA AAC TGA TGA GTC CGT GAG GAC GAA ACA TTG TTT TAG-3'
Rz1 11/10 c GUC	5'-AAT TCT AAA ACA ATG TTT CGT CCT CAC GGA CTC ATC AGT TTA TCT TCA-3'
Rz 14//13 w GUC	5'-AAT TTC TTT GAA GAT AAA CTG ATG AGT CCG TGA GGA CGA AAC ATT GTT TTA TAT G-3'
Rz1 14/13 c GUC	5'-AAT TCA TAT AAA ACA ATG TTT CGT CCT CAC GGA CTC ATC AGT TTA TCT TCA AAG A-3'

For ribozyme *in vitro* transcription

RPR1 tsp	5'-TAA TAC GAC TCA CTA TAG GGA GAG TTT TAC GTT TGA GGC C-3'
RPR1 ter	5'-AAA AAG AAA GAT TAA ATT GGA-3'

For sequencing

RPR1-1	5'-GTG TAT TCT TCC TGC TCC AAG C-3'
rpr1# 1	5'-GTC AAC AGG ATA TGT TA-3'
Pgk1-10	5'-GAA ATA AAT TGA ATT GAA TTG-3'

For Reverse Transcription

Pgk1-11	5'-AAT TCC TTA GCA ACT GGA GCC AAA GAG TAT-3'
---------	---

### 3.1.6 Media, buffers and solutions

Media

*Escherichia coli*

LB	1 % Tryton; 0,5 % yeast extract; 1 % NaCl
LB +Amp	LB + 100 µg/ml Ampicilline
LB +Amp+IPTG/XGal	To 500 ml LB + Amp were added 5 ml 100mM IPTG and 600 µl X-Gal (40.85 mg/ml) (Solid medium was prepared by adding 1,5 % Agar-agar)

*Saccharomyces cerevisiae*

YE	2 % Glucose; 0.5 % Yeast extract; pH 6,3
YEGE	2 % Glycerol; 2 % Ethanol; 0.5 % Yeast extract
YE + G418	YE + 50-200 µg/ml G418
YEGE + G418	YEGE + 50-200 µg/ml G418
YEPD	2 % Glucose; 2 % Peptone; 0.5 % Yeast extract; pH 6.3

YNB	0.67 % Yeast Nitrogen Base w/o Aminoacids (DIFCO), 2 % Glucose, 40 mg/L aminoacids (depending on the strain used)
Presporulation	10 % Glucose, 0.8 % Yeast extract; 0.3 % Peptone
Sporulation	0.05 % Glucose, 1 % Potassium acetate; 0.1 % Yeast extract (Solid medium was prepared by adding 1.5 % Agar-agar)

### Buffers

PBS	10 mM NaPO <sub>4</sub> ; 150 mM NaCl
1M Phosphate buffer	1 M Na <sub>2</sub> HPO <sub>4</sub> ; 1M NaH <sub>2</sub> PO <sub>4</sub> adjusted to pH7.0
20 x SSC	3 M NaCl; 0.3 Na <sub>3</sub> -citrat; pH 7.0
TAE	2 mM EDTA; 20 mM Na-acetate; 40 mM Tris; pH 8.3 with Acetic acid
TBE	9 mM Tris; 9 mM Boracic acid; 0.25 mM EDTA; pH 8.2 – 8.4
TE	10 mM Tris; 1 mM EDTA; pH 8.0

### Solutions

Denaturing PAA (5%)	8M Urea; 5% PAA; 1 x TBE
DEPC – H <sub>2</sub> O	0.1% DEPC
Ethidium Bromide	10 mg / ml Ethidium Bromide
MgCl <sub>2</sub> – Tris-HCl	10 mM Tris; 100 mM MgCl <sub>2</sub> 6H <sub>2</sub> O; pH 7.6
CaCl <sub>2</sub> – Tris-HCl	10 mM Tris; 100 mM CaCl <sub>2</sub> 6H <sub>2</sub> O; pH 7.6
8 % PEG Solution	8% PEG <sub>2000</sub> ; 1 mM EDTA; 0.2 M NaCl; 10 mM Tris HCl; pH 7.6

## **3.1.7 Cultivation conditions**

### *Escherichia coli*

*E. coli* strains were cultivated in LB medium at 37°C. Recombinant clones were selected in LB plates supplied with 100µg/ml Ampicilline or were identified by blue-white screening on indicator plates (IPTG; X-Gal).

### *Saccharomyces cerevisiae*

Wild type *S. cerevisiae* strains were grown in YEPD plates at 28°C. Transformants were grown in YNB or in YE + G418 medium. For pre-cultures a medium size yeast colony was picked and transferred to 50 ml medium and grew at 28°C overnight. The selection of the medium inoculated depended on the strain.

Aerobic cultures. 100 ml shake-flask cultures were inoculated with 0.1-1 % of pre-cultures and grown at 28°C on an orbital shaker at 160 rpm for 24-48 hours.

Anaerobic cultures. The batch fermentations were performed in 100 ml Erlenmeyer flasks containing YNB medium supplied with the appropriate aminoacids for each strain. The cultures were stirred continuously at 300 rpm after closing the vessels with air locks, which ensured the exclusion of oxygen allowing the release of gases.

### **3.2 DNA and RNA isolation**

#### **3.2.1 Isolation of plasmid DNA from *E.coli* strains**

Plasmid DNA was isolated from 1 ml of overnight cultures according to “miniprep” method developed by Ish-Horowicz and Burke for analysis of transformants (Ish-Horowicz & Burke, 1981). Large-scale plasmids isolations from 50-100 ml cultures were performed according to the manual of the Qiagen Pack-100/500 purification kit. The DNA concentration was determined by spectrophotometry (Sambrook et al., 1989).

#### **3.2.2 Isolation of genomic DNA from *S. cerevisiae* strains**

10 ml YEPD were inoculated and the cells were grown overnight at 28°C. The cells were harvested at 8K rpm for 3 min, resuspended in 0.5 ml distilled water, and transferred to an Eppi tube. The cells were newly harvested at 10K rpm for 3 min and resuspended in 200 µl lysis buffer (2 % Triton -100, 1 % SDS, 100 mM NaCl, 1 mM EDTA, 10 mM Tris-Hcl; pH 8.0). 0.3 g of glass beads (0.45-0.5 mm dia), 100 µl Phenol and 100 µl Chloroform/Isoamylalcohol (24:1) were added and vigorously mixed for 3-4 min. After of that 600 µl TE was added and centrifuged at 10K rpm for 5 min. The aqueous phase was recovered and transferred to a fresh tube with 1 ml of ethanol and centrifuged at 10K rpm for 10 min at 4°C. The supernatant was discarded and the pellet was resuspended in 400 µl TE containing 3 µl of RNase A (10 mg /ml) and incubated at 37 degrees for 5 min. After incubation 10 µl 5 M ammonium acetate were added and the nucleic acids were precipitated by adding ethanol and centrifugation at 10K rpm for 10 min at 4°C. The recovered pellet was washed with 70 % ethanol, dried at room temperature and finally gently resuspended in 50 µl TE.

#### **3.2.3 Isolation of plasmid DNA from *S. cerevisiae***

Colony was picked and transferred to 200 µl of lysis buffer for plasmid isolation (100 mM NaCl, 10 mM Tris-HCl pH 8.0, 1 mM EDTA, and 0.1 % SDS). Equal volume of glass beads (0.45 mm dia) were added and vortex at top speed for 1 min. The extraction was made one time with 200 µl of phenol/CHCl<sub>3</sub> (2/1). Plasmids were precipitated with ethanol, after of that washed with 80 % ethanol, dried for being resuspended in 100 µl TE and used to transform *E. coli*.

#### **3.2.4 Isolation of RNA from *S. cerevisiae***

YEPD (50 ml) overnight cultures were harvested at 3-5K rpm for 5 min at 4°C and put on ice. Cells were resuspended in 10 ml citrate buffer (1.2 M sorbit, 20 mM K<sub>2</sub>HPO<sub>4</sub>, 1 mM EDTA; pH 5.8), incubated with 1-5 mg/ml of Lytic enzyme (ISN) for 20-30 min at 37°C, and spun down at 5K rpm for 5 min at 4°C. Secondly, the cell were broken by suspending in 5 ml of denaturing solution (250g Guanidinthiocyanate, 293 ml DEPC-water, 24,6 ml 10% Sarkosyl, 17,6 ml 0,75 M sodium citrate, pH 7,0; heated at 65°C for diluting) and 5 ml of DEPC water, vortex for 1 min. Then 0.5 ml of 2M Na-acetate (pH 4,0), 5 ml phenol, and 1ml

CHCl<sub>3</sub>/Isoamylalcohol (24:1) were added, this solution was vortex vigorously for 10 sec and placed on ice for 15 min. After centrifugation at 10K rpm for 20 min at 4°C the aqueous phase was pulled off to a fresh tube and precipitated with 5 ml of Isopropanol at -20 °C overnight. On the next day, the nucleic acids were centrifuged at 10K rpm for 20 min at 4°C. The pellet was washed with 80 % Ethanol, spun down at 10K rpm for 5 min, dried in a Speed-Vac as short as possible and dissolved in 300 µl of DEPC-water.

Additionally, 250 µl of total RNA isolation were used for poly (A)<sup>+</sup> mRNA isolation using the Oligotex mRNA kit (Qiagen), the protocol was performed according to the manual described by the manufacturer. After isolation a volume of 20-30 µl of poly (A)<sup>+</sup>mRNAs was purified usually.

### **3.2.5 Isolation of DNA from Agarose gels**

DNA fragments were isolated from gels using the Jet-Sorb gel elution kit (Genomed). The method was accurately follow how was described by the manufacturer. The base of this method is the DNA absorption on a matrix and its subsequent extraction. The DNA samples were mixed with 10 µl/ml ethidium bromide before running on agarose gels, after run the DNA was identified with 354 nm UV light and the interesting band was cut out and purified with the chemicals supplied by the supplier.

### **3.2.6 Isolation of labelled RNA from PAA gels**

For purification after *in vitro* transcription, labelled RNAs were separated on polyacrylamide gels. Gels were autoradiographed immediately afterwards to detect the desired band, which was cut out and transferred to a 0.5 ml tube with 400 µl Elution buffer (0.5 M NH<sub>4</sub>OAC, 0.1 % SDS, 0.1 M EDTA; pH 8) and placed at 4°C overnight. The supernatant was transferred to a fresh tube with 800 µl ethanol and centrifuged at 10K rpm for 20 min, the supernatant was discarded and the pellet was dissolved in 10 µl DEPC-water.

## **3.3 DNA *in vitro* recombination methods: Restriction, dephosphorylation, and ligation**

Restriction analyses were performed according to Sambrook et al. (1989), with 1-7 Units enzyme per µg DNA. For dephosphorylation 1 unit of alkaline phosphatase (AP) was added. To inactivate the AP activity 2 µl EGTA were added and incubated at 65°C for 10 min, after of that the samples were ready for ligation. The DNA fragments were described as was described above by Jet-sorb Extraction method. The ligation reaction was carried out with 1 µl Ligase for a total volume of 20 µl and incubated overnight at 14°C.

## **3.4 General PCR Method**

The reaction was performed in 20 µl volume in a 0,2 ml reaction tube and the following solutions were pipetted: 9.8 µl H<sub>2</sub>O, 1,6 µl 2.5 mM dNTP's (Boehringer, Mannheim), 5 µl 4x reaction buffer (MBI Fermentas, St. Leon-Rot), 1 µl 10 pmol from each primer, 1 µl DNA (1ng plasmid DNA or 100-200 ng genomic DNA), and 0,2 µl *Taq* polymerase (4 U/ µl; MBI Fermentas, St. Leon-Rot).

The PCRs were carried out in TGradient Whatman (Biometra, Goettingen) equipment. In general the following program was used: pre-treatment at 94°C for 2 min, 25 or 30 cycles when the target was plasmid or genomic DNA respectively, followed of incubation for 30 sec at 56-64°C (annealing), 72°C for 15-120 sec (elongation) and 94°C (denaturation) for 15 sec. Post-treatment comprised end-elongation at 72°C for 5 min. The annealing temperature was calculated by the G/C rule as  $T_{\text{annealing}} = 1.42(\Sigma \text{ nt} + .\Sigma \text{G/C}) + 22^\circ\text{C}$ . The elongation time depended on the fragment length, thus 15 sec were used for short fragments until 600 bp and for longer fragment the elongation time was estimated by the *Taq* polymerase activity, i.e., 40 bases/sec are incorporated in the new synthesized strand.

### 3.5 Gel Electrophoreses

DNA electrophoresis was carried out horizontally; the agarose percent (1.0-2.5 %) depended on the size of the fragment to be separated in TAE (160 bp to 9 Kbp). Midi and mini size of gels were used: 18 x 10 x 0.5 cm and 12 x 10 x 0.5 cm, respectively. Gels were run at 100 V for 1-1.5 hours. Generally, the size markers used were  $\lambda$  DNA digested with *HindIII* and GeneRuler™ (100 bp DNA Ladder Plus; MBI, St. Leon-Rot).

RNA electrophoresis was done horizontally in formaldehyde gels 1 % agarose. Midi and mini size of gels were used: 18 x 10 x 0.5 cm and 12 x 10 x 0.5 cm. The protocol was followed how it was described by Odgen and Adams (1987). Gels were run at 100 V for 1-4 hours. Size marker used was RNA ladder, low range (MBI Fermentas, St. Leon-Rot).

Nucleic acids were detected by staining the agarose gels with ethidium bromide (1 µg/ml) and UV light (254 nm).

Radiolabelled RNA was separated for purification and cleavage analysis through denaturing RNA gels, 3.5 or 5 % acrylamide with Bis-acrylamide at 19:1, respectively and 8 M urea as denaturant (Sambrook et al., 1989). All the solutions were previously treated against Rnases using DEPC-water. The size of the gels was 16 x 14 x 0.5 cm. Gels were run at 40 mA for 1.5-2.5 hours. After run, the gels were embedded in 10% methanol, 10 % acetic acid for 20 min in order to fix the gels to Whatman 3 MM paper by drying at 80° C for 1 hour. Gels were exposed in X-ray cassettes and frozen at -70 °C.

### 3.6 Northern blot analyses

Northern blot analyses were performed according to Sambrook et al. (1989). After gel electrophoresis, the RNA was transferred to a Qiabran Nylon membrane (Qiagen) using a Possiblot™ pressure blotter and UV crosslinked. Probes were labelled using [ $\alpha$ -<sup>32</sup>P] dATP. Hybridization was performed with Rapid buffer according the protocol supplied by the manufacturers (Amersham). Membranes were put in X-ray cassettes and incubated at 70 ° C.

### 3.7 Transformation methods

#### 3.7.1 Transformation of *E. coli*

*E. coli* transformations were performed according the heat shock method developed by Himeno et al. (1984). Competent cells were obtained by  $\text{CaCl}_2$  treatment; these cells were directly used or stored at  $-70^\circ\text{C}$  in 100 mM  $\text{CaCl}_2$ , 15 % Glycerin. To 200  $\mu\text{l}$  of fresh cells or 240  $\mu\text{l}$  of freeze competent cells, 100  $\mu\text{l}$  of 8 % PEG<sub>2000</sub> (8 % PEG<sub>2000</sub>, 1 mM EDTA, 0.2 M NaCl, 10 mM Tris-HCl pH 7.6) and 20  $\mu\text{l}$  of DNA were added. Cells were gently mixed, placed on ice for 30 min and a heat shock was applied for 1 min at  $42^\circ\text{C}$ . Adding 1 ml of LB medium and the incubation at  $37^\circ\text{C}$  for 90 min made the regeneration. Cells were plated on the appropriated selection agar. Transformation efficiencies were about 104-106 CFU/ $\mu\text{g}$  DNA.

#### 3.7.2 Transformation of *S. cerevisiae*

Transformation of *S. cerevisiae* was made according the lithium acetate/PEG method (Gietz & Woods, 2002). 20 ml YEPD was inoculated and the cells were grown overnight at  $28^\circ\text{C}$  and 120 rpm. 100 ml YEPD shake-flask cultures were inoculated at different concentrations (0.01 %, 0.05 %, and 0.1 %). Cells were grown overnight until  $\text{OD}_{600} = 0.5$ , harvested at 5K rpm for 5 min and washed with 10 ml 0.1 M Li-acetate (0.1 M lithium acetate, TE pH 8.0) and resuspended in 2 ml 0.1 M Li-acetate. The mixture of transformation was done with 100  $\mu\text{l}$  cells, 5  $\mu\text{l}$  DNA (1-5  $\mu\text{g}$ ), 5  $\mu\text{l}$  salmon sperm DNA (10 mg/ml), and 600  $\mu\text{l}$  PEG (40 % PEG<sub>4000</sub>, 0.1 M lithium acetate, TE pH 8.0), gently mixed and incubated at  $42^\circ\text{C}$  for 30 min. Cells were harvested at 5K rpm for 5 min and plated on selective medium at different dilutions (1:10, 1:100, and undiluted). For selection on YE + G418 the cells were regenerated in 5 ml YE for 3-4 hour after plating.

Fast method. A shorter form of the lithium acetate method was also used. A picked colony (3 mm dia) was transferred to 1 ml distilled water in a 0.5 ml tube and spun 5K rpm for 5 min. Pellets were washed in 1 ml 0.1 M Li-acetate and resuspended in 0.5 ml 0.1 M Li-acetate. The next steps were performed as before, regarding that the transformation mixture was carried out with a higher concentration of DNA about 5-10  $\mu\text{g}$ .

### 3.8 Radioactive labelling of DNA

Random primer labelling using [ $\alpha$ - $^{32}\text{P}$ ] dATP (Hartmann Analytic) was performed for generating hybridization probes of PCR products (Megaprime labeling kit, Amersham). Single stranded oligonucleotides were labelled with [ $\gamma$ - $^{32}\text{P}$ ] d ATP (Hartmann Analytic) using T<sub>4</sub> Polynucleotide Kinase (Biolabs) according to Sambrook et al. (1989).

### 3.9 Ribozyme cleavage activity

#### 3.9.1 *In vitro* transcription reaction by T7 polymerase

The reaction was carried out using eluted PCR product as templates.

Non-radioactive *in vitro* transcription of Ribozymes. The mixture reaction was done with 4 µl 4 x Transcription buffer (MBI Fermentas, St. Leon-Rot), 1 µl RNAsin (20 U/ µl; Promega), 1 µl 2.5 mM rNTPs (Boehringer, Mannheim), 10 µl PCR product (1 µg/ µl), and 1 µl T7 polymerase (20 U/µl; MBI Fermentas, St. Leon-Rot). The mixture was incubated at 37°C for 2 hours, then 1 µl DNase I Rnase free (2 U/ µl; Pharmacia) was added and incubated at 37°C for 15 min. The volume of the mixture was pull up to 100 µl and mixed with 15 µl NH<sub>4</sub>-acetate 7 M. The mixture was extracted with equal volume of phenol/CHCl<sub>3</sub>: Isoamylalcohol (24:1), the aqueous phase was carefully transferred to a fresh tube and precipitated with 2 volume ethanol and centrifuged at 13K rpm for 25 min. Pellet was dried in a Speed-Vac as short as possible and dissolved in 20 µl DEPC-water.

Radioactive *in vitro* transcription of *PGK1*. The transcription reaction was modified by adding 1 µl [ $\alpha$ -<sup>35</sup>S] UTP (Hartmann Analytic) to the mixture reaction and after incubation at 37°C for 1 hour, immediately after the transcription products were separated on 3.5 % PAA 8 M urea gels (3.5) and purified (3.2.6).

#### 3.9.2 *In vitro* trans-cleavage reaction

*PGK1* transcript (50 mM) was combined with increased ribozyme concentrations between 50-500 mM combined in 17 µl with 1 µl 1 M Tris-HCl pH 7.6, heated at 95°C for 1 min, cooled to room temperature for 15 min. The initiation was made by adding 2 µl 0.1 M MgCl<sub>2</sub> and the reactions were incubated at 37°C for 1 hour and stopped with 1 volume of stop solution (95% formamide, 20 mM EDTA, 0.05% bromophenol, 0.05% xylene cyanol). The cleavage products were separated by 5 % PAA 8 M urea gels and the detection was made by Autoradiography (3.5).

#### 3.9.3 Primer extension

For first strand of cDNA synthesis, volumes between 3-9 µl of poly (A)<sup>+</sup> mRNA isolations (0.5-1.5 µg; 3.2.4) were prepared in a sterile tube with 20 pmol of sequence specific primer P<sub>gk1-11</sub> (3.1.5) and pull up to 11 µl. Simultaneously, 0.5 µg of *in vitro* *PGK1* transcript and/or 9 µl of cleavage reaction (described above) were used as control. After incubation at 70°C for 5 min, the samples were placed on ice for 10 min. 4 µl 5X reaction buffer (MBI Fermentas, St. Leon-Rot), 2 µl 10 mM dNTP (Boehringer, Mannheim), 1 µl RNAsin (20 U/ µl; Promega), and 1 µl [ $\alpha$ -<sup>35</sup>S] ATP (Hartmann Analytic) were added and pull up to 19 µl. The reaction mixtures were pre-incubated at 37°C for 5 min, after that the reaction started by adding 1 µl of M-MuL V Reverse Transcriptase (40 U/ µl; MBI Fermentas, St. Leon-Rot) and incubated at 37°C for 4 hours. Reactions were stopped by adding 10 µl of loading buffer and heating at 70°C for 10 min. The extended products were separated by 8% PAA 8 M urea gels and the detection was made by autoradiography (3.5).



The size marker used was a mixture of chain-terminated fragments generated from a ddCTP sequencing reaction using the T7 Sequencing kit from USB Corporation (USB Corporation, Ohio) and following rigorously the provided protocol. The DNA template was a PCR fragment used for *in vitro* transcription of *PGK1*. The labelling was made by adding 1 µl [ $\alpha$ -<sup>35</sup>S] ATP (Hartmann Analytic) to the sequencing reaction.

### **3.10 Ribozyme DNA construction**

For annealing of the sense and antisense ribozyme strands, the following mixture was used: 1 µl from each oligomer (10 ng/µl), 500 mM NaCl and 7 µl distilled water. This sample was heated up to 70°C and let to cold until room temperature. For phosphorylation, 2 µl of this sample was pipetted to a 1.5 ml tube with 10 mM ATP, 2 µl 10 x Polynucleotide kinase buffer (BioLabs), 2 µl Polynucleotide kinase (10 KU/ml; BioLabs) and 12 µl distilled water. The mixture was incubated at 37°C for 60 min and the phosphorylation activity was inactivated by incubation at 65°C for 10 min. After that the DNA oligomer duplexes were ready for cloning into the vectors.

### **3.11 Sequence analysis of DNA**

Sequencing was carried out at the Freie Universitaet Berlin (Dr. Martin Meixner): The sequencing primers were listed under point 3.1.5.

### **3.12 Protein analyses and Glycerol determination**

#### **3.12.1 Isolation of total protein from *S. cerevisiae***

The strains were inoculated in 50 ml YNB pre-cultures and grown overnight (strains with slower growth were grown for 2 days) until OD<sub>600</sub> = 1.0-1.5. Samples of 200 µl – 400 µl were inoculated to 100 ml YNB and grew overnight until OD<sub>600</sub> = 0.6-0.7. The same volume of culture was transferred to two SS34 tubes (40 ml) per strain and centrifuged at 3K rpm during 15 min. Liquid phases were taken off and maintained always in ice. The cells were washed with 6 ml PBS and centrifuged in 6 ml tubes at 3K rpm for 5 min at 4°C. The liquid phase was discarded, the cells were resuspended in 500 µl PBS, 1% Triton, 1 mM PMSF and the suspension was transferred to a 0.5 ml fresh tube. For breaking the cells, one volume of glass beads was added and vigorously vortexed 1 min for 5 times, the suspension was centrifuged at 12K rpm during 15 min and the aqueous phase was carefully transferred to a fresh tube.

#### **3.12.2 Activity and protein concentration**

*PGK1* activity. The method was performed according to Scopes, 1975. For *PGK1* activity measuring 50 µl crude extracts (diluted 1/10 with PBS; twice for each sample), 850 µl *PGK1* activity buffer (stock buffer: 30 mM Triethanolamine, 10mM 3-phosphoglycerate, 50 mM KCl, 5 mM MgCl<sub>2</sub>, 0.2 mM EDTA to this were freshly added 0.2 mg/ml BSA, 20-40 µg/ ml Glyceraldehyde phosphate dehydrogenase (50-100 IU/mg) and 0.1 mM NADH) were mixed and placed previously in spectrophotometer at 30°C to measure undesired contamination.

Adding 100 µl 50 mM ATP pH 7.5 (adjusted with KOH) started the reaction. Activity measurements were carried out at 340 nm by oxidation of NADH for every molecule of 3-phosphatoglycerate phosphorylated.

Protein concentration. The protein amount present in the samples was estimated according the BIO-Rad protocol described by the manufacturer.

### **3.12.3 Glycerol determination**

The protocol was carried out according to Nevoigt & Stahl, 1996. 50 ml YNB pre-cultures were inoculated and grew overnight at 28°C and 160 rpm until OD<sub>600</sub>= 1.3-1.5. Fermentations were carried out in 100 ml YNB medium inoculated with 10% pre-cultures. Anaerobic cultures were grown overnight at 28°C and stirred at 300 rpm until OD<sub>600</sub>= 1.3-1.5. Samples of 10 ml of culture were harvested at 5 K rpm for 10 min in pre-weighed 10 ml tubes, 1.5 ml supernatants were transferred to a 1.5 ml fresh cry-tube and frozen by shock with liquid N<sub>2</sub> and placed at -20 °C. When the determination was taken place 100 µl were incubated for 10 min at 80°C to stop possible enzymatic reactions and the samples were diluted 1:5 for analyses of glycerol production. Glycerol concentration was determined by Glycerol kit (R-Biopharm; Boehringer, Mannheim) and the supplied protocol was followed rigorously.

Pellet obtained were washed two times in distilled water and the tubes were dried for 48 hours at 100°C, cooled in a desiccator and reweighed for biomass analyses.

### **3.13 Tetrad analysis**

Strains were grown 2 days in presporulation medium and sporulated after 3-5 days after transferring to sporulation medium. The plates were checked for sporulation by microscopy. Cells were transferred to a 1.5 ml tube with 600µl distilled water for washing and spun at 5K rpm for 5 min, resuspended in 50 µl distilled water, 2.5 µl β-Glucuronidase (Sigma) were added and samples were incubated at room temperature for 8 min, 10 µl were diluted with 90 µl ice cooled water and the mixture was carefully transferred onto thin YE plates using a sterile loop. The four spores were then separated from each other and moved to isolated positions on the YE plate using the micromanipulator. The spores germinated and formed colonies 3-4 days after dissection. The phenotypes were scored by replica plating onto appropriated media.

## 4 Results

### 4.1 Selection of the hammerhead target sites

As a general rule, the requirement in the target to be cleaved by a hammerhead ribozyme is the presence of the NUH triplet where N is any nucleotide and H is any nucleotide except G. However, in terms of the cleavage rate the natural GUC triplet is the best target for being selected (Amarzguioui & Prydz, 1998). The sequence of the *PGK1* mRNA contains 24 GUC triplets as possible hammerhead target sites. In order to establish which should lead to an efficient catalytic activity, it was analyzed the accessibility of the potential target sites for *trans*-acting ribozymes. The secondary structure fold of the target mRNA was predicted at different temperatures (25, 30 and 37°C) applying the “RNA draw” computer program (Matzura & Wennborg, 1996). Only two of the 24 GUC triplets could be shown to be placed in a single stranded region of the RNA for at least two of the tested temperatures: target site one, which is located next to the translation start codon and target site nine, nt position at 318 of the ORF. Both of the sites were chosen to design hammerhead ribozymes (HH Rz 1 and HH Rz 9) (Fig.7). As a negative control a third ribozyme was designed (HH Rz 5, ORF position 78 nt), which is located in a region of the *PGK1* messenger clearly predicted as double-stranded RNA.

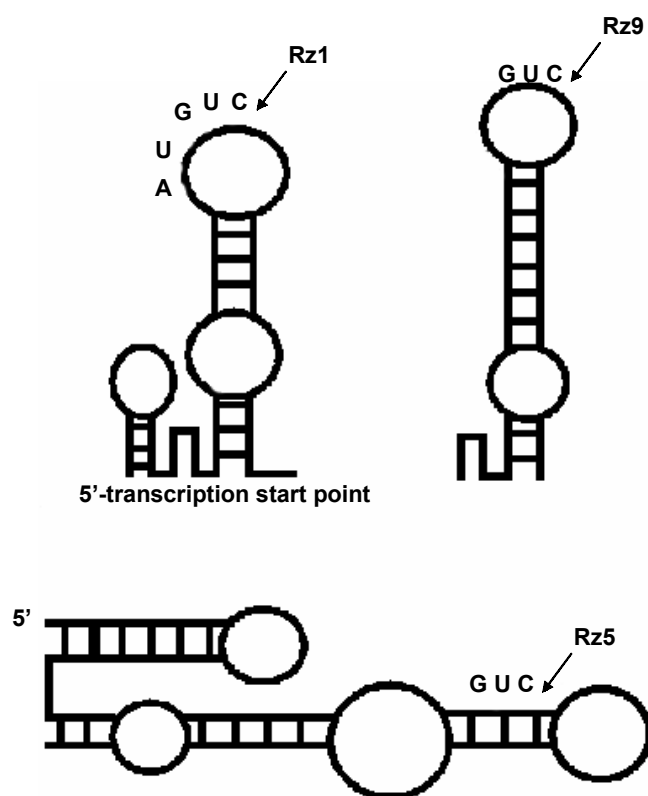


Figure 7: Secondary structure of three different regions of the *PGK1* mRNA selected by “RNA draw”. The arrows mark the GUC triplets selected to design *trans*-acting hammerheads for *PGK1* mRNA cleavage.

## 4.2 Designing and cloning of hammerhead ribozymes

For optimal *in vivo* ribozyme activity, it is well known that the two sequence stretches flanking the conserved region of the *trans*-acting ribozyme, stem I and stem III (see fig. 2) should be composed of 15 nucleotides in asymmetrical arrangement (9 and 6 or 8 and 7 nt). Thus, DNA oligomer duplexes for the chosen target sites were synthesized, each containing the 22 nt of the conserved region and the two flanks of 8 and 7 nt complementary to the different target sites (Fig. 8). The 5' ends were designed as *EcoRI* overhangs for the cloning of the ribozyme sequences into the single *EcoRI* site of the pIIIEx423 RPR plasmid series downstream from the polymerase III promoter (Good & Engelke, 1994).

Rz1 8/7 w GUC:

5'-AAT TAG ATA AAC **TGA TGA GTC CGT GAG GAC GAA** ACA TTG TTG-3'

Rz1 8/7 c GUC:

5'-AAT TCA ACA ATG TTT **CGT CCT CAC GGA CTC ATC AGT** TTA TCT-3'

Rz5 w GUC:

5'-AAT TTC CAA TGG **CTG ATG AGT CCG TGA GGA CGA** AAC GTT GAA G-3'

Rz 5 c GUC:

5'-AAT TCT TCA ACG TTT **CGT CCT CAC GGA CTC ATC AGC** CAT TGG A-3'

Rz9 w GUC:

5'-AAT TAA GCC TTC **TGA GTC CGT GAG GAC GAC GAA** ACA GCG GCG-3'

Rz 9 c GUC:

5'-AAT TCG CCG CTG TTT **CGT CCT CAC GGA CTC ATC AGA** AGG CTT-3'

Figure 8: DNA sequence of the Watson and Crick strand (w and c, respectively) of the three cloned *trans*-acting ribozyme genes. The constructs contain the conserved sequence of the hammerhead ribozyme (bold type), the complementary flanks of the targets and the *EcoRI* overhangs for cloning (underlined).

### 4.3 Cloning of the ribozyme DNAs into vectors of the pIIIEx423 series

In order to get a high ribozyme expression in yeast cells, we used the shuttle plasmid pIIIEx423 RPR (see appendix). These vectors, generously provided by D.H. Engelke (University of Michigan, Ann Arbor), were derived from the pRS vector series developed by Sikorski and Hieter (1989) to promote the accumulation of small RNAs in yeast. The high expression is based on the presence of a promoter which is transcribed under the control of the polymerase III system. The pIIIEx423 RPR plasmids contain the intragenic promoter from the *S. cerevisiae* RNase P RNA gene (*RPR1*). This promoter consists of an A box and B box within the transcribed leader which is normally removed from the “mature” domain of the RNase P RNA. The fusion of this leader to RNAs that are not recognized in RNase P maturation process leads to stable accumulation of these molecules (Fig. 9) (Good & Engelke, 1994).

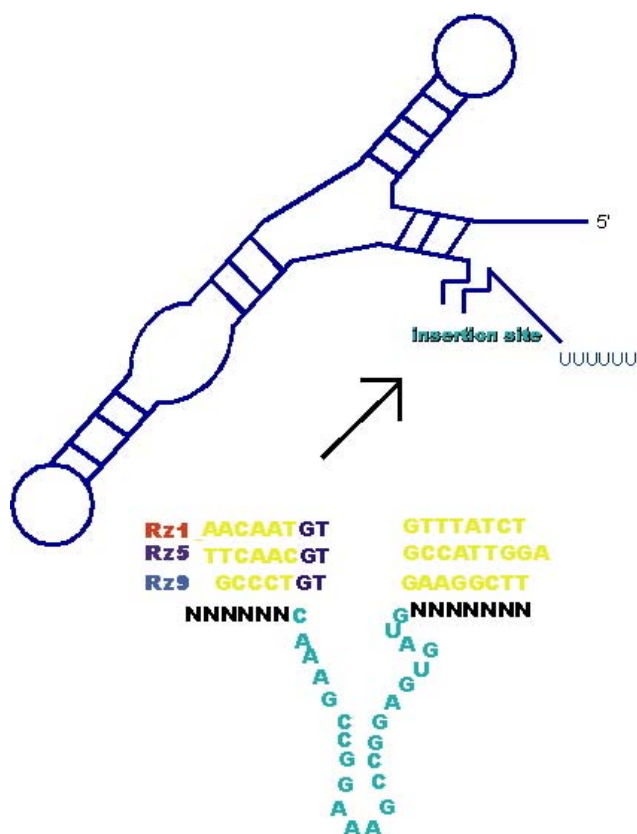


Figure 9: Schematic representation of the insertion site used for cloning of hammerhead ribozymes in the *RPR1* leader RNA designed by Good and Engelke (1994). Thus, the hammerhead ribozyme encoding sequences were inserted into single *EcoRI* site of pIIIEx423 RPR.

The correct integration of the ribozyme genes in plasmid pIIIEx423 RPR Rz1, Rz5, and Rz9 was confirmed by restriction analysis with *Bam*HI/ *Eco*RI and separation on a 2.5% agarose gel (see fig. 10, lanes 2, 3, and 4). The *Bam*HI/ *Eco*RI restriction fragment of about 400 bp corresponds to the sequence between the *Bam*HI restriction site used to clone the *RPR1* leader into the plasmid pRS423 and the *Eco*RI insertion site used to clone the ribozyme DNAs. The ribozyme DNAs were designed to maintain one *Eco*RI site at the 3'-end, hence producing about a 40 nt longer sequence after cloning.

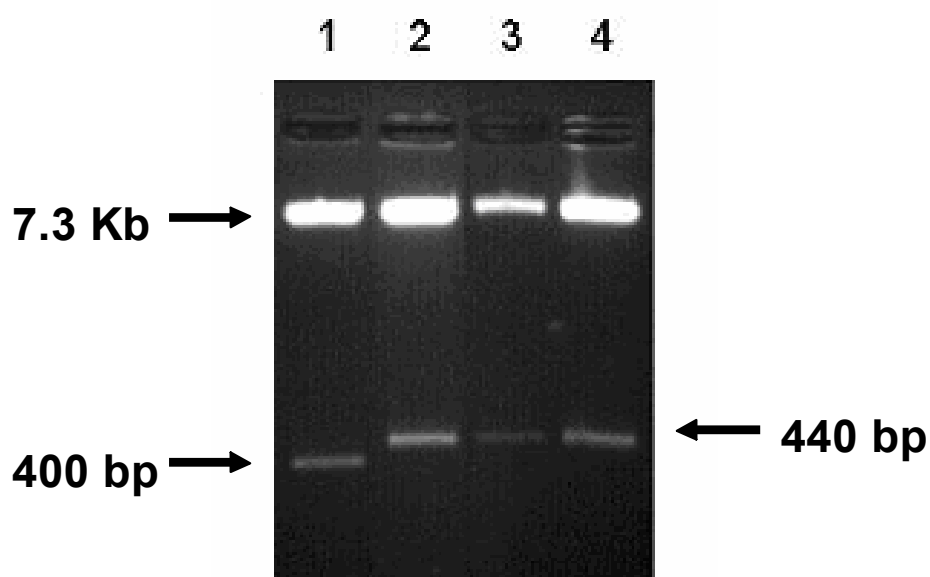


Figure 10: Checking the correct insertion of the ribozyme DNAs by restriction-analysis with *Bam*HI/*Eco*RI and separation on a 2.5% agarose gel. Digestion of plasmids pIIIEx423 RPR without ribozyme DNA (lane 1), Rz1, Rz5, and Rz9 (lanes 2, 3, and 4, respectively). The right arrow shows the bands corresponding to the *Bam*HI/*Eco*RI fragments carrying the correct insertion of the ribozyme expression cassette of about 440 bp.

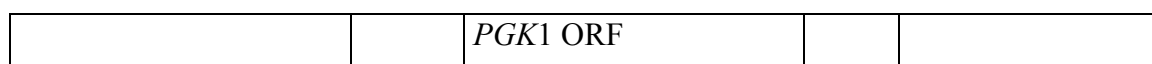
#### 4.4 *pgk1*-knock-out strain

For disruption of the chromosomal copy of the *PGK1* gene, a PCR-based knock-out strategy was chosen. The deletion cassette with a kanamycinMX module as a dominant resistant marker was amplified from plasmid pUG6 (Gueldener et al., 1996) via PCR using two long primers (60 nt) whose 40 nt long sequence stretches at their 5' ends are homologue to specific upstream and downstream sequences of the *PGK1* ORF (see chapter 3.1.5).

Due to the difficulty in manipulating the *pgk1* knock-out phenotype (inhibited growth on glucose), the development of a  $\Delta pgk1$  strain made it necessary to use a diploid strain as the starting material in order to ensure the viability of this strain. For this reason, the strain CEY (see materials and methods) was transformed with the disruption cassette and the transformants were selected on glucose media plates containing 100µg/ml Kanamycin resistance marker, geneticin 418 (G418). The detection of the correct integration was achieved by diagnostic PCR. The kanamycin-resistant diploid transformants contain both the sequence corresponding to the inserted disruption cassette in the *PGK1* ORF (3917 bp) and the sequence encoding for the wild-type *PGK1* gene (3244 bp) (Fig. 11, lane 8). Subsequently, the transformants were submitted to tetrad analysis and the spore-isolates from tetrads, were analyzed with respect to their expected phenotype for the  $\Delta pgk1$  strain isolate by growth on different carbon sources (Fig. 12). Figure 12 shows that two spore-isolates from each tetrad have the phenotype described for  $\Delta pgk1$ , which is in accordance with a meiotic segregation. Therefore, these isolates do not grow on glucose plates but are able to grow on glycerol/ethanol plates (YEGE) in the presence of G418. This is the exact knock-out phenotype expected and the analysis of the disruption events by PCR of the ORF on these haploid isolates revealed a correct integration of the disruption cassette into the *PGK1* gene (Fig. 13).



**Primers used for PCR analyses**  
***PGK1***



pgk1-5              pgk1-3              G1  
 $\Rightarrow$                      $\Rightarrow$                      $\Rightarrow$

**Disrupted gene**

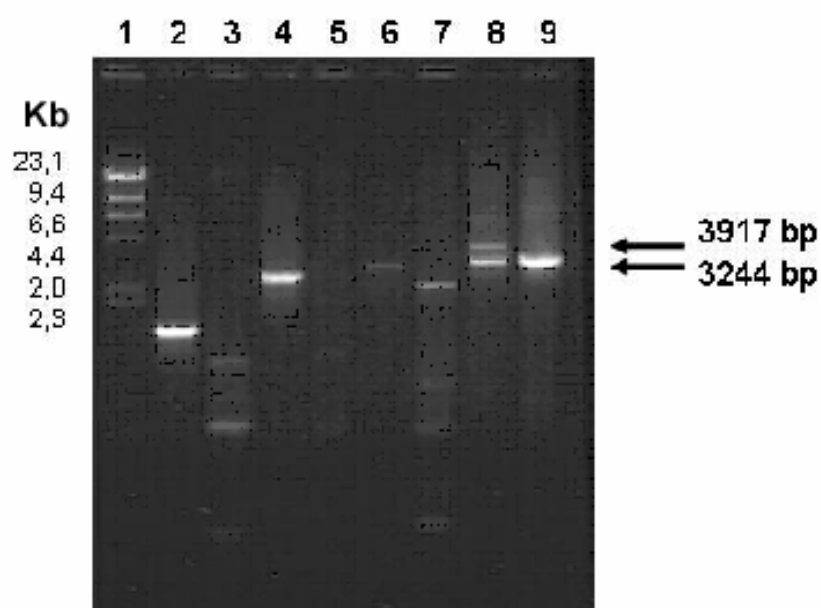
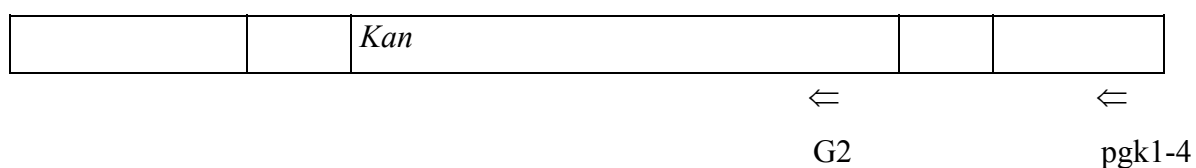


Figure 11: PCR analysis of the correct integration of the kan cassette in kanamycin resistant diploid CEY transformants.  $\lambda$  DNA /*Hind*III marker (lane 1); amplified DNA of a Kan resistant transformant using pgk1-4 and G1 (lane 2), pgk1-3 and G2 (lane 4), pgk1-5 and G2 (lane 6), and pgk1-3 and pgk1-4 (lane 8); amplified DNA of the wild-type strain CEY using pgk1-4 and G1 (lane 3), pgk1-3 and G2 (lane 5), pgk1-5 and G2 (lane 7), and pgk1-3 and pgk1-4 (lane 9) as a control.

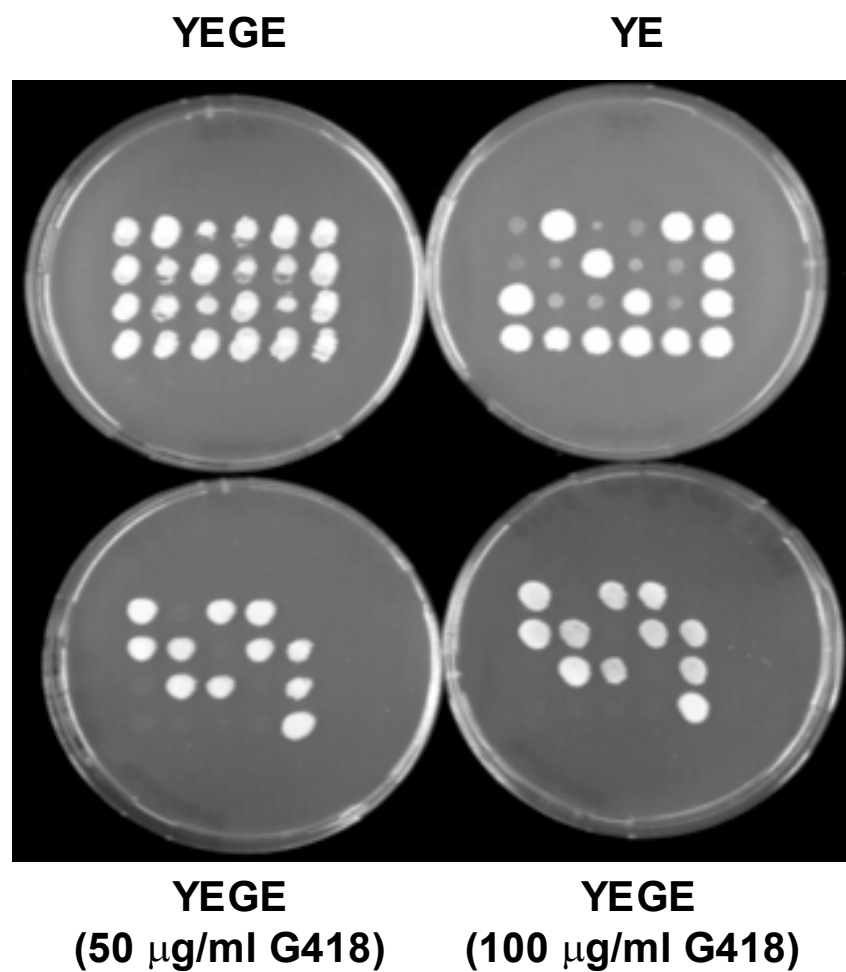


Figure 12: Growth characteristics of different spore-isolates from tetrads of the diploid strain CEY PGK1/*pgk1*::KanMX. The haploid *pgk1* knock-out strains are known to grow only on media with non-fermentable carbon sources like ethanol and/or glycerol (YEGE), but cannot grow on glucose medium (YE). The spore isolates carrying the Kan resistance cassette grow on YEGE plates with Geneticin 418 (G418), but are unable to grow on glucose containing media.

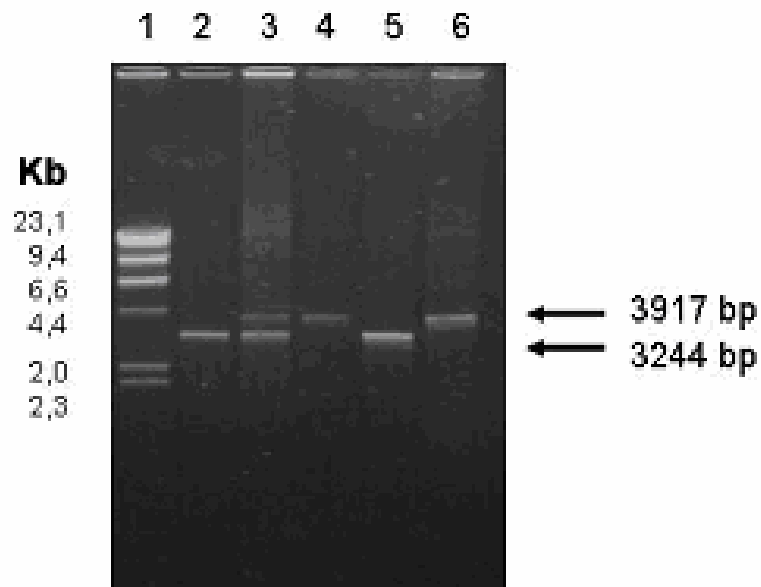


Figure 13: PCR analysis of correct integration of the kan cassette in kanamycin resistant diploid transformants and haploid spore isolates using *pgk1-3* and *pgk1-4*.  $\lambda$  DNA /*Hind*III (lane 1); diploid wild-type CEY (lane 2); diploid Kan transformant (lane 3); haploid spore a1 with  $\Delta pgk1$  phenotype (lane 4); haploid spore a2 with *PGK1* phenotype (lane 5) and haploid spore a3 with  $\Delta pgk1$  phenotype (lane 6).

## 4.5 Delivery of hammerhead ribozymes

In order to analyze the factors that are involved in the catalytic *in vivo* activity, the hammerhead ribozymes and the *PGK1* gene were delivered into the *pgk1* knock-out and wild-type strain using three different approaches (Fig. 14):

**1. Two-plasmid-system**: The *PGK1* gene was amplified from total yeast DNA by PCR using *pgk1*-3 and *pgk1*-4 primers (see above), and cloned into vector pGEM-T. The *PGK1* gene was re-cloned from pGEM-T as a *SacII/SpeI* fragment into yeast/*E. coli* shuttle vector pRS416 (Sikorski & Hieter, 1989) to give rise to pRS416-*PGK1* and co-localized with the pIIIEx423 RPR ribozyme constructs (see appendix). The  $\Delta pgk1$  strain was subsequently transformed with pRS416-*PGK1* and the pIIIEx423 RPR plasmids, with and without ribozymes. This strategy is straight to analyze the effects of the nuclear localization of the ribozymes and the target molecule in the cleavage activity.

**2. One-plasmid-system**: The pIIIEx423 RPR Rz and pIIIEx423 RPR were digested with *BamHI/XhoI* and the fragments carrying the expression cassette with and without ribozymes (as a negative control) were inserted into the single *BamHI/XhoI* sites of plasmid pRS416-*PGK1* (see appendix). The correct insertion was checked by restriction assays (see figure 7, lanes 1, 3 and 5). The  $\Delta pgk1$  strain was transformed with the pRS416-*PGK1*-RPR1 Rz and pRS416-*PGK1*-RPR1 plasmid, respectively. This approach might produce a highly productive ribozyme-target interaction since the delivery of both genes is via a co-expressing trans-acting ribozyme/target plasmid.

**3. Simple-plasmid-system**: The wild-type strain was transformed with the pIIIEx423 RPR plasmids with and without ribozymes. This model should shed light on how the chromosomal target localization influences ribozyme activity. The activities obtained using this system can be compared to those from the one- and two-plasmid-system where the target *PGK1* gene is localized on a plasmid.

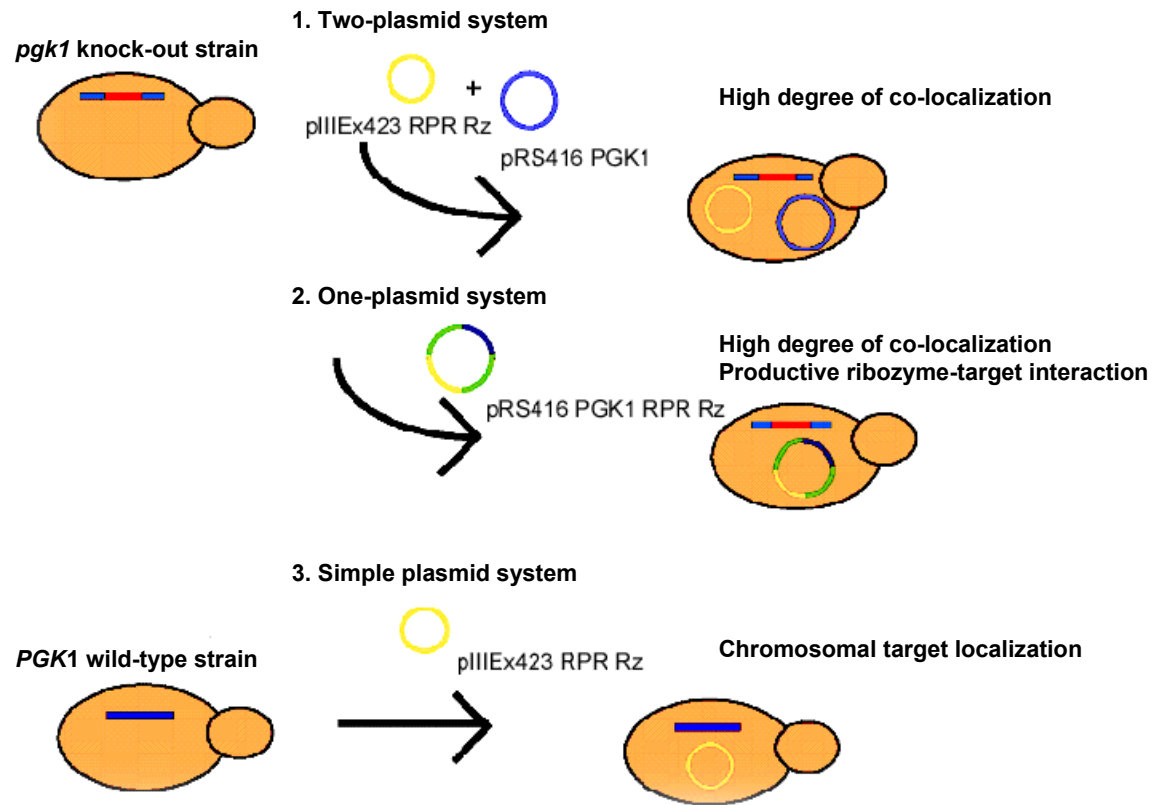


Figure 14: Ribozyme-delivery strategy. This schematic model presents the three systems used for ribozyme expression in yeast cells for determining cellular factors involved in cleavage activity.

## 4.6 Detection of cleavage activity

The ribozyme cleavages activities were tested by *in vitro* and *in vivo* assays.

### 4.6.1 *In vitro* assays

To examine whether the ribozymes had the predicted cleavage activity from their secondary structures and to establish the influence of the ribozyme insertion into the *RPR1* leader on the cleavage reaction, the cleavage activities were compared *in vitro*. RNA was synthesized *in vitro* with T7 RNA polymerase. Different primers were designed to amplify the corresponding encoding ribozymes and the target sequences were under the control of the T7 promoter control. These fragments were used for *in vitro* transcription where the **complete** *PGK1* mRNA was labelled by [ $\alpha^{32}\text{P}$ ] UTP incorporation. The transcription products were used to test the cleavage activity by cleavage reaction assays for every ribozyme (Fig. 15). Cleavage reactions were performed at 37°C for 60 min and cleavage products were separated on a denaturing polyacrylamide gel. As the template for transcription a *PGK1* fragment of 1379 bp was amplified from pRS416 using the primers pgk1-tsp and pgk1-ter. The Rz templates were amplified from the pIIIEx423 RPR with and without ribozymes genes by using the primers rpr1-tsp and rpr1-ter. RPR1 means *RPR1* leader without ribozyme. The cleavage control used was substrate incubated without ribozyme in presence of 10 mM  $\text{Mg}^{2+}$ . As expected, the cleavage reaction of Rz1, showed a weak band corresponding to the small 40 nt 5' cleavage product of *PGK1* RNA and its accumulation increased when a greater concentration of RZ1 was added in the cleavage reaction, i.e. single turnover was established. On the contrary, there was no evidence for any cleavage activity of Rz5 and Rz9. But the resolution of this assay by using long *PGK1* transcripts as substrates was not sensitive enough to draw clear conclusions.

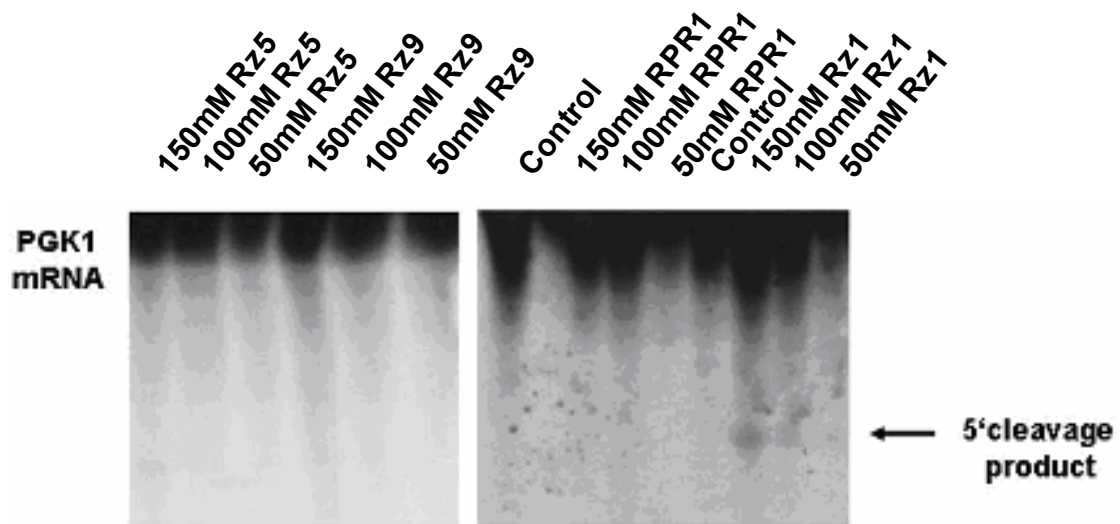


Figure 15: Cleavage of the *PGK1* target by hammerhead ribozymes. The *PGK1* RNA fragment was internally labelled with [ $\alpha^{32}$ P] UTP and incubated with each of the individual ribozyme cassettes to cleave the selected sites.

#### 4.6.1.1 Improving the *in vitro* assays

Due to the difficulties found when detecting the *in vitro* cleavage activity, a new cleavage reaction was performed under different conditions. A short 5' fragment from the *PGK1* sequence was amplified at the start transcription codon, considering also the 3' sites selected, thus a 422 nt substrate was obtained to be cleaved by ribozymes. Furthermore, in order to improve the resolution, an internal label procedure was developed by the incorporation of [ $\alpha^{35}\text{S}$ ] UTP. The [ $\alpha^{32}\text{P}$ ] UTP results in diffuser and bigger bands that hamper the detection of sequences with little differences in size (smaller than 40 nt). The labelling of probes with [ $\alpha^{35}\text{S}$ ] UTP generates thin bands after detection by autoradiography. However, it is not known until now how the cleavage activity is affected due to the incorporation of [ $\alpha^{35}\text{S}$ ] labelled UTP at the GUC codon.

The cleavage reaction was performed under standard conditions. The cleavage products were separated on a denaturing polyacrylamide gel. As the template for transcription a *PGK1* fragment of 422 bp was amplified from pRS416 using the primers pgk1-tsp and pgk1-9. The Rz templates were amplified from the pIIIEx423 RPR carrying the ribozyme genes by using the primers rpr1-tsp and rpr1-ter. The cleavage control used was substrate incubated without ribozyme in presence of  $\text{Mg}^{2+}$ . The cleavage activity of Rz1 with the expected 3' cleavage product (382 bases long) was observed. Single turnover was confirmed by using increased concentrations of ribozymes (Fig. 16 B).

To analyze the influence of longer flanks, we designed two new ribozymes (Fig.16 A). These constructs were cloned, amplified and *in vitro* transcribed as mentioned above for expressing ribozymes. The cleavage activities were enhanced and the expected 3'-cleavage product was accumulated (Fig. 16 B). The reaction was increased about 20 % by using 11/10 flanks and 40% by using of 14/13 flanks. Furthermore, we tested the catalytic activities of Rz5 and Rz9. As expected and demonstrated previously, no cleavage activity was detected for Rz5. However, Rz9 did not show the cleavage activity predicted. Only very weak bands corresponding to the 5'-cleavage products were observed despite the increased Rz concentration. Thus, the cleavage activity of hammerhead ribozymes *in vitro* could be partially deduced from their computer-generated secondary structures. Additionally, we designed the Rz transcripts that contained the whole secondary structure of the ribozyme cassette. With this experiment it was demonstrated that the ribozymes inserted into this folding sequence could bind and cleave the target molecule appropriately, at least *in vitro*.



Moreover, the cleavage activity assays revealed that the use of internally labelled RNA by radioactive [ $\alpha^{35}\text{S}$ ] UTP does not have an inhibitory effect on catalysis.

#### A. Oligonucleotides

Rz1 11//10 w GUC:

5'-AAT TTG AAG ATA AAC **TGA TGA GTC CGT GAG GAC GAA** ACA TTG TTT TAG-3'

Rz1 11/10 c GUC:

5'-AAT TCT AAA ACA ATG TTT **CGT CCT CAC GGA CTC** ATC AGT TTA TCT TCA-3'

Rz1 14//13 w GUC:

5'-AAT TTC TTT GAA GAT AAA **CTG ATG AGT CCG TGA GGA CGA** AAC ATT GTT TTA TAT G-3'

Rz1 14/13 c GUC:

5'-AAT TCA TAT AAA ACA ATG TTT **CGT CCT CAC GGA CTC** ATC AGT TTA TCT TCA AAG A-3'

#### B

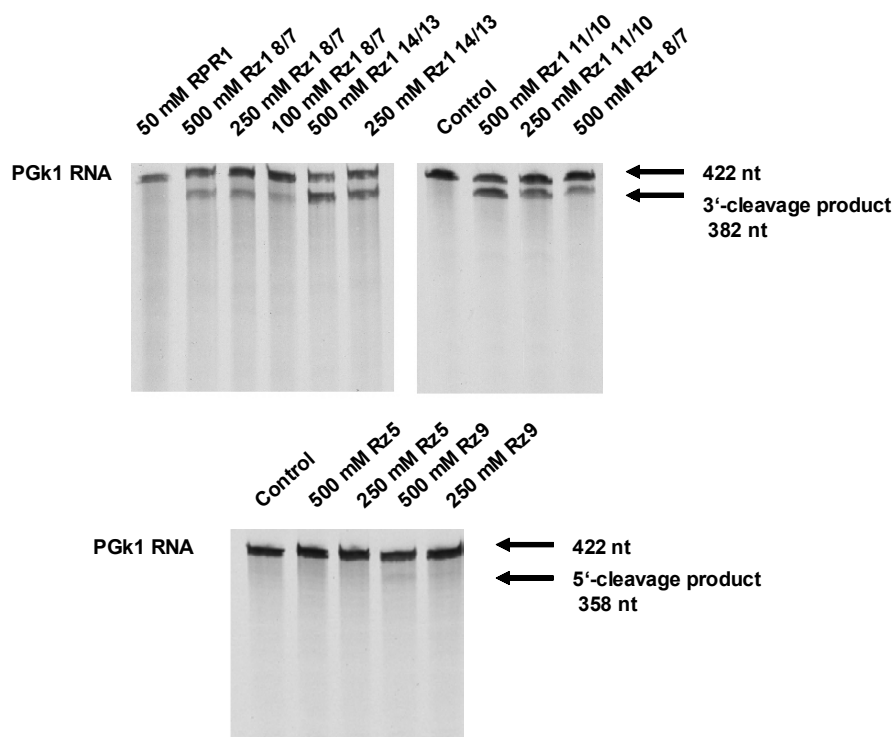


Figure 16: Cleavage activity detection. A. DNA sequence of both strands (w and c) of the two cloned trans-acting ribozyme genes designed with longer flanks. The constructs contain the conserved sequence of the hammerhead ribozyme (bold type), the complementary flanks of the targets and the *EcoRI* overhangs for cloning (underlined). B. Cleavage reaction of the *in vitro* *PGK1* small transcript internally labelled with [ $\alpha^{35}\text{S}$ ] UTP. The *PGK1* transcript was incubated with each of the individual ribozyme cassettes to cleave the selected sites. Cleavage reactions were started by adding magnesium and performed at 37°C for 60 min.

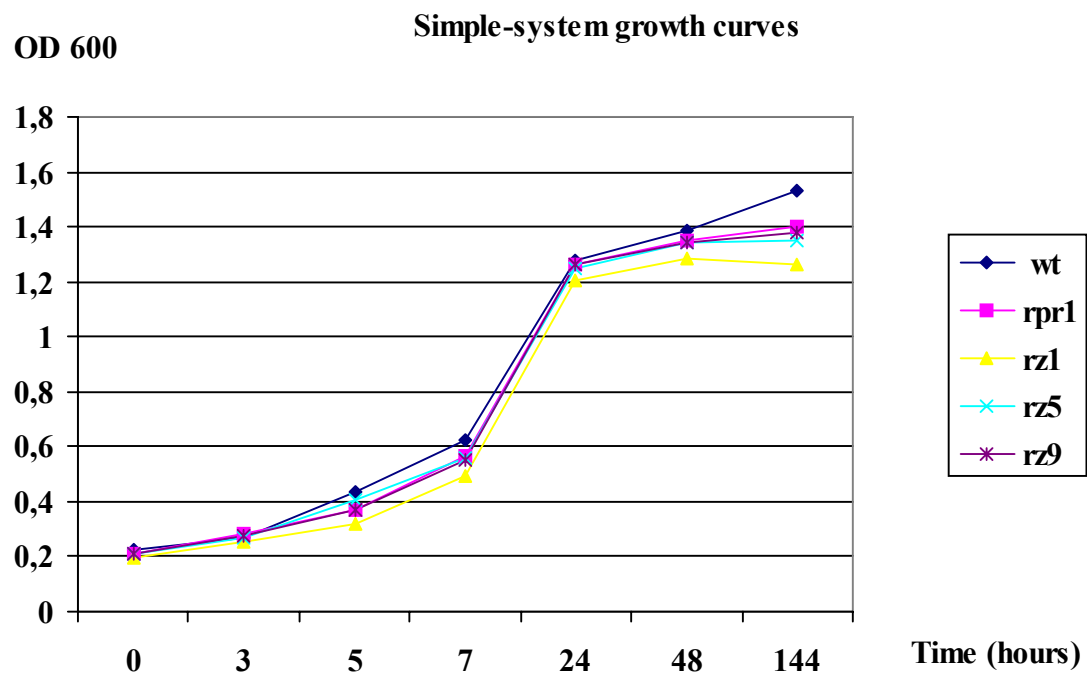
## 4.6.2 *In vivo* assays

### 4.6.2.1 Effects of ribozyme-delivery on growth rates

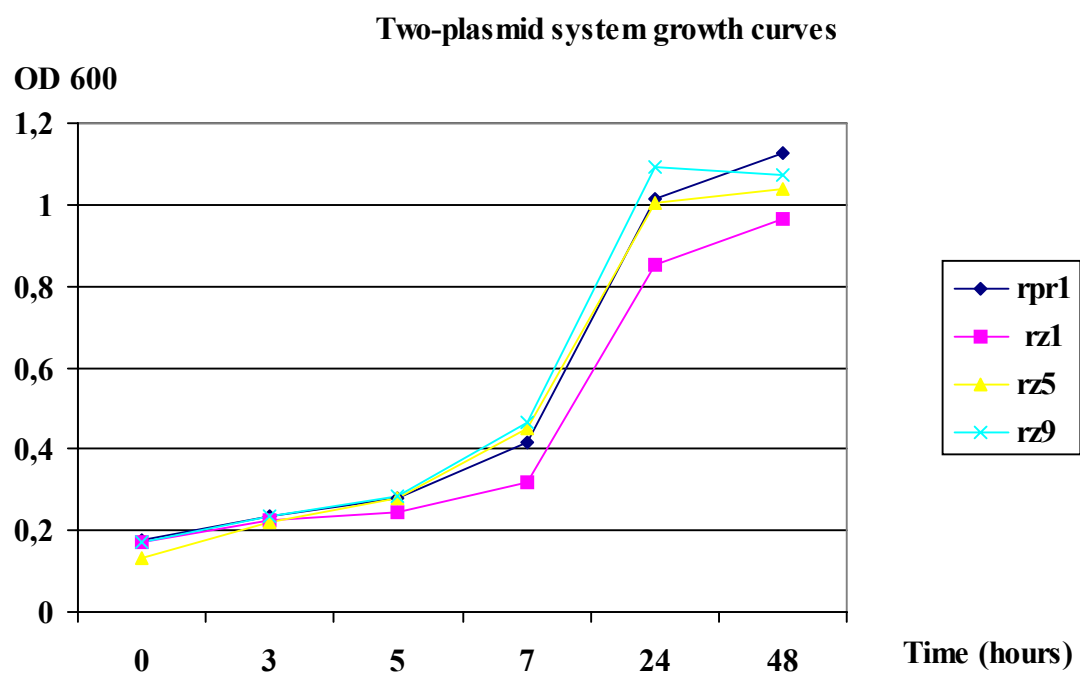
For an initial physiological characterization and to enable comparison of ribozymes directed to different *PGK1* RNA sites, the wild-type and  $\Delta pgk1$  strains were transformed following the described strategy. The growth rates were determined in shake-flask cultures on minimal media with glucose at 30°C in aerobic conditions. This determination should indicate the direct influence of the transformation procedure and the plasmid type used on growth.

In minimal medium, all the transformants have a slower growth than the wild-type strain. The growth rates of strains transformed with Rz1 in the simple- and two-plasmid system differ from the wild-type and the control strain transformed with plasmids without ribozyme, showing a slower growth than any of the other strains (compare fig. 17 A and 17 B). This result might be consistent with the fact that the phosphoglycerate kinase is involved in glucose metabolism and a low expression during growth on glucose containing media leads to a reduction of the specific growth rate. Nevertheless, the one-plasmid system transformant for Rz1 did not show any effect as neither did the Rz5 and Rz9 transformants. This is expected from the results obtained for both ribozymes Rz5 and Rz9 in the *in vitro* assays. Considering that the ribozyme expression cassette is cloned into a low-copy-number plasmid, the presumably low level of expression reached might lead to Rz1 activities being too low to be detected.

A.



B.



C.

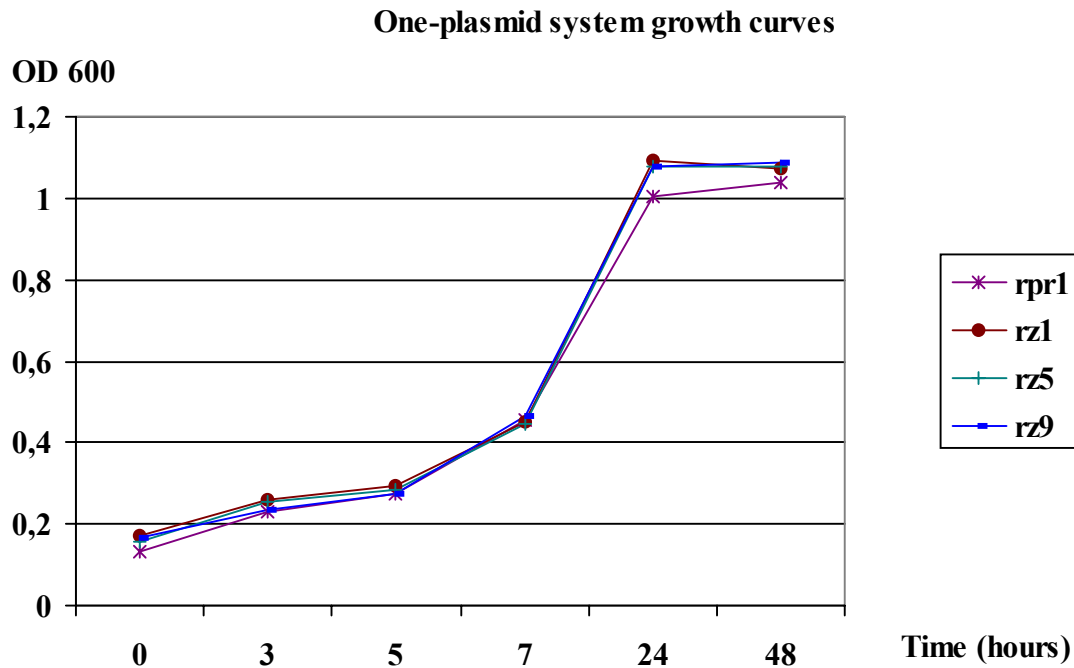


Figure 17: Growth rates of *S. cerevisiae* strains on minimal media containing glucose as the sole carbon source (YNB).

A. Growth curves for Simple system. Wt correspond to wt strain (CEY 1118-6B). Rpr1, rz1, rz5, and rz9 correspond to the strains derived after transformation of the wild-type strain with pIIIEx423 RPR without Rz, carrying Rz1 8/7, Rz5, and Rz 9, respectively.

B. Growth curves for Two-plasmid system transformants. Rpr1, rz1 8/7, rz5, and rz9 correspond to the  $\Delta pgk1$  strain transformed with pRS 416-PGK1 and pIIIEx423 RPR without Rz, carrying Rz1 8/7, Rz5, and RZ9, respectively.

C. Growth curves One-plasmid system. Therefore, rpr1, rz1, rz5, and rz9, correspond to  $\Delta pgk1$  strain transformed with pRS 416 PGK1 RPR1 without Rz, carrying Rz1 8/7, Rz5, and Rz9.

Shake-flask cultures were grown at 30°C in aerobic conditions.

#### 4.6.2.2 Analysis of *PGK1* gene expression and RNA cleavage activity of the transformants

To compare the level of *PGK1* transcripts in the transformants with the wild-type haploid strain, we analyzed *PGK1* RNA accumulation by northern analysis (Fig. 18). The transformants were grown on YEPD media and total RNA was isolated. When looking for cleavage activity, two probes were tested; one probe was directed to the *PGK1* ORF to look for the 3' cleavage products present (Fig. 18 top panel) and a second probe was developed for hybridization to the 5' untranslated region (5'UTR) (Fig. 18 middle panel). The analysis of transcription level and presence of 5' cleavage products was performed with a 611 bp fragment from the *Pgk1* coding region (orf probe) generated by PCR using primers *pgk1-6* and *pgk1-7*. For determining the presence of 5' cleavage products, oligonucleotide *pgk1-0* was labelled by polynucleotide kinase. The samples were balanced with *S. cerevisiae* actine. The actine probe was generated by PCR using primers *Actine-1a* and *Actine-1e*. The strains transformed with the plasmid carrying the *Rz1* with 8/7 flanks from each system were used in this experiment.

The analyses showed similar *PGK1* mRNA levels for all the transformants. Thus, it was not possible to verify the presence of any cleavage products for any of the tested transformants from this experiment.

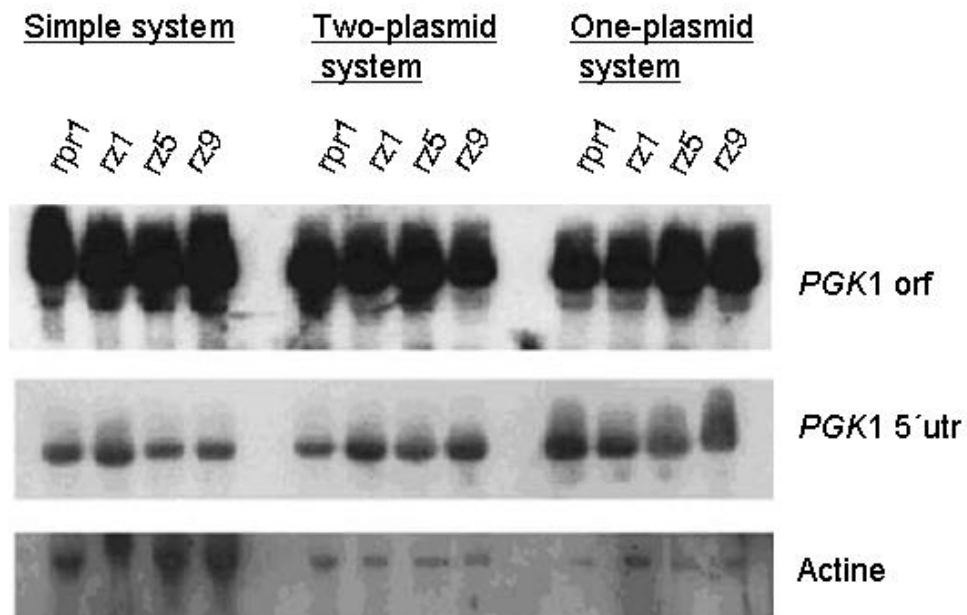


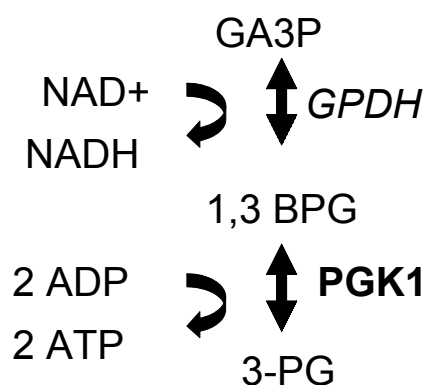
Figure 18: *PGK1* expression analyses by Northern blotting. The transformants and wt strains were grown on YEDP at 30 °C and total RNA was isolated, blotted and hybridized with the *PGK1* probes. The *S. cerevisiae* actine was used as internal control for balanced RNA loading.

### 4.6.2.3 P<sub>gk1</sub> activity assays

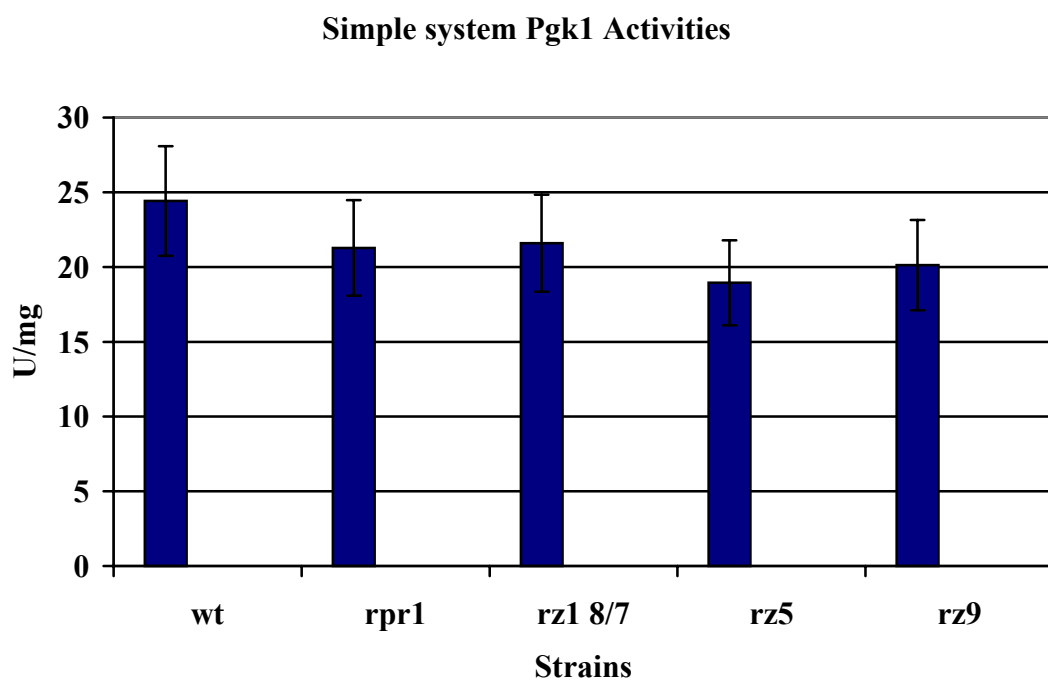
Effects of *trans*-cleavage ribozyme activity on the phosphoglycerate kinase were investigated by measuring enzyme activity in cell-free extracts of wild-type *S. cerevisiae*, CEY 1118-6B, and in transformants from simple, one-plasmid, and two-plasmid systems. The assay principle is based on the phosphoglycerate kinase reaction which is coupled to the previous enzyme in the glycolytic pathway, glyceraldehydes-3-phosphate dehydrogenase, resulting in the oxidation of 1 molecule of NADH for every molecule of 3-phosphoglycerate phosphorylated (see fig. 19 A). Thus, the decrease in the *PGK1* expression can be measured by a decrease in the absorbance of NADH at 340 nm. The cells were grown in minimal media containing glucose as the carbon source at 30°C. To ensure reproducible results, all cultures were grown to OD<sub>600</sub> = 0.5- 0.7. The activities were related to the total protein content.

Phosphoglycerate kinase activities in simple and one-plasmid-system strains transformed with plasmids carrying ribozymes were not significantly different from the activities in strains transformed with the control plasmid without ribozymes. The activities in Rz5 and Rz9 transformants strains of the two-plasmid system did not show any reduction. However, the Rz1 transformant strain for this system showed a lower activity in comparison to the control strain. The reduction of the P<sub>gk1</sub> activity might be a direct effect of the Rz1 catalytic activity on the *PGK1* expression (Fig. 19 D).

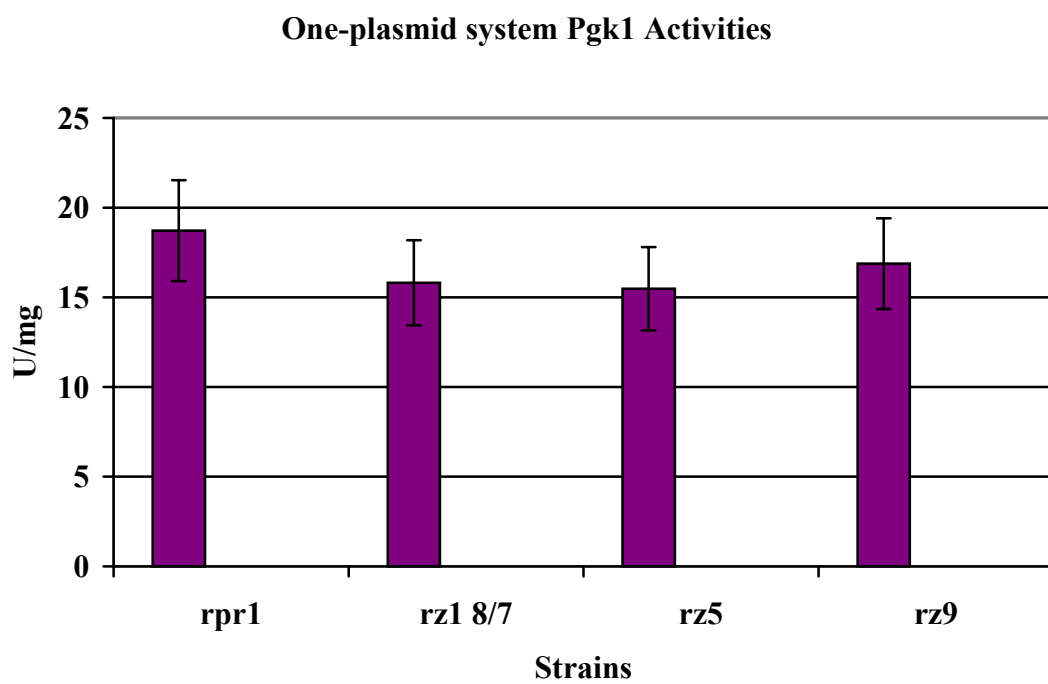
#### A. P<sub>gk1</sub> activity assay



B.



C.





D.

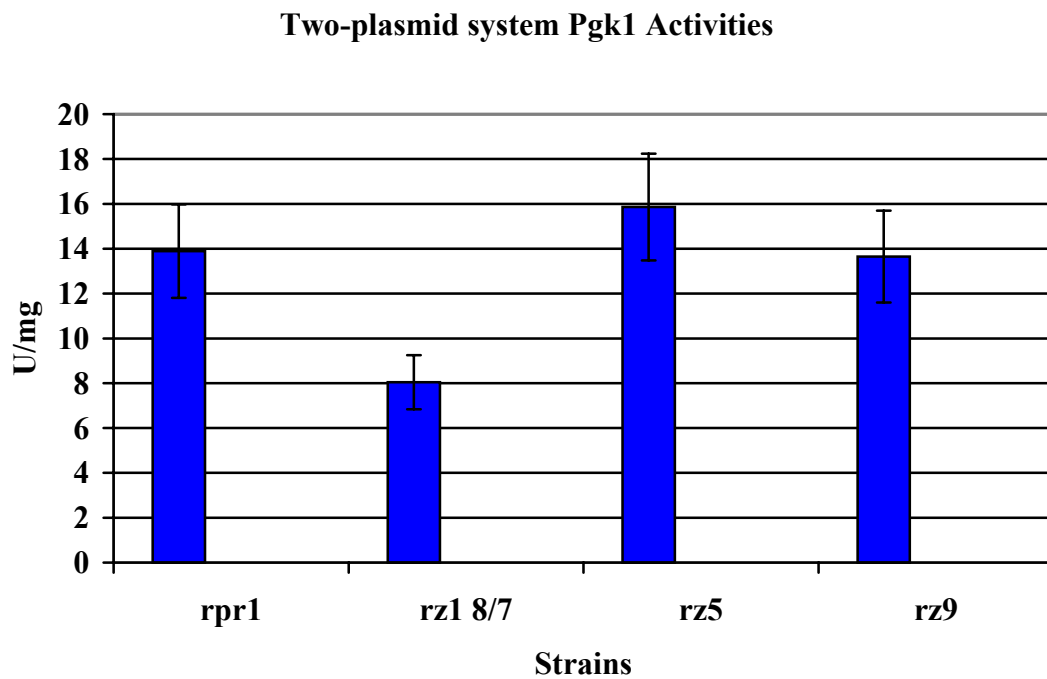


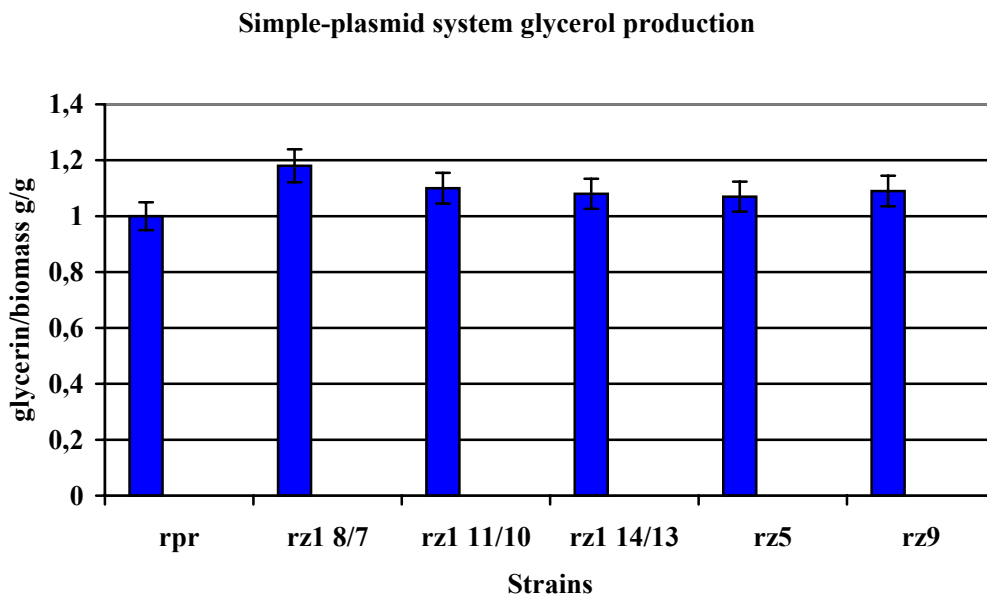
Figure 19: Analyses of the P<sub>gk1</sub> activity. A. Schematic representation of the glycolytic pathway part used to determine the P<sub>gk1</sub> activity. B, C, D. Specific phosphoglycerate kinase activities of transformant strains. For enzyme activity assays, free extracts were obtained from log phase cells grown on minimal medium (YNB).

#### 4.6.2.4 Effects of ribozymes on glycerol production

From the activity assays, it was not possible to clearly determine to what extent the *PGK1* expression was influenced by *trans*-acting ribozyme when measuring indirectly the enzyme activity. Therefore, it was decided to analyze the effect of the *PGK1* expression on glycerol synthesis, which is formed as a by-product when *S. cerevisiae* ferments sugar to ethanol. If the *PGK1* expression is reduced, this should lead to an increase of the glycerol-3-phosphate production. To carry out this analysis, we determined the concentration of glycerol secreted into the media in relation to biomass for each strain after growth under anaerobic conditions in minimal medium. The measuring of glycerol in anaerobic conditions avoids the consumption of this metabolite as carbon source in the stationary phase.

The results obtained from the simple system showed, as it was expected that Rz5 (as inactive ribozyme control) and Rz9 did not exhibit any influence on the glycerol production. An increment on the glycerol yield in the Rz1 transformed strain was detected. However this increment is not relevant for strains transformed with Rz1 designed with longer flanks. Thus the level of glycerol production was similar to the control strain transformed without ribozymes (Fig. 20 A). These results are consistent with approaches reported by Lieber and Strauss. They observed that despite good *in vitro* activity, ribozymes designed with longer flanks did not show the expected *in vivo* activity (Lieber & Strauss, 1995). For this reason, only the RZ1 with 8/7 flanks transformants were analyzed in the one-plasmid and two-plasmid systems. Comparing the glycerol production for the different systems transformed with Rz1, an increment was observed with the two-plasmid system but no effect could be detected for the one-plasmid system (Fig. 20 B). The controls used in these systems produced less amounts of glycerol than the wild-type strain. This could indicate the influence on the glycolytic pathway caused by transformation with this kind of plasmid and/or the promoter types used.

A.



B.

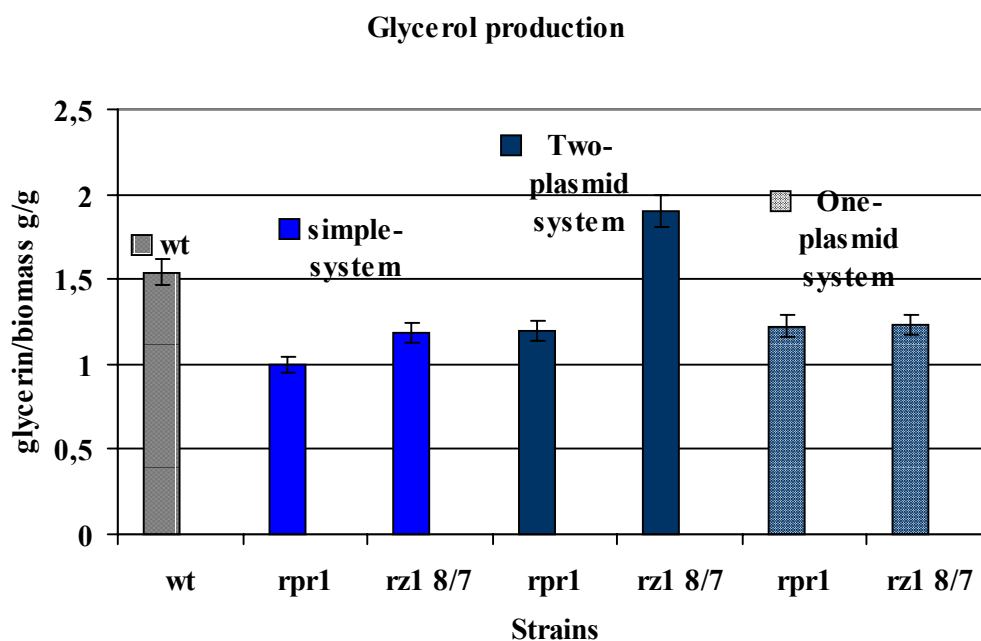
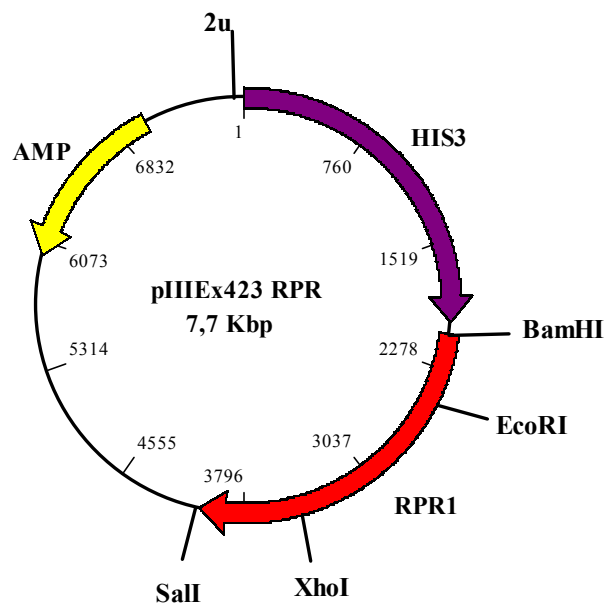


Figure 20: Glycerol amounts in transformed strains after anaerobic growth in minimal medium. Glycerol yields were expressed in relation to biomass (as dry weight). The strains were grown under anaerobic conditions on minimal medium with glucose for 24h (starting up  $OD_{600} = 0.1-0.15$ ), to the early stationary phase, and collected for glycerol and dry weight analysis. A. Comparison of glycerol production in Simple system transformants and the influence of longer flanks. B. Glycerol production from Rz1 8/7 transformants in all three systems.

## 4.7 Ribozyme expression

Based on the data presented previously (see chapter 4.6.2), it is important to know whether or not the ribozyme cassette is expressed at the expected level for every system. The simple and two-plasmid system must have a high ribozyme expression, because the pIIIEx423 RPR vector is a derivative of a high-copy-number plasmid including the *RPR1* promoter which has a high transcription rate (Fig. 21 A). Besides, the one-plasmid system should have less transcript accumulation since pRS416 is a low copy plasmid (one or two copies per cell) (see appendix). Because of this, the ribozyme expression was analyzed by northern blot. The probe was generated by PCR using the *rpr1* ter and *rpr1* tsp primers for amplifying the sequence corresponding to the whole ribozyme cassette (See material and methods). The analyses confirmed a high transcript accumulation in the high-copy-number plasmid used for ribozyme expression, i.e. the simple and the two-plasmid system. As can be seen in fig. 21 B, cassettes carrying the ribozymes migrate slower on 1.2% agarose-formaldehyde gels than cassettes without ribozymes (see fig 21 B line *rpr1* in relation to *rz1*, *rz5*, and *rz9*). This confirms again, effective ribozyme insertions into the plasmids. The one-plasmid system however showed a very weak signal for ribozyme expression. This might be consistent with the absence of cleavage activity detected (Chapter 4.6.2.4) although the same nuclear localization of ribozymes and *PGK1* target gene is present in this system. Unexpectedly, a high ribozyme expression is observed for *Rz5* and *Rz9* inserted into high copy numbers plasmids. The data also support the previously obtained results, i.e. these *Rzs* are not catalytically active *in vitro* as well as *in vivo* in spite of the high accumulation shown. Moreover, it was possible to detect the accumulation of the endogenous wild-type *RPR1* transcript in every transformant.

A:



B.

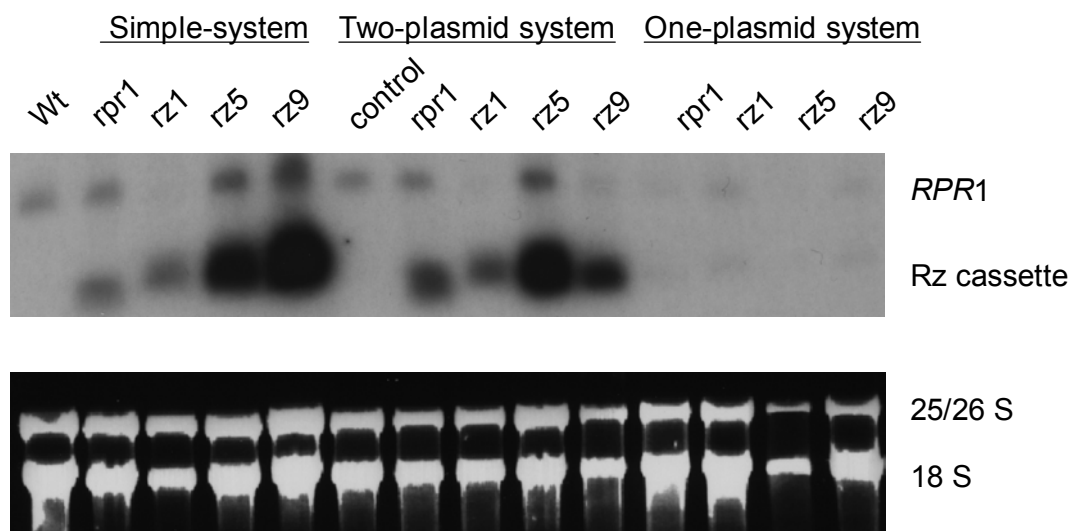


Figure 21: Ribozyme expression analysis. A. vector map of pIIIEx423 RPR used for ribozyme expression. B. Ribozyme expression of the different systems using Northern blot analysis. Total RNAs were isolated, blotted and hybridized with the *RPR1* probes. The *S. cerevisiae* 25/26 S and 18 S RNAs were used as internal control for equivalent RNA loading. The wild-type strain, a two-plasmid system control strain ( $\Delta pgk1$  transformed with pRS416 *PGK1* used as expression control) and the transformants were grown at 30 °C in minimal medium.

#### 4.8 Improving the co-localization of ribozyme and target RNA

In order to have a higher catalytic efficiency on the Rz1 transformed strains, we decided to take advantage of the properties of some messenger RNAs to localize within specific sub-cellular compartments. In eukaryotic cells, sub-cellular localization signals for several mRNAs are positioned in the 3'UTRs. Recently, it was shown for *S. cerevisiae* that the *ASH1* mRNA localizes into a discrete particle that is maintained at the bud tip and *cis*-acting sequences within the 3'untranslated region for this mRNA are recognized by specific target molecules that are required for its nuclear export and localization (Beach et al., 1999). Later on it was reported that the behavior of mRNAs in nuclear transport mutants is different. Under stress conditions some transcripts appear to fill the nucleus and others accumulate in the nucleolus when the export is blocked. Thus, these results show the existence of a link between mRNA processing and nuclear export (Brodsky & Silver, 2000). In human cells and *Drosophila* oocytes the use of catalytic RNAs to reduce the expression was successful when they were co-localized to the same intracellular compartment by using the discrete 3'UTR of the target RNA. These signals were fused to the targets and ribozymes, and it was possible to achieve a two- to three-fold enhancement of ribozyme function compared with non-co-localized transcript (Lee et al., 2001 and 1999). Based on these approaches a new ribozyme transcript was created. The terminator region of the *RPR1* was replaced by a sequence amplified from the pRS416 *PGK1* plasmid containing the 3'UTR sequence of *PGK1* described by Brodsky and Sylver (2000). The Rz1 8/7 was inserted into the pIIIEx423 RPR vector as described above. Primers 3'UTR stp (1) and 3'UTR ter (2) were used for amplifying the corresponding *PGK1* 3'UTR from the pRS416 *PGK1* plasmid. This fragment was digested with *EcoRI/XhoI* and ligated to the pIIIEx423 RPR Rz1 8/7 plasmid. The pIIIEx423 RPR Rz1 8/7+ *PGK1* 3'UTR was used for transforming the wild-type strain CEY 1118-6B (see fig. 22).

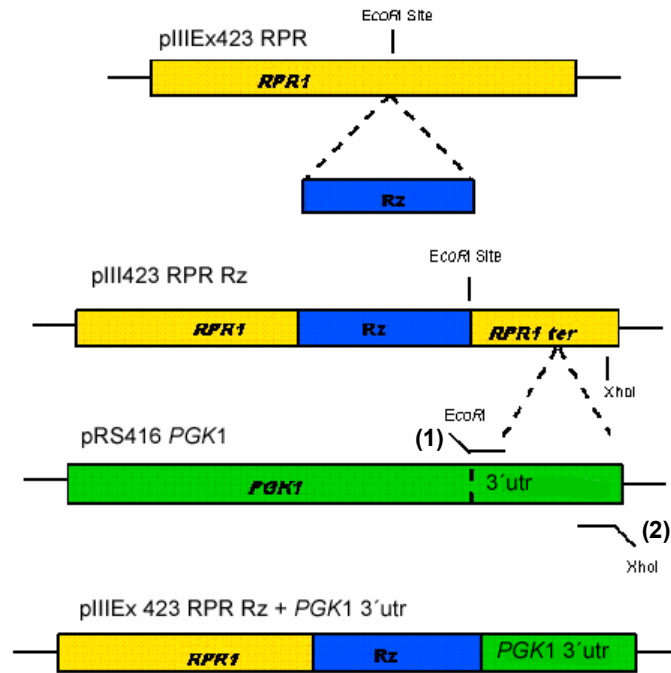


Figure 22: Schematic representation of the construction of the cassettes used for testing ribozyme target co-localization with the *PGK1* 3'UTR.

The Simple system was used to establish the influence on the glycerol production. This system was chosen due to its better growth-rate of the *Rz1* transformant compared to the two-plasmid system. Therefore, the wild-type strain was again transformed with this new plasmid. The effects of introducing the *PGK1* 3'UTR sequence were compared with the *Rz1* 8/7 transformant and the control strain (without ribozyme) by glycerol formation (Fig. 23). The introduction of the *PGK1* 3'UTR yield a 20% increased glycerol production in relation to the control strain without *Rz*. This enhancement on the glycerol production was observed in all of the six transformants analyzed. As an example, the value shown here belongs to the transformant strain number 2 (*pIIIEx423 RPR Rz1 + PGK1 3'UTR* (2)).

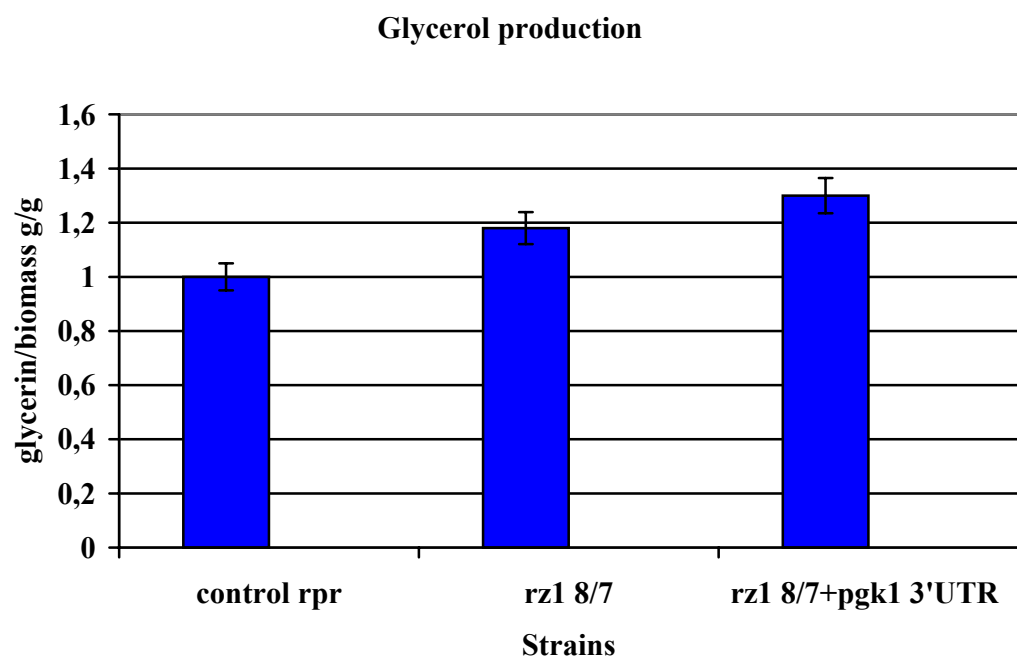


Figure 23: Glycerol production following introduction of the *PGK1* 3'UTR into the ribozyme expression cassettes.

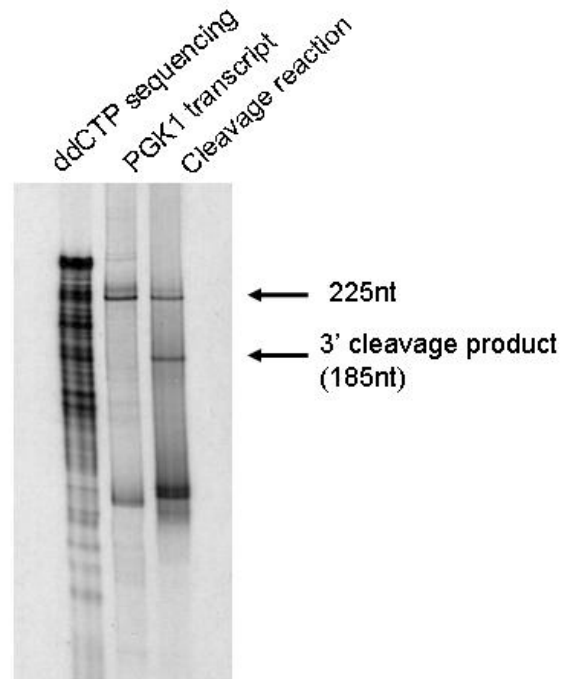


#### 4.9 Determining *in vivo* catalytic activity using primer extension

The experiments analyzed until now show an influence on the glycerol production in the simple and the two-plasmid system by insertion of Rz1 8/7 into the *RPR1* cassette. This accumulation could be due to the cleavage of the *PGK1* mRNA. However, so far no cleavage activity could be detected. The northern blot experiments did not show any presence of the expected cleavage products. Considering that Rz1 is cleaving only 40 nt downstream of the transcription start point, the resulting size of the 5'-cleavage product also makes the detection difficult. Thus, to determine the presence of a cleavage product, a primer extension was carried out. To test the primer extension conditions (reverse transcription, synthesis of cDNA) with the 3' cleavage product as template, samples from successful *in vitro* cleavage reaction were analyzed (Fig. 24 A). The cleavage product corresponding to the 3' end could be detected by primer extension. Therefore, in order to confirm cleavage activity *in vivo*, poly (A)<sup>+</sup> mRNA was isolated and subjected to reverse transcription (Fig. 24 B). The Rpr1, rz1 8/7, rz1 14/13, and rz1+ 3'UTR lines, correspond to the reverse transcription reactions from wild-type strain transformed with pIIIEx423 RPR without Rz, with Rz1 8/7, Rz1 14/13, and Rz1 8/7 + *PGK1* 3'UTR, respectively. All the samples were incubated for 4 hours with M-MuL V reverse transcriptase and primer pgk1-11 at 37°C, DNA fragments were internally labelled with [ $\alpha^{35}$ S] ATP.

Despite all the efforts made for having an amplification of the 3'cleavage product, modification of the test conditions, incubation time, binding time, and specific primers, it was not possible to detect the expected cleaved product.

A.



B.

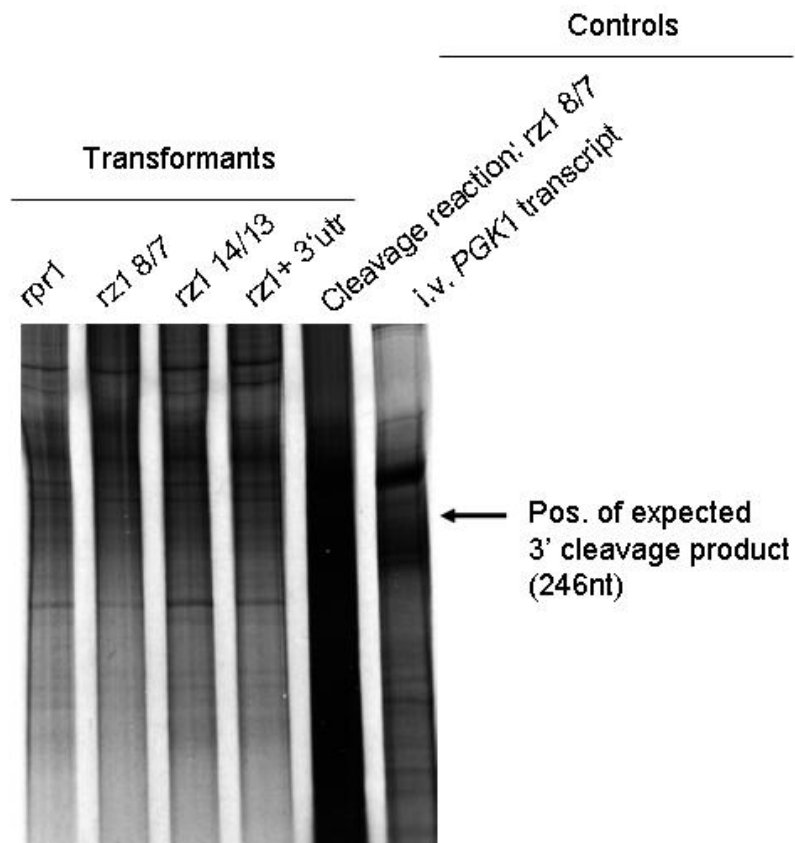


Figure 24: Primer extension analysis of the *in vitro* and *in vivo* ribozyme cleavage activity. A. Detection by primer extension of ribozyme mediated cleavage by RZ1 8/7 on the *in vitro* *PGK1* transcript fragment; *pgk1-8* was used as nested primer. B. poly (A)+ mRNA isolated from Simple system transformants were analyzed by primer extension.

#### 4.10 Regulated ribozyme delivery

While investigating whether the delivering of ribozymes can be regulated, the *CUP1* promoter was tested to transcribe hammerhead ribozymes. This analysis was carried out within the framework of a diploma thesis. The pYEX-BX, which has the *CUP1* promoter, was used to clone ribozymes-encoding sequence into the *EcoRI* site. The *RPR1* carrying the Rz cassettes was also cloned into the *BamHI/PstI* of pYEX-BX restriction sites for comparing the catalysis by delivering ribozymes inserted into the stable secondary structure of *RPR1* transcripts (see fig. 24). The *in vivo* cleavage activity was determined by glycerol formation by growing the transformant strains on different copper concentrations. These experiments did not show any improvement on the glycerol production, and the transformants showed a lower level of glycerol formation than the wild-type indicating that the high copper concentration was to same extent toxic for *S. cerevisiae* (for more details please refer to the diploma thesis of Nicole Abdallah “Expression of *trans*-acting ribozymes in *Saccharomyces cerevisiae* under the control of the *CUP1* promoter, TU-Berlin 2003”).

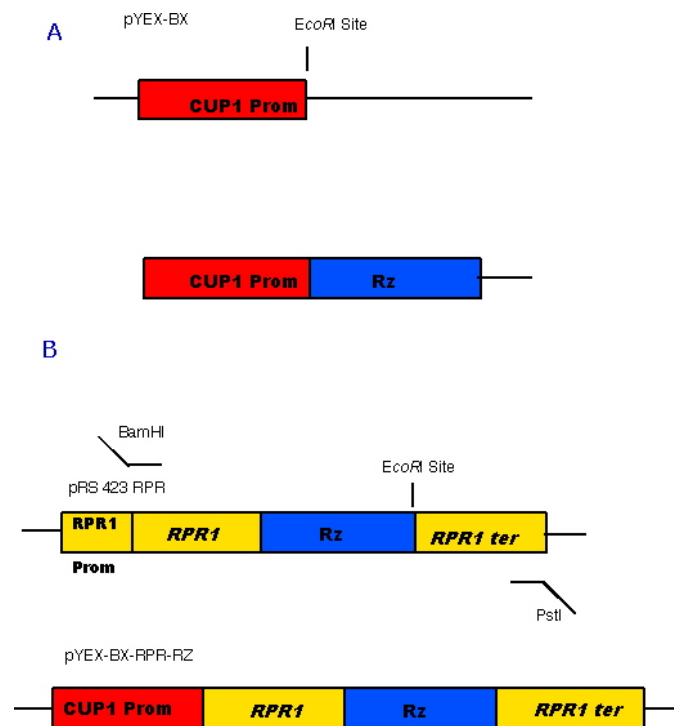


Figure 25: Schematic representation for the construction of regulated expression vectors. A. Design of pYEX-BX-RZ plasmid. B. Design of pYEX-BX RPR1 ribozymes plasmids.

## 5 Discussion

### 5.1 Selection of sites for ribozyme design

The ribozyme cleavage activity was tested using *in vitro* and *in vivo* standard methods. The *in vitro* assays revealed that Rz1 and Rz5 had the expected cleavage activities (Chapter 4.6.6.1). Hence, the level of accuracy of the computer algorithms used for secondary structure predictions is questionable and additionally they do not predict higher order structure.

The analysis of *in vitro* experiments to predict *in vivo* cleavage activity is limited. Many factors inside the cell affect the cleavage reaction. Low free  $Mg^{+2}$  concentrations, stability and compartmentalization of ribozymes must be considered, as well as substrate RNA conformation and RNA binding proteins. The mRNAs are associated with heterogeneous nuclear ribonucleoproteins in the nucleus. When transport to cytoplasm takes place they are replaced by cytoplasmic ribonucleoproteins. All of these proteins can hamper or have an influence on the RNA folding and thus avoid the access of ribozymes to the targets.

The *in vitro* activity does not guarantee efficient *in vivo* activity, although the relative efficacy *in vivo* can be expected to correlate with the relative efficacy *in vitro* (Birikh et al, 1997).

It was confirmed that ribozymes designed at the 5'-end had much more efficacy. Rz9 located at 318 nt of the ORF the *in vitro* activity was almost undetectable and did not have *in vivo* activity. On the contrary, Rz1 was designed for cleaving at the start codon site which was previously successfully reported for reducing the *ADE1* expression in yeast. This sequence is located in a region which is accessible and therefore effective for the designing of *trans*-acting hammerhead ribozymes (Ferbeyre, et al, 1995). The 5'-end was also a good target for hammerhead ribozymes to suppress telomerase activity in mammalian cells. A ribozyme targeting 13 nucleotides downstream from the 5'-end of hTERT, a catalytic subunit of human

telomerase, exhibited the strongest telomerase-inhibitory activity. The future trial is the application of this hammerhead ribozyme as a potential anti-cancer agent which indicates the confidence in this design (Yokoyama et al., 2000).

The sequence analyses revealed that all the ribozyme genes were inserted at the right position into the ribozyme expression cassette in pIIIEx423 RPR plasmids. Therefore, ribozyme sequences obtained for Rz1 8/7, Rz1 11/10, Rz1 14/13, and Rz9 had the expected sequences corresponding to the chemically synthesized oligonucleotides created for this purpose (see appendix). Moreover, the *RPR1* terminator region was switched correctly by the *PGK1* untranslated region in pIIIEx423 RPR Rz1 8/7.

Unfortunately, the sequence analysis of Rz5 revealed a punctual deletion. Hereby a base deletion was observed corresponding to G at the catalytic core sequence (see Fig. A 8): 5' GTG AG(G) ACG AAA 3' (Fig. 27). However, whether this change had an influence on the absence of catalytic activity reported here is unknown. This base was a G placed at stem II and does not belong to the two stretches of highly conserved sequences reported previously by Haselhoff and Gerlach (1988) 5'-CUGANGA and 5'GAAG, respectively. The length of the stem II has a larger influence on ribozyme activity than the nucleotide loop that terminates the stem II. Stems shorter than two base pairs are less active than those with two or more bases pairs. However, some ribozymes designed with shorter stem II which could cleave with almost full activity have been reported. These ribozymes could also cleave long RNA transcripts faster than wild-type ribozymes (Birikh et al, 1997, McCall et al., 2000). Nevertheless, the cleavage reaction carried out with Rz5 revealed that this ribozyme was inactive under any conditions.

With respect to the asymmetrical design chosen, the catalytic activities obtained in this work confirm the fact that for single turnover, the length of the arms is important for an efficient catalytic *in vitro* activity. In this experiment, high concentrations of ribozymes were

used, so that all the substrate molecules should be in a complex with the ribozymes. *In vitro*, the ribozyme designed with 13 and 14 bp flanks respectively, was the most active one. However, *in vivo* this ribozyme did not show the expected cleavage activity that is consistent with previous results obtained by Lieber and Strauss. They conclude that *in vivo* the most active ribozyme is a molecule with a 7 and an 8 bp helix (Lieber & Strauss, 1995). *In vivo*, the dissociation rate must be considered when multiple turnovers are required, in order to cleave most of the target molecules. The rate of dissociation of cleavage products is expected to consistently decrease with increasing length arms (McCall et al, 2000; Ferbeyre et al., 1996).

## 5.2 Use of pIIIEx423 RPR for ribozyme delivery and its influence on the metabolism

The plasmids constructed to transform the yeast for ribozyme delivery have a direct influence on the metabolism. In the *in vivo* assays, measuring the effects of the ribozyme on the growth rates and glycerol production (chapters 4.6.2.1 and 4.6.2.4), a comparison of the transformants with the wild-type strain revealed that the transformants have a slower growth and slower glycerol production than the untransformed strain. This observation has been reported previously. In recombinant gene expression, the possibilities to introduce a non-specific "metabolic burden" negatively affecting the growth have been described in numerous organisms. In yeast, reductions of the specific growth rate, biomass, respiratory capacity, and stability have been observed along with a decrease in the glycolytic flux and an increase in the maintenance energy requirement. This effect increases with the production levels, either due to the plasmid copy number amplification or an increase in the strength of the recombinant promoter. The effect of the cloned expression may be associated with either energetic cost of extra protein synthesis or the competitive effect. The dilution of native proteins was also suggested as a major mechanism causing a decrease in the flux through the glycolysis and in the maximum specific growth rate. The foreign protein synthesis during plasmid replication, toxicity of recombinant proteins and the negative consequences of small amounts of read through transcripts may also play an important role. In multi-copy plasmid transformed strains, factors such as the quantities or activities of the transcription and translation initiation factors, enzymes essential for expression, the amount of ribosomes, ribosomal activity, availability of biosynthetic precursors and metabolic energy needed for gene expression plus protein synthesis, may be the bottleneck for efficient gene expression (Goergens et al., 2001; Van der Aar et al., 1992).

It has been reported that the transformation with a gene which is already contained in the host, is not a selective advantage and may place a "metabolic burden" on the transformed strain inducing a low growth rate and poor mass yields (Ayub et al., 1992). pIIEx423 RPR used for ribozyme expression has a truncated copy of the *RPR1* gene, its wild-type gene is also found on the host used for transformation. Thus, the *RPR1* gene used as the cassette for ribozyme delivery could indeed cause slow growth of the transformants.

Moreover, in budding yeast actively transcribed pol III genes can negatively regulate adjacent RNA polymerase II (pol II)-transcribed promoters. This silencing was observed by sub-nuclear localization of the tRNAs. The association of early tRNAs to the nucleolus had a negative influence on the *HIS4* expression when this promoter was cloned adjacent to the *HIS4* gene in a (ars6/cen4) copy plasmid. The proximity to pol III transcription units might be used as a regulatory strategy in eukaryotes, the pol II transcription units near tRNA genes is non-random and the proximity affects the pol II units (Kendall et al., 2000).

Taken together these observations it is likely that the use of high-copy-number plasmids designed for expressing a high level of ribozymes in order to suppress the expression of a glycolytic gene negatively affects the glucose metabolism.

Despite the influence of pIIEx423 RPR on the metabolism, the catalytic function of the ribozymes seems not to be affected by the vector. The cleavage activity could even be determined by an increment of glycerol production in Rz1 transformants. Moreover, the *RPR1* cassette was successful in expressing high levels of ribozymes. The northern-blot analyses demonstrated the high ribozyme transcript accumulation reached in the transformants (chapter 4.7). Furthermore, the secondary structure of the *RPR1* leader did not interfere with the *in vivo* and *in vitro* cleavage-activity of the ribozymes. The *in vitro* cleavage-activity analyses revealed that the ribozymes expressed into the *RPR1* secondary structure were able to bind and cleave the *PGK1* target efficiently (chapter 4.6.11). *In vivo* analyses also demonstrated



that strains transformed with Rz1 expressing-plasmids, accumulated greater glycerol than the controls (chapter 4.6.2.4) which confirms the use of the *RPR1* leader as successful cassette for ribozyme expression.

### **5.3 High interaction of target and ribozymes (one-plasmid system)**

Despite the close location of the ribozymes and the target *PGK1* genes when using the pRS416 *PGK1 RPR1*, the ribozyme activity was not effective in the one-plasmid system. The activity assays and glycerol-production determination did not show any effects caused by ribozyme activity. When compared to the simple-plasmid system and the two-plasmid system this could be a result of the low level of ribozyme expression obtained. Northern-blot analyses confirmed a low accumulation of ribozymes transcripts in these strains (See chapter 4.7). Thus, the amount of ribozyme molecules might be not sufficient to cleave the *PGK1* transcripts in order to get any influence on the protein and glycerol level.

However, another factor that could be involved is the different polymerase machineries used for each gene expression: pol II for *PGK1* and pol III for the ribozyme. It has been documented that the RNA polymerase II transcription process is located in specialized places. The sub-nuclear location of the transcription machinery in eukaryotic cells was investigated by computer assisted-microscopy. These results show that RNA polymerase II transcription takes place at discrete sites scattered throughout the nucleoplasm and that these sites are also the locations of pre-mRNA processing. The active polymerases appear to be grouped into clusters at each transcription site, and certain sub-nuclear domains appear specialized for the expression or silencing of particular genes with a dynamic arrangement of transcription in the nucleus (Szentirmai & Sawadogo, 2000). Therefore, when an event takes place such as the transcription itself, it is possible that the organization of the whole nucleus makes the

expected ribozyme-target interaction unsuccessful in the one-plasmid system. The spatial organization important for gene-expression involves a different distribution of the transcripts.

Moreover, it has been described that tRNA processing is located in the nucleolus alongside ribosomal biogenesis. The RNase P which cleaves the 5' termini of pre-tRNAs, and pre-tRNAs were accumulated at this place, suggesting that the biogenesis of at least some tRNAs begins with the transcription at the nucleolus or nascent transcripts are transported to the nucleolus for being processed (Bertrand et al., 1998). Therefore, it is possible that ribozymes which are inserted into an RNase P RNA leader and the *PGK1* transcripts are spatially separated both during and after transcription. This spatial distribution did not have any influence on the other tested systems simple and two-plasmid system, since the high ribozyme expression obtained might be feasible to influence the glycerol yield.

#### **5.4 High degree of compartmentalization (two-plasmid system)**

The effects observed for the two-plasmid system in comparison with the simple system, did not show major differences despite the slower rate of growth reached in the two-plasmid system than in simple system Rz1 transformants (Chapter 4.6.2). Such an approach could indicate a greater effect on the glycolysis due to a greater reduction of the *PGK1* expression which would directly affect the growth in glucose.

The two-plasmid system has a *PGK1* copy cloned into pRS416 which is a low-copy-number plasmid designed to have an episomal replication. In the simple system, the *PGK1* gene is located at the wild-type locus. Therefore, the nuclear co-localization of the ribozyme and the target gene seems to be less important in comparison to the messenger co-localization and high level of ribozyme expression.

## 5.5 Enhancement on the glycerol production by ribozyme co-localization signals

A higher ribozyme/target interaction could be possible when the 3' UTR of the *PGK1* was used as terminator in the *RPR1* cassettes. This could lead to a cytoplasmic accumulation of ribozymes. The level of glycerol reached in Rz1 8/7 + *PGK1* 3' UTR transformants was greater than in the strain transformed with Rz1 8/7 + *RPR1* terminator sequence (See chapter 4.8). The co-localization of ribozymes and their target RNAs is the major determinant of high level activity of ribozymes *in vivo*. The transport, anchoring and translation regulation of localized transcript are governed by proteins that form large ribonucleic complexes with the mRNAs. Messenger RNA molecules are exported from nuclei as ribonucleoprotein particles. Many components which play a crucial role in poly (A)<sup>+</sup> RNA export have been characterized as nucleoporines, shuttling transport factors, helicases and exonucleases (Hurt et al., 2000). The process of specific localization is often mediated by *cis*-acting elements within the 3' untranslated region of the transcript. For instance, the 3' UTR of the *PGK1* gene directs the localization of hybrid GFP mRNAs to free cytoplasmic polysomes indicating the importance of the RNA structure in export events (Corral-Debrinski et al., 2000). The *RPR1* terminator region may direct the ribozymes to remain in the nucleus where the *RPR1* function is required. Thus, it could be demonstrated that the activity of the exported ribozyme was more efficient. Therefore, the export of ribozymes efficiently and specifically to cytoplasm has been used to obtain significantly higher cleavage activity of hammerhead ribozymes in mammalian cells (Kuwabara et al., 2001; Kato et al, 2001).

## 5.6 High target gene expression

*PGK1* is a highly expressed gene (Holland & Holland, 1978). The long half-life of its transcripts was one of the major characteristic evaluated as important in allowing the detection of intact cleavage products. However, the high level of expression for this gene could also affect the detection of cleavage activity. The range of reduction that must be reached in order to observe an effect in the glycerol production is not known. Perhaps, the multiple turnovers could not be satisfied with our ribozyme expression system despite high levels of transcription reached. Nevertheless, this system could be tested and more efficiently exploited when the cleavage activity is thought to suppress a gene with slower level of expression.

## 5.7 Differential expression of transcripts

In *Saccharomyces cerevisiae* the transition from logarithmic growth to the stationary phase is accompanied with a 50% decrease in total RNA and a decline in the ribosomes to less than 25% of the maximum amount (Sethy et al., 1995). The *PGK1* mRNAs levels decreased as cells entered the stationary phase (Dickson & Brown, 1998). Starvation involves a transition from active growth to growth arrest and involves changes in multiple environmental parameters over time such as cell density, pH, and the successive depletion of nutrients which contribute to the complex temporal pattern of gene expression (Gasch et al., 2000).

The RNAs transcribed by pol III are not limiting for cell growth under normal conditions but are available for cellular processes including protein secretion, synthesis and RNA processing. However, some reports have determined that the tRNA transcription is down regulated during transition from logarithmic to stationary phase growth (Sethy et al., 1995). Therefore, the fact of almost no effect determined on the *PGK1* activity may be explained due to the high expression of the *PGK1* gene in the early logarithmic phase used for this analysis. Likewise in the stationary phase the catalytic activity could be measured as glycerol production due to the decreased level of *PGK1* transcripts present and the maintenance of enough ribozyme transcripts under these conditions where glycerol is accumulated.

Furthermore, it must be considered that the partial influence on the *PGK1* activity could be also observed with a cleaved mRNA molecule which generates a truncated protein *in vivo*, which could contribute to the total protein activity. Considering that the Rz1 was designed to cleave at the start translation codon (See chapter 4.1), it is not possible that the cleavage activity mediated by Rz1 generates a truncated *PGK1* which is still active. A report in human cells has shown the substantial accumulation of a truncated protein of Apolipoprotein B mRNA caused by cleavage activity of hammerhead ribozymes; in this case, most of the truncated protein was degraded intracellularly (Wang et al., 1999).

The undetected ribozyme activity determined by P<sub>gk1</sub> activity assays could be an effect of the method principle itself. This method is based on the indirect measuring of the NADH oxidation coupled to the phosphoglycerate kinase reaction. The NADH consumption might also be caused by other enzymes present in the system what could leads to unspecific values.

## 5.8 PGK1 and glycolysis

The reduction of the *PGK1* to influence the glycolytic pathway in order to increase the glycerol production seems to depend on many factors. The level of glycerol accumulated in the transformants compared with the controls strains does not differ significantly (chapter 4.8). A 20% enhancement in the glycerol yield was reached in the transformants. Decreasing the *PGK1* mRNA level to influence the glycolytic flux may not cause the expected physiology of lower glycolysis rate. Some experiments showed that the glycolytic flux is conditionally correlated to the ATP concentration. A strong negative correlation between the glycolytic flux and the intracellular ATP content, i.e. a higher rate of glycolysis was not accompanied with an increased level of glycolytic enzymes (Larsson et al., 1997). On the other hand, the overexpression of individual glycolytic enzymes in yeast did not increase fermentation rates (Shaaff et al., 1989). These contrasting views of this metabolic pathway confirm the existence of many other factors that control the metabolic flux such as the ATP consumption and the cytosolic redox balance. Furthermore, the metabolic control analysis revealed that numerous metabolites as well as ATP/ADP and NADH/NAD<sup>+</sup> ratios affect glycerol formation. The metabolites concentrations vary in magnitude as does the relative proportion at different phase of growth. Thus, the parameters that affect the glycerol flux early in fermentation have not the same extent of influence later (Cronwright et al., 2002).

Moreover, under fermentative conditions the levels of pyruvate kinase and other glycolytic enzyme influence both the rate and direction of the carbon flux. The consequences of disturbing the transcriptional and post-transcriptional regulation of *PYK1*, *PFK1* and *PFK2* genes as well as the Pyk1 and Pfk1 levels were that under fermentative growth conditions, the gene regulation plays a minor role in the control of the glycolytic flux. Pyk1 had unexpected control effects. A decrease in Pyk1 caused an increase in the TCA cycling, i.e. an apparent

switch from fermentative to respiratory metabolism via an unknown mechanism (Pearce et al., 2001). Thereby, the understanding of the factors which control the *in vivo* metabolic flux is relatively limited.

## 5.9 No evidence for cleavage products

In RNA decay studies, it was observed that *PGK1* mRNAs are stable due to the sequence context of the *PGK1* translation start codon. The 3' UTR has no influence on the RNA decay. The regions around the start codon are sensitive to changes and this destabilization brought about a reduction on the translational efficiency (LaGrandeur & Parker, 1999). This report might be consistent with the fact that no 3'-cleavage product was found in Rz1 transformants by primer extension (chapter 4.9). The Rz1 was designed for cleaving the *PGK1* mRNA at a site including the start codon. Thus, the probability of detecting the 5'-cleavage product (about 40 nt) after isolation is low since it could be exposed to a rapid 5'-to-3' exonucleolytic degradation.

The *in vivo* assays revealed an enhancement in the glycerol production when Rz1 was used as catalytic RNA. However, this effect could be caused by an anti-sense activity without cleavage by the ribozyme. This might also explain the absence of the 3'-cleavage product detected by northern blot and primer extension assays (Chapters 4.6.2.2 and 4.9). Nevertheless, considering that the ribozyme was inserted into the *RPR1* leader, an antisense activity due to 15nt (8 and 7 nt for each helix) in relation to the whole expressed molecule (ca. 165 nt) is questionable. A cleavage reaction should take less time to act than an antisense binding in order to reduce the gene expression. The ribozyme and target secondary structures should interfere to capture the target for longer times in order to avoid the translation process.

The possible use of an inactive RZ1 form could help to determine the factor involved in the detected ribozyme activity.

In the northern blot assays, the absence of cleavage products and the similar RNA expression detected in the transformants and control strains might be an effect of the low resolution of the technique. The wild-type *PGK1* mRNA is only 40 nt longer than the cleaved RNA, thus this difference is difficult to be confirmed by this method.

This approach has also been reported in other systems where the hammerhead ribozymes do not significantly reduce the protein expression. A hammerhead ribozyme which self cleave a  $\beta$ -galactosidase reporter has been analyzed. In *E. coli* the *in vivo* efficiency of this ribozyme was 45-50% in spite of the good catalytic activity found *in vitro* with 70-80% efficiency. Moreover, northern blot analyzes were unable to detect cleavage products. The hammerhead ribozymes ability appeared also weak or nonexistent for the tested systems which also give an impression of the difficulties in detecting *in vivo* ribozyme activity (Drew et al., 1999).



## 5.10 Intracellular Ribozyme applications

In yeast, most of the positive advances have been carried out with hammerhead ribozymes acting in *cis* for studying yeast RNA processing *in vivo* and for optimization of *in vitro* transcription of yeast transcripts (Duevel et al., 2002; Fechter et al., 1998). However *in vivo cis*-acting activity has been related with suppression of gene expression by interfering with splice site selection or translation initiation and not *in vivo* cleavage of the transcripts (Castanotto et al., 1998, Yim et al., 2000).

Only a few cases of *in vivo* detectable cleavage products have been reported. Ferbeyre et al. (1996) have suggested that these negative results could be explained due to the fact that the yeast metabolism is very fast to observe a ribozyme-based cleavage activity; only when the cell-cycle was arrested, a hammerhead cleavage action was promoted. This factor could also be observed in the analysis of glycerol production. The measuring was carried out at the stationary phase where the cell-cycle is arrested. Hence, the influence on the *PGK1* expression was detected at the stationary phase but no clear evidence was found at logarithmic phase of growth.

In *S. cerevisiae*, *trans*-acting ribozymes were reported with 100% efficiency *in vivo* when localization signals were added to ribozymes (Samarzky, 1999). Many protein factors are involved in the intracellular processing and transport on mRNAs immediately after transcription. Such factors could inhibit the binding of ribozymes with the target in the nucleus and the transport of mRNA to the cytoplasm seems to be more rapid than the attack by nuclear ribozymes (Koseki et al., 1999). Therefore, the knowledge and new advances of RNA structure and its physical cellular localization as well as transport/export machinery, are important to ensure co-localization and like this to have access to the tools for creation of models for high efficient suppression mediated by ribozymes in yeast.

Interestingly, in a recent publication, Khvorova and colleagues (2003) could show that the minimal sequence conserved hammerhead-ribozyme motif is sufficient to support a cleavage at high  $Mg^{2+}$  concentrations but not at low  $Mg^{2+}$  concentrations characteristic of intracellular environments. The hammerhead ribozyme requires non-conserved sequence elements outside of the conserved catalytic core to allow intracellular cleavage activity. These elements should stabilize the hammerhead ribozyme in an active conformation via tertiary interactions. Hammerhead ribozymes stabilized by such interactions cleave efficiently at physiological  $Mg^{2+}$  concentrations and are functional *in vivo*. In this work, the enhancement of glycerol production by application of anti-sense hammerhead ribozymes was only 20%. The low efficiency achieved could also be a consequence of the low intracellular  $Mg^{2+}$  concentrations of yeast cells. The use of stabilized hammerhead ribozyme to achieve good efficiency in the *in vivo* cleavage activity could be also tested as a new tool to reduce gene expression in yeast.

The application of ribozyme in mammalian cells has been extensively tested. *Trans*-cleaving ribozymes have been used in a small number of patients with infectious diseases and cancer. The delivery of ribozymes to the patients has been either by gene therapy methods or by direct injection of a synthetic ribozyme. The huge progresses in gene therapy application has been carried out in individuals with the human immunodeficiency virus (HIV), where CD4<sup>+</sup> cells from the patient were transfected with retroviral vectors carrying anti HIV-ribozymes *ex vivo* and infused into the patient. Three synthetic ribozymes have been directed to target RNAs that are associated with induction or cancer progression; the ribozyme directed against the *flt-1* mRNA, which encodes the high affinity receptor for the angiogenic protein vascular endothelial factor (VEGF), has been evaluated in breast and colorectal cancer. The other two targets correspond to the human epidermal growth-factor receptor type 2 which is overexpressed in breast cancer and the hepatitis C virus (HCV), which is associated with liver

cirrhosis and hepatocellular carcinoma. Most of the critical factors found for an effective therapy are the ability to deliver ribozymes into the appropriate cells *in vivo*, as well as both level and duration of the target inhibition (Sullenger & Gilboa, 2002). Efficient ribozyme delivery, efficient high expression, co-localization of the ribozyme with the target, specificity of ribozyme for the desired mRNA, and an enhancement of the ribozyme-mediated substrate turnover are the obstacles which must be overcome for ribozymes to become generally useful surrogate genetic tools and realistic therapeutic agents (Castanotto et al., 2002).

Recently, in mammalian cells to improve the efficiency of ribozymes *in vivo* a novel ribozyme with the ability to access and cleave at the specific target site has been created through the combination of the hammerhead ribozymes with the unwinding activity of the endogenous RNA helicase eIF4AI. To connect the helicase to the ribozyme a poly(A) sequence was added to the 3' end of the ribozymes. This sequence is a naturally occurring RNA motif of the RNA helicase. Thus, targets on the mRNA previously inaccessible to cleavage were effective substrates for these ribozymes (Kawasaki & Taira, 2002). For yeast cells, this could also be a new approach for the generation of effective ribozymes using the helicase activity to enhance the cleavage efficiency *in vivo*.

## 6 Summary and future prospects

In this work, a novel strategy was developed to decrease the expression of the *PGK1* gene encoding the phosphoglycerate kinase of the glycolytic pathway by *trans*-acting hammerhead ribozymes. We selected and designed ribozymes for cleavage of the *PGK1*mRNA based on the prediction of its secondary structure. To deliver the ribozymes three different systems were tested. These systems required the creation of a *pgk1* knock-out strain and plasmid constructs expressing *PGK1*/Ribozyme to achieve a stable accumulation of ribozymes co-localizing with the target mRNA. The ribozymes were inserted into the *RPR1* cassette using the pIIIEx423 RPR plasmid to allow high ribozyme expression. RPR plasmids contain the intragenic polymerase III promoter from the *S. cerevisiae* RNase P RNA gene (*RPR1*). The fusion of this leader to RNAs leads to stable accumulation of these molecules. In order to analyze the ribozyme *trans*-cleavage activity and its effects on the polymerase II dependent expression of *PGK1*, different techniques to investigate the cleavage activity were applied (northern blot, primer extension, P<sub>gk1</sub> activity assay and glycerol production analysis).

The computer prediction supported by *in vitro* experiments is an initial step of the target selection. The ribozyme cleavage analyses confirmed the Rz site located at the start translation codon as accessible and efficient for the design of *trans*-acting hammerhead ribozymes. This site contains the consensus sequence AUGUC found in many yeast genes. Furthermore, the 3' untranslated region of the target gene, which contains *cis* sequences to specifically localize the transcript, is useful in ribozyme design. The fusion of the *PGK1* 3'untranslated region to the Ribozyme which is directed to the consensus sequence AUGUC lead to a better result of ribozyme activity in terms of glycerol production. Thus, its use in *trans*-ribozyme delivery has been newly confirmed. As a rule, a combination of both sequences can be feasible for ribozyme design. Likewise, the northern blot analyses confirmed the use of the *RPR1* leader as useful for high ribozyme expression. The secondary

structure of the *RPR1* leader did not interfere with the *in vivo* and *in vitro* cleavage activity of the ribozymes.

The understanding and knowledge of RNA metabolism seem to be an important issue for developing effective ribozyme design in yeast. The co-localization of ribozyme and target genes on the same plasmid does not guarantee cleavage activity when different transcription machineries play a role in their gene expression. The spatial distribution of polymerases II and III systems and the nuclear organization when transcription takes place, hampers an efficient interaction between target and ribozymes. The numerous proteins and factors binding the RNA, either in processing and trafficking, as well as the transport of ribozymes from nucleus to cytoplasm and the high level of expression are all important factors to be considered for designing more efficient ribozymes. Moreover, the use of high-copy-number episomal plasmids caused reduced yeast vitality that complicated the determination of the ribozyme effect.

Thus, to avoid this effect the future work should be focused on the creation of integrative vectors for delivery of the optimized ribozyme (RPR-cassette and 3' untranslated region). The use of more than one ribozyme-expression-cassette into integrative vectors could ensure a high expression level. Furthermore, it would be favorable to select a reporter target gene that allows direct determination of the expression level. The gene encoding the green fluorescence reporter-protein (GFP) should be useful as a target gene to test the ribozyme catalytic activity. Moreover, the *trans*-acting hammerhead ribozyme design might also consider the stabilization by sequence elements outside the conserved core to allow efficient cleavage *in vivo* (see also Khvorova et al., 2003).

## 7 Zusammenfassung und Ausblick

In der vorliegenden Arbeit wurde eine neue Strategie entwickelt, um die Expression des *PGK1* Gens, das für die Phosphoglycerat-Kinase der Glycolyse kodiert, mittels trans-agierenden Hammerhead Ribozymen zu verringern. Die Ribozyme wurden anhand der Computer vorausgesagten Sekundärstruktur von *PGK1*mRNA konzipiert und ausgewählt. Es wurden drei verschiedene Systeme getestet, um die Ribozyme an ihren Bestimmungsort zu bringen. Diese Systeme machten die Erstellung eines *pgk1* knock-out Stamms und die Entwicklung von *PGK1*/Ribozym-exprimierenden Plasmiden nötig, um eine stabile Akkumulation von Ribozymen und die Co-Lokalisation mit der Ziel mRNA zu erreichen. Um einen hohen Expressionslevel der Ribozyme zu gewährleisten, wurden die Ribozyme unter Verwendung des pIIIEx423 RPR Plasmids in dessen *RPR1* Kassette eingefügt. RPR Plasmide enthalten den intragenischen Polymerase III Promotor des *S. cerevisiae* RNase P RNA Gens (*RPR1*). Die Fusion dieser Sequenz mit Ribozym-Sequenzen führt zu einer stabilen Akkumulation der RNA-Moleküle. Um die Transspaltungs-Aktivität der Ribozyme und deren Effekt auf die Polymerase II abhängige Expression des *PGK1* Gens zu untersuchen, wurden verschiedene Techniken angewendet, die es erlauben, die Spaltungsaktivität zu messen (Northern Blot, Primer Extension, *Pgk1* Aktivitätsmessungen, Analyse der Glycerinproduktion).

Computergestützte Vorhersagen der Sekundärstruktur, die durch *in vitro* Experimente ergänzt wurden, sind ein erster Schritt bei der Auswahl von Ziel-RNAs. Spaltungs-Untersuchungen der Ribozyme bestätigten, dass die am Startcodon der Translation lokalisierte Sequenz als ein zugängliches und effizientes Ziel zur Entwicklung von trans-agierenden Hammerhead Ribozymen genutzt werden kann. Diese Sequenz ist häufig als Consensus Sequenz AUGUC am Beginn von Hefe-Genen zu finden. Des weiteren ist die 3' nicht-translatierte Region des Zielgens, die cis Sequenzen enthält, die zur spezifischen Lokalisation des Transkripts führen, nützlich in der Ribozymentwicklung. Die Fusion der 3' nicht-

translatierten Region des *PGK1* Gens mit dem Ribozym für den AUGUC Consensus führte zu einer erhöhten Glycerinproduktion, was auf eine verbesserte Spaltungsaktivität hindeutet. Der positive Effekt der 3' nicht-translatierten Region in der Lokalisation von trans-agierenden Ribozymen konnte somit bestätigt werden. In der Regel ist eine Kombination der beiden genannten Sequenzbereiche zum Ribozymdesign sinnvoll. Auch bestätigte die Analyse durch Northern Blots, dass die Verwendung der *RPR1* Sequenz zur erhöhten Expression von Ribozymen führt. Die Sekundärstruktur der *RPR1* Sequenz behinderte die *in vivo* und *in vitro* Spaltungsreaktion der Ribozyme nicht.

Das Verständnis und Wissen über den RNA Stoffwechsel sind eine wichtige Grundlage für die Entwicklung effektiv spaltender Ribozyme in Hefe. Die Co-Lokalisation von Ribozym- und Ziel Gen auf demselben Plasmid garantieren nicht eine hohe Spaltungsaktivität, wenn für die RNAs verschiedene Transkriptionssysteme verwendet werden. Die räumliche Verteilung der Polymerase II und III Systeme und die Organisation im Kern während der Transkription lassen eine effiziente Interaktion zwischen Ziel-Sequenz und Ribozym kaum zu. Zahlreiche Proteine und Faktoren, die in der Prozessierung und beim Transport an die RNA binden, wie auch der Transport von Ribozymen vom Kern zum Cytoplasma und ein hoher Expressionslevel sind wichtige Größen, die die Wirkung eines Ribozyms beeinflussen. Hierbei muss allerdings berücksichtigt werden, dass die Verwendung hochexprimierender, episomaler Vektoren zu einer Reduzierung der Vitalität der Hefe führen kann, die die Bestimmung der Ribozymwirkung erschwert.

Es wäre daher interessant, in weiterführenden Arbeiten optimierte Ribozyme (RPR-Kassette, 3' nicht-translatierte Region) in das Hefegenom zu integrieren, um die genannten Effekte zu vermeiden. Die Integration von mehr als einer Ribozymexpressionskassette könnte einen hohen Expressionslevel sichern. Darüber hinaus wäre die Auswahl eines Zielgens wünschenswert, dessen Expressionsreduktion einfacher meßbar ist. Das GFP Gen, welches für das „Green Flurescent Protein“ kodiert, könnte ein nützliches Ziel sein, um

Ribozymaktivität zu testen. Seit kurzem ist auch bekannt, dass die trans-agierenden Hammerhead Ribozyme durch Sequenzelemente außerhalb des konservierten Kerns stabilisiert werden können, was zu einer wesentlich besseren Spaltung *in vivo* führt (siehe Khvorova et al., 2003).



## 8 References

- Amarzguiou M & Prydz H (1998) Hammerhead ribozymes design and application. *Cell Mol. Life Sci.* 54: 1175-1202.
- Ayre BG, Koehler U, Goodman HM, Haseloff J (1999) Design of highly specific cytotoxins by using trans-splicing ribozymes. *Proc. Natl. Acad. Sci.* 96: 3507-3512.
- Ayub MAZ, Astolfi-Filho S, Mavituna F, Oliver SG (1992) Studies on plasmid stability, cell metabolism and superoxide dismutase production by P<sub>gk</sub><sup>-</sup> strains of *Saccharomyces cerevisiae*. *Appl. Microbiol. Biotechnol.* 37: 615-620.
- Arndt GM & Atkins D (2001) RNA Catalysis in Fungi. In: Eckstein F and Lilley DMJ (eds) *Nucleic Acids and Molecular Biology*. Springer-Verlag. Berlin. Heidelberg. 10: pp 343-366.
- Atkins D & Gerlach WL (1994) Artificial Ribozyme and Antisense Gene Expression in *Saccharomyces cerevisiae*. *Antisense Res. Dev.* 4: 109-117.
- Beach DL, Salmon ED, Bloom K (1999) Localization and anchoring of mRNA in budding yeast. *Curr. Biol.* 9(11): 569-578.
- Bertrand E, Houser- Scott F, Kendall A, Singer RH, Engelke DR (1998) Nucleolar localization of early tRNA processing. *Genes & Dev.* 12: 2463-2468.
- Birikh KR, Heaton PA, Eckstein (1997) The structure, function and application of the hammerhead ribozyme. *Eur. J. Biochem.* 245: 1-16.
- Blancafot P, Ferbeyre G, Sariol C, Cedergren R (1997) *PoII*-driven integrative expression vectors for yeast. *J. Biotechnol.* 56: 41-47.
- Blount KF & Uhlenbeck OC (2002) The hammerhead ribozyme. *Biochem. Soc. Trans.* 30(6):1119-1122.
- Brodsky AS & Silver PA (2000) Pre-mRNA processing factors are required for nuclear export. *RNA* 6(12): 1737-1749.
- Castanotto D, Rossi JJ, Deshler JO (1992) Biological and Functional Aspects of Catalytic RNAs. *Critical Rev. in Eukaryotic Gene Expression* 2(4): 331-357.
- Castanotto D, Li H, Chow W, Rossi JJ, Deshler JO (1998) Structural Similarities Between Hammerhead Ribozymes and the Spliceosomal RNAs Could Be Responsible for Lack of Ribozyme Cleavage in Yeast. *Antisense & Nucleic Acid Drug Dev.* 8: 1-13.
- Castanotto D, Chow WA, Li H, Rossi JJ (1998) Unusual Interactions Between Cleavage Products of a Cis-Cleaving Hammerhead Ribozyme. *Antisense & Nucleic Acid Drug Dev.* 8: 499-506.
- Castanotto D, Scherr M, Rossi JJ (1999) Intracellular Expression and Function of Antisense Catalytic RNAs. In Phillips MI (ed) *Methods in Enzymology*. Academic Press Inc, New York. 313:pp. 401-420.

Castanotto D, Li JR, Michienzi A, Langlois MA, Lee NS, Puymirat J, Rossi JJ (2002) Intracellular ribozymes applications. *Biochem. Soc. Trans.* 30(6): 1140-1144.

Chambers A, Tsang JSH, Stanway C, Kingsman AJ, Kingsman SM (1989) Transcriptional Control of the *Saccharomyces cerevisiae* *PGK1* Gene by *RAP1*. *Mol. Cell. Biol.* 9(12): 5516-5524.

Ciriacy M & Breitenbach I (1979) Physiological Effects of seven Different Blocks in Glycolysis in *Saccharomyces cerevisiae*. *J. Bacteriol.* 139(1): 152-160.

Corral-Debrinski M, Blugeon C, Jacq C (2000) In Yeast the 3' Untranslated Region or the Presequence Is Required for the Exclusive Localization of Its mRNA to the Vicinity of Mitochondria. *Mol. Cell. Biol.* 20(21): 7881-7892.

Cronwright GR, Rohwer JM, Prior BA (2002) Metabolic Control of Glycerol Synthesis in *Saccharomyces cerevisiae*. *App. Env. Microbiol.* 68(9): 4448-4456.

Curtis EA & Bartel DP (2001) The hammerhead cleavage reaction in monovalent cations. *RNA* 7(4): 546-552.

Dickson LM & Brown JP (1998) mRNA translation in yeast during entry into stationary phase. *Mol. Gen. Genet.* 259: 282-293.

Donahue CP & Fedor M (1997) Kinetics of hairpin ribozymes cleavage in yeast. *RNA* 3: 961-973.

Doherty EA & Doudna JA (2000) Ribozyme Structures and Mechanisms. *Annu. Rev. Biochem.* 69: 597-615.

Drew HR, Lewy D, Conaty J, Rand KN, Hendry P, Lockett T (1999) RNA hairpin loops repress protein synthesis more strongly than hammerhead ribozymes. *Eur. J. Biochem.* 266: 260-273.

Duevel K, Valerius O, Mangus DA, Jacobson A, Braus GH (2002) Replacement of the yeast TRP4 3' untranslated region by a hammerhead ribozymes results in a stable and efficiently exported mRNA that lacks a poly(A) tail. *RNA* 8: 336-344.

Eckstein F, Kore AR, Nakamaye KL (2001) *In vitro* Selection of Hammerhead Ribozyme Sequence Variants. *Chembiochem* 2: 629-635.

Egli CM & Braus GH (1994) Uncoupling of mRNA 3' Cleavage and Polyadenylation by Expression of a hammerhead Ribozyme in Yeast. *J. Biol. Chem.* 269(44): 27378-27383.

Ferbeyre G, Bratty J, Chen H, Cedergren R (1995) A hammerhead ribozymes inhibits *ADE1* gene expression in yeast. *Gene* 155: 45-50.

Ferbeyre G, Bratty J, Chen H, Cedergren R (1996) Cell Cycle Arrest Promotes *trans*-Hammerhead Ribozyme Action in Yeast. *J. Biol. Chem.* 271(32): 19318-19323.

Gasch AP, Spellman PT, Kao CM, Carmel-Harel O, Eisen MB, Storz G, Botstein D, Brown PO (2000) Genomic Expression Programs in the Response of Yeast Cells to Environmental Changes. *Mol. Biol. Cell.* 11: 4241-4257.

Gaughan DJ & Whitehead AS (1999) Function and biological applications of catalytic nucleic acids. *Biochim. Biophys. Acta* 1445: 1-20.

Gietz D & Woods RA (2002) Transformation of Yeast by Lithium Acetate/Single-Standed Carrier DNA/Polyethylene Glycol method. *Methods in Enzymol.* 350: 87-96.

Goergens JF, van Zyl WH, Knoetze JH, Hahn-Haegerdal B (2001) The metabolic Burden of the *PGK1* and *ADH2* Promoter Sytems for Heterologous Xylanase Production by *Saccharomyces cerevisiae* in Defined Medium. *Biotechnol. Bioeng.* 73(3): 238-245.

Good PD & Engelke DR (1994) Yeast expression vectors using RNA ploymerase III promoters. *Gene* 151: 209-214.

Guedener U, Heck S, Fiedler T, Beinhauer J, Hegemann JH (1996) A new efficient gene disruption cassette for repeated use in budding yeast. *Nucleic Acids Res.* 24(13): 2519-2524.

Hamman C & Tabler M (1999) Generation and Application of Asymmetric Hammerhead Ribozymes. *Methods* 18: 273-280.

Hasselhoff J & Gerlach WL (1998) Simple RNA enzymes with new and highly specific endonuclease activities. *Nature* 334: 585-591.

Hendry P & McCall M (1996) Unexpected anisotropy in substrate cleavage rates by asymmetric hammerhead ribozymes. *Nucleic Acids Res.* 24(14): 2679-2684.

Himeno M, Shibata T, Kawabara Y, Hanaoka Y, Komano T (1984) Effect of polyethylene glycol in plasmid DNA on transformation of CaCl<sub>2</sub>-treated *Escherichia coli* cells. *Agric. Biol. Chem.* 46:657-662.

Hitzeman RA, Hagie FE, Hayflick JS, Chen CY, Seeburg PH, Derynck R (1982) The primary structure of the *Saccharomyces cerevisiae* gene for 3-phosphoglycerate kinase. *Nucleic Acids Res.* 10(23): 7791-7808.

Holland MJ & Holland JP (1978) Isolation and Identification of Yeast Messenger Ribonucleic Acids Coding for Enolase, Glyceraldehyde-3-phosphate Dehydrogenase, and Phosphoglycerate kinase. *Biochemistry* 17(23): 4900-4907.

Hurt E, Straesser K, Segref A, Bailer S, Schlaich N, Presutti C, Tollervey D, Jansen R (2000) Mex67p Mediates Nuclear Export of a Variety of RNA Polymerase II Transcripts. *J. Biol. Chem.* 275(12): 8361-8368.

Ish-Horowicz D & Burke JF (1981) Rapid and efficient cosmid cloning. *Nucleic Acids Res.* 9: 2989-2998.

Kato Y, Kuwabara T, Warashina M, Toda H, Taira K (2001) Relationships between the Activities *in Vitro* and *in Vivo* of Various Kinds of Ribozyme and Their Intracellular Localization in Mammalian Cells. *J. Biol. Chem.* 276(18):15378-15385.

Kawasaki H & Kazunari T (2002) Identification of genes by hybrid ribozymes that couple cleavage activity with the unwinding activity of an endogenous RNA helicase. *EMBO*. 3(5): 443-450.

Kendall A, Hull MW, Bertrand E, Good PD, Singer RH, Engelke DR (2000) A CBF5 mutation that disrupts nucleolar localization of early tRNA biosynthesis in yeast also suppresses tRNA gene-mediated transcriptional silencing. *Proc. Natl. Acad. Sci.* 97(24): 13108-13113.

Khvorova A, Lescoute A, Westhof E, Jayasena SD (2003) Sequence elements outside the hammerhead ribozyme catalytic core enable intracellular activity. *Nat. Struct. Biol.* 10(3): 708-712.

Kuwabara T, Warashina M, Koseki S, Sano M, Ohkawa J, Nakayama K, Taira K (2001) Significantly higher activity of a cytoplasmic hammerhead ribozyme than a corresponding nuclear counterpart: engineered tRNAs with an extended 3' end can be exported efficiently and specifically to the cytoplasm in mammalian cells. *Nucleic Acids Res.* 29(13): 2780-2788.

Laemmli UK (1970) Cleavage of structural proteins during the assembly of the head of bacteriophage T<sub>4</sub>. *Nature* 227: 680-685.

LaGrandeur T & Parker R (1999) The cis acting sequences responsible for the differential decay of the unstable *MFA2* and stable *PGK1* transcripts in yeast include the context of the translational start codon. *RNA*. 5: 420-433.

Larsson C, Nilson A, Blomberg A, Gustafsson L (1997) Glycolytic Flux is Conditionally Correlated with ATP Concentration in *Saccharomyces cerevisiae*: a Chemostat with ATP Study under Carbon-or Nitrogen-Limiting Conditions. *J. Bacteriol.* 179(23): 7243-7250.

Lee NS, Sun B, Williamson R, Gunkel N, Salvaterra PM, Rossi JJ (2001) Functional colocalization of ribozymes and target mRNAs in *Drosophila* oocytes. *FASEB J.* 15(13): 2390-2400.

Lee NS, Bertrand E, Rossi J (1999) mRNA localization signals can enhance the intracellular effectiveness of hammerhead ribozymes. *RNA* 5(9): 1200-1209.

Lieber A & Strauss M (1995) Selection of efficient Cleavages Sites in Target RNAs by Using a Ribozyme Expression Library. *Mol. Cell. Biol.* 15(1): 540-551.

Lilley DMJ (1999) Structure folding and catalysis of the small nucleolytic ribozymes. *Curr. Opin. Struct. Biol.* 9: 330-338.

Lott WB, Pontius BW, von Hippel PH (1998) A two-metal ion mechanism operates in the hammerhead ribozyme-mediated cleavage of an RNA substrate. *Proc. Natl. Acad. Sci.* 95: 542-547.

McCall MJ, Hendry P, Mir AA, Conaty J, Brown G, Lockett TJ (2000) Small, Efficient Hammerhead Ribozymes. *Mol. Biotechnol.* 14: 5-16.

McKay D & Wedekind JE (1999) Small Ribozymes. In: The RNA World. 2th edition, Cold Spring Harbor, USA: Cold Spring Harbor Laboratory Press. pp 265-287.

Marschall P, Thomson JB, Eckstein F (1994) Inhibition of Gene Expression with Ribozymes. *Cell. Mol. Neurobiol.* 14(5): 523-538.

Matzura, O. & Wennborg, A. (1996) RNA draw: an integrated programm for RNA secondary structure calculation and analysis under 32-bit Microsoft Windows. *Comput. Appl. Biosci.* 12 (3), 247-249.

Moore PA, Sagliocco FA, Wood RMC, Brown AJP (1991) Yeast Glycolytic mRNAs Are Differentially Regulated. *Mol. Cell. Biol.* 11(10): 5330-5337.

Nasr F, Bécam AM, Brwn SC, Nay DD, Slonimski PP, Herbert CJ (1995) Artificial antisense RNA regulation of *YBR1012* (YBR136w), an essential gene from *Saccharomyces cerevisiae* which is important for progression through G1/S. *Mol Gen Genet.* 249: 51-57.

Nevoigt E & Stahl U (1996) Reduced Pyruvate Decarboxylase and Increased Glycerol-3-phosphate Dehydrogenase [NAD<sup>+</sup>] Levels Enhance Glycerol Production in *Saccharomyces cerevisiae*. *Yeast* 12: 1331-1337.

Odgen RC & Adams DA (1987) Electrophoresis in agarose and acrylamide gels. In Berger SI and Kimmel AR (eds) *Methods in Enzymology*. Academic Press Inc, New York. 152:pp 61-87.

Olsson L, Larsen ME, Rønnow B, Mikkelsen JD, Nielsen J (1997) Silencing *MIG1* in *Saccharomyces cerevisiae*: Effects of Antisense *MIG1* Expression and *MIG1* Gene Disruption. *App. Env. Microbiol.* 63(6): 2366-2371.

Ostergaard S, Olsson L, Nielsen J (2000) Metabolic Engineering of *Saccharomyces cerevisiae*. *Microbiol. Mol. Biol. Rev.* 64(1): 34-50.

Overkamp KM, Bakker BM, Koetter P, Luttik MAH, van Dijken JP, Pronk JT (2002) Metabolic Engineering of Glycerol Production in *Saccharomyces cerevisiae*. *App. Env. Microbiol.* 68(6): 2814-2821.

Pearce AK, Crimmins K, Groussac E, Hewlins MJE, Dickinson R, Francois J, Booth IA, Brown JP (2001) Pyruvate kinase (Pyk1) levels influence both the rate and direction of carbon flux in yeast under fermentative conditions. *Microbiology.* 147: 391-401.

Piper PW, Curran B, Davies MW, Hirst K, Lockheart A, Seward K (1988a) Catabolite control of the elevation of *PGK1* mRNA levels by heat shock in *Saccharomyces cerevisiae*. *Mol. Microbiol.* 2(3): 353-361.

Piper PW, Curran B, Davies MW, Hirst K, Lockheart A, Odgen JE, Stanway CA, Kingsman AJ, Kingsman SM (1988b) A heat shock element in the phosphoglycerate kinase gene promoter of yeast. *Nucleic Acids Res.* 16(4): 1333-1348.

Rossi JJ (1999) Ribozymes, genomics and therapeutics. *Chemistry & Biology.* 6: R33-R37.

Sagliocco FA, Zhu D, Vega Laso MR, McCarthy JEG, Tuite MF, Brown AJP (1994) Rapid mRNA Degradation in Yeast Can Proceed Independently of Translation Elongation. *J. Biol. Chem.* 269(28): 18630-18637.

Samarsky DA, Ferbeyre G, Bertrand E, Singer RH, Cedergren R, Fournier MJ (1999) A small nucleolar RNA:ribozymes hybrid cleaves a nucleolar RNA target *in vivo* with near-perfect efficiency. *Proc. Natl. Acad. Sci.* 96: 6609-6614.

Sambrook J, Fritsch EF, Maniatis T (1989) *Molecular cloning: A laboratory manual*. 2<sup>th</sup> edition, Cold Spring Harbor, USA: Cold Spring Harbor Laboratory Press.

Schmidt, U., Lehmann, K. & Vilches, C. (2001) Ribozyme in der Bäckerhefe *Saccharomyces cerevisiae*. Funktionanalyse und biotechnologische Anwendung. *BIOForum* 24, 672-676.

Scopes RK (1975) 3-Phosphoglycerate Kinase o Baker's Yeast. *Methods Enzymol.* 42: 134-138.

Scott WG, Murray JB, Arnold JRP, Stoddard BL, Klug Aaron (1996) Capturing the structure of a Catalytic RNA Intermediate: The Hammerhead Ribozyme. *Science* 274: 2065-2069.

Sethy I, Moir RD, Librizzi M, Willis IM (1995) In vitro evidence for Growth Regulation of tRNA Gene Transcription in Yeast. *J. Biol. Chem.* 270(47): 28463-28470.

Shaaft I, Heinisch J, Zimmermann FK (1989) Overproduction of glycolytic enzymes in yeast. *Yeast* 5: 285-290.

Sikorski RS & Hieter P (1989) A System of Shuttle Vectors and Yeast Host Strains Designed for Efficient Manipulation of DNA in *Saccharomyces cerevisiae*. *Genetics* 122: 19-27.

Sullenger BA & Gilboa E (2002) Emerging clinical applications of RNA. *Nature* 418: 252-258.

Szentirmay MN & Sawadogo M (2000) Spatial organization of RNA polymerase II transcription in the nucleus. *Nucleic Acids Res.* 28(10): 2019-2025.

Tanner NK (1999) Ribozymes: The characteristics and properties of catalytic RNAs. *FEMS Microbiol. Rev.* 23: 257-275.

Takagi Y, Warashima M, Stec W J, Yoshinari K, Taira K (2001) Recent advances in the mechanisms of action of ribozymes. *Nucleic Acids Res.* 29: 1815-1834.

Vaish NK, Kore AR, Eckstein F (1998) Recent developments in the hammerhead ribozyme field. *Nucleic Acids Res.* 26(23): 5237-5242.

Van der Aar PC, Van den Heuvel JJ, Roeling WFM, Raue HA, Stouhamer AH, Van Verseveld HW (1992) Effects of Phosphoglycerate Kinase Overproduction in *Saccharomyces cerevisiae* on the Physiology and Plasmid Stability. *Yeast* 8: 47-55.

Velculescu VE, Zhang L, Zhou W, Vogelstein J, Basrai MA, Bassett DE, Hieter P, Vogelstein B, Kinzler KW (1997) Characterization of the Yeast Transcriptome. *Cell* 88: 243-251.

Verma S, Vaish NK, Eckstein F (1997) Structure-function studies of the hammerhead ribozymes. *Curr. Opin. Chem. Biol.* 1: 532-536.

Wang JP, Enjoji M, Tiebel M, Ochsner S, Chan L, Teng BB (1999) Hammerhead Ribozyme Cleavage of Apolipoprotein B mRNA Generates a Truncated Protein. *J. Biol. Chem.* 274(34):24161-24170.

Warashima M, Takagi Y, Stec WJ, Taira K (2000) Differences among mechanisms of ribozymes-catalyzed reactions. *Curr. Opin. Biotechnol.* 11: 354-362.

Yim SH, Park I, Ahn JK, Kang C (2000) Translational suppression by hammerhead ribozymes and inactive variants in *S. cerevisiae*. *Biomol. Engineering* 16: 183-189.

Yokoyama Y, Takahashi Y, Shinohara A, Wan X, Takahashi S, Niwa K, Tamaya T (2000) The 5'-End of hTERT mRNA Is Good Target for Hammerhead Ribozyme to Suppress Telomerase Activity. *Biochem. Biophys. Res. Commun.* 273: 316-321.

Zhao JJ & Lemke G (1998) Rules for Ribozymes. *Mol. Cell. Neurosci.* 11: 92-97.

Zuker M (1994) Prediction of RNA secondary structure by energy minimization. *Methods Mol. Biol.* 25: 267-294.

## 9 Appendix

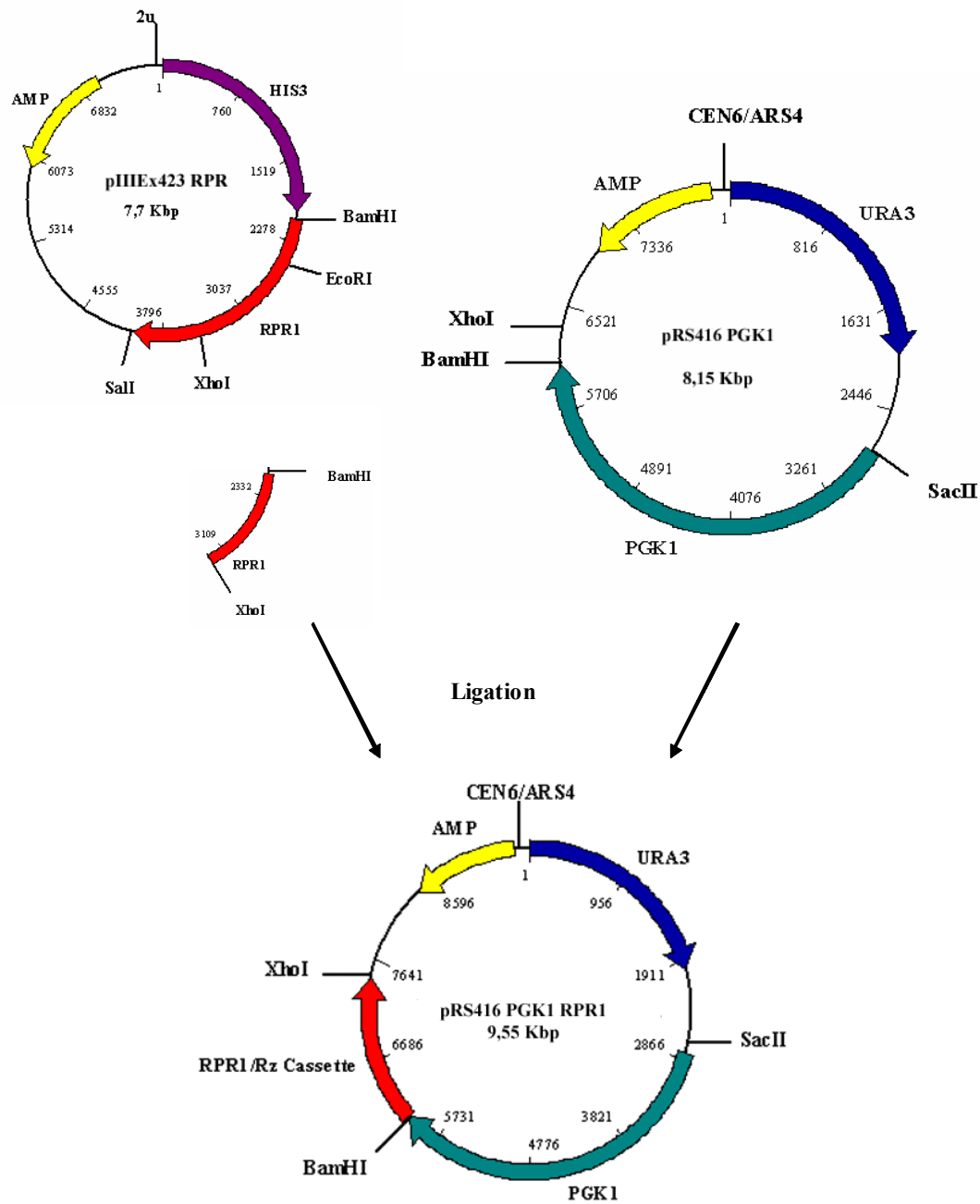


Figure A 1: Construction of the pRS416 vector carrying *PGK1* gene and the ribozyme expression cassette. Abbreviations: *AMP*: ampicilline resistance gene, *HIS4*: histidinol dehydrogenase, *PGK1*: phosphoglycerate kinase gene, *RPR1*: Rnase P RNA ribozyme expression cassette, *URA3*: uracil 3 gene.



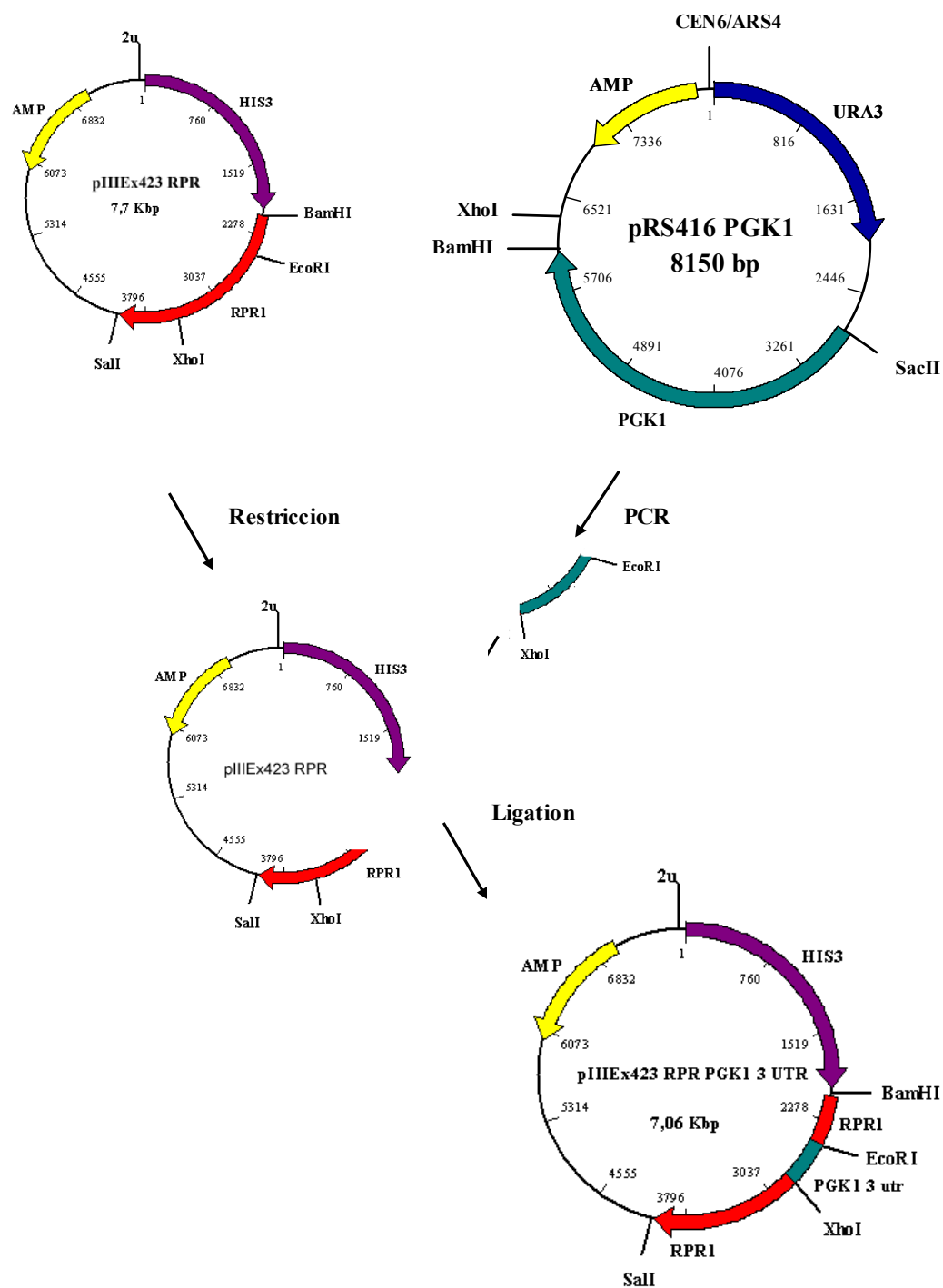
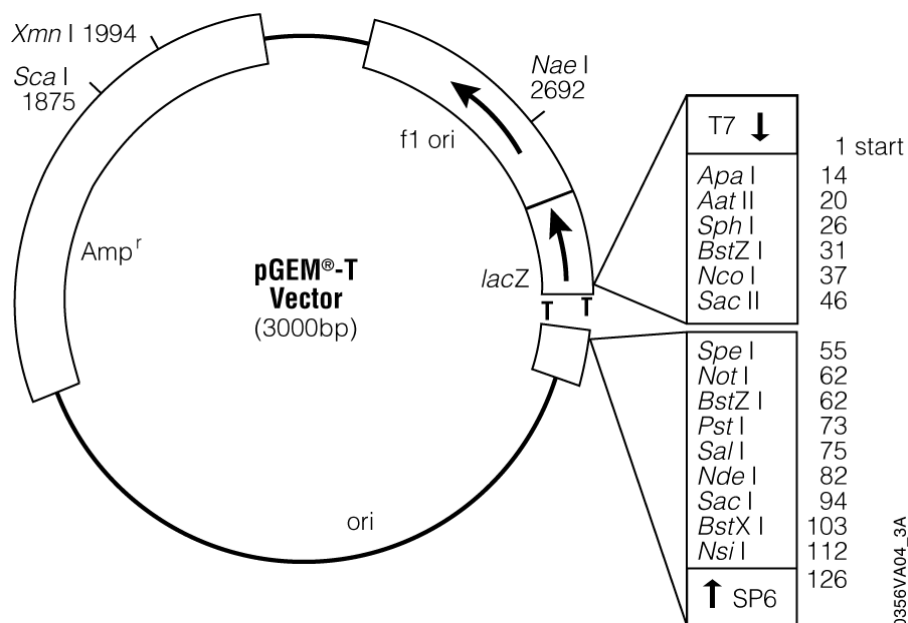


Figure A 2: Construction of the pRS423 *RPR1* vector carrying the terminator region of *PGK1*. Abbreviations: *AMP*: ampicilline resistance gene, *HIS4*: histidinol dehydrogenase, *PGK1*: phosphoglycerate kinase gene, *PGK1* 3'UTR. Phosphoglycerate kinase 3' untranslated region, *RPR1*: Rnase P RNA ribozyme expression cassette, *URA3*: uracil 3 gene.



pGEM®-T Vector sequence reference points:

Base pairs	3000
T7 RNA polymerase transcription initiation site	1
multiple cloning region	10-113
SP6 RNA polymerase promoter (-17 to +3)	124-143
SP6 RNA polymerase transcription initiation site	126
pUC/M13 Reverse Sequencing Primer binding site	161-177
lacZ start codon	165
lac operator	185-201
beta-lactamase (Amp <sup>r</sup> ) coding region	1322-2182
phage f1 region	2365-2820
lac operon sequences	2821-2981, 151-380
pUC/M13 Forward Sequencing Primer binding site	2941-2957
T7 RNA polymerase promoter (-17 to +3)	2984-3

Figure A 3: pGEM®-T Vector Map. This vector has been linearized with EcoR V at base 51 (\*) and a T-residue has been added to both 3'-ends. The pGEM®-T Vector is prepared by cutting Promega's pGEM®-5Zf(+) Vector with EcoRV and adding a 3' terminal thymidine to both ends. These single 3'-T overhangs at the insertion site greatly improve the efficiency of ligation of a PCR product into the plasmid by preventing recircularization of the vector and providing a compatible overhang for ligation of PCR products generated by certain thermostable polymerases.

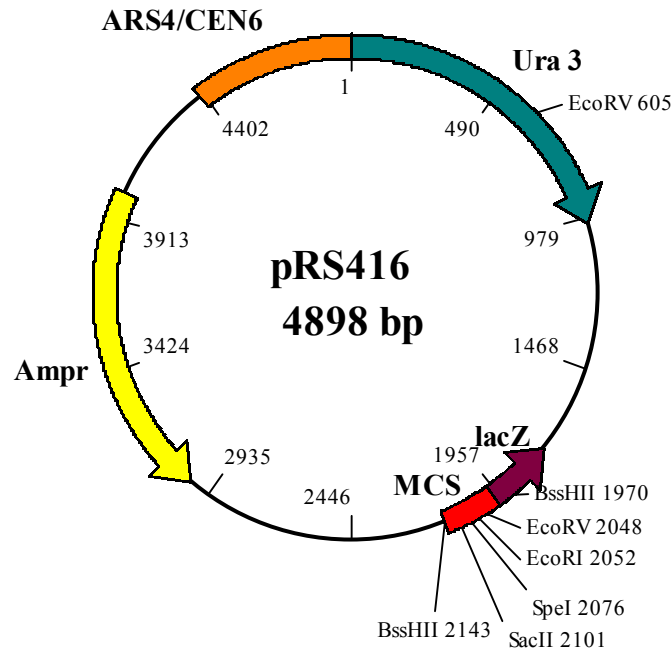


Figure A 4: Plasmid map of the yeast shuttle vector pRS416. The pRS416 vectors are yeast centromere plasmids (YCps) derived from the Yip vectors. These vectors include a CEN6/ARS4 cassette that provides mitotic stability and the ability to be autonomously replicated.

### RPR1 Promoter

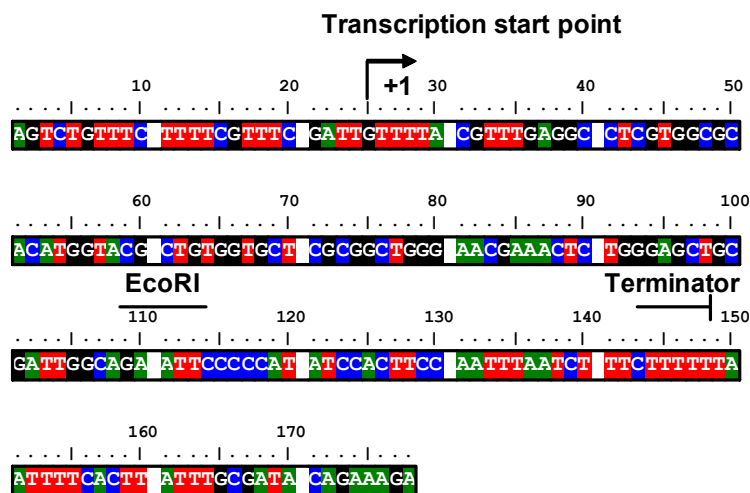


Figure A 5: Sequence of pol III promoter construct published by Good and Engelke (Good & Engelke, 1994). The sequence of the *RPR1* promoter construct is given from upstream of the transcription start point (marked with bent arrows). The *EcoRI* insertion site for Ribozyme genes and terminator sequence are marked with over lines.

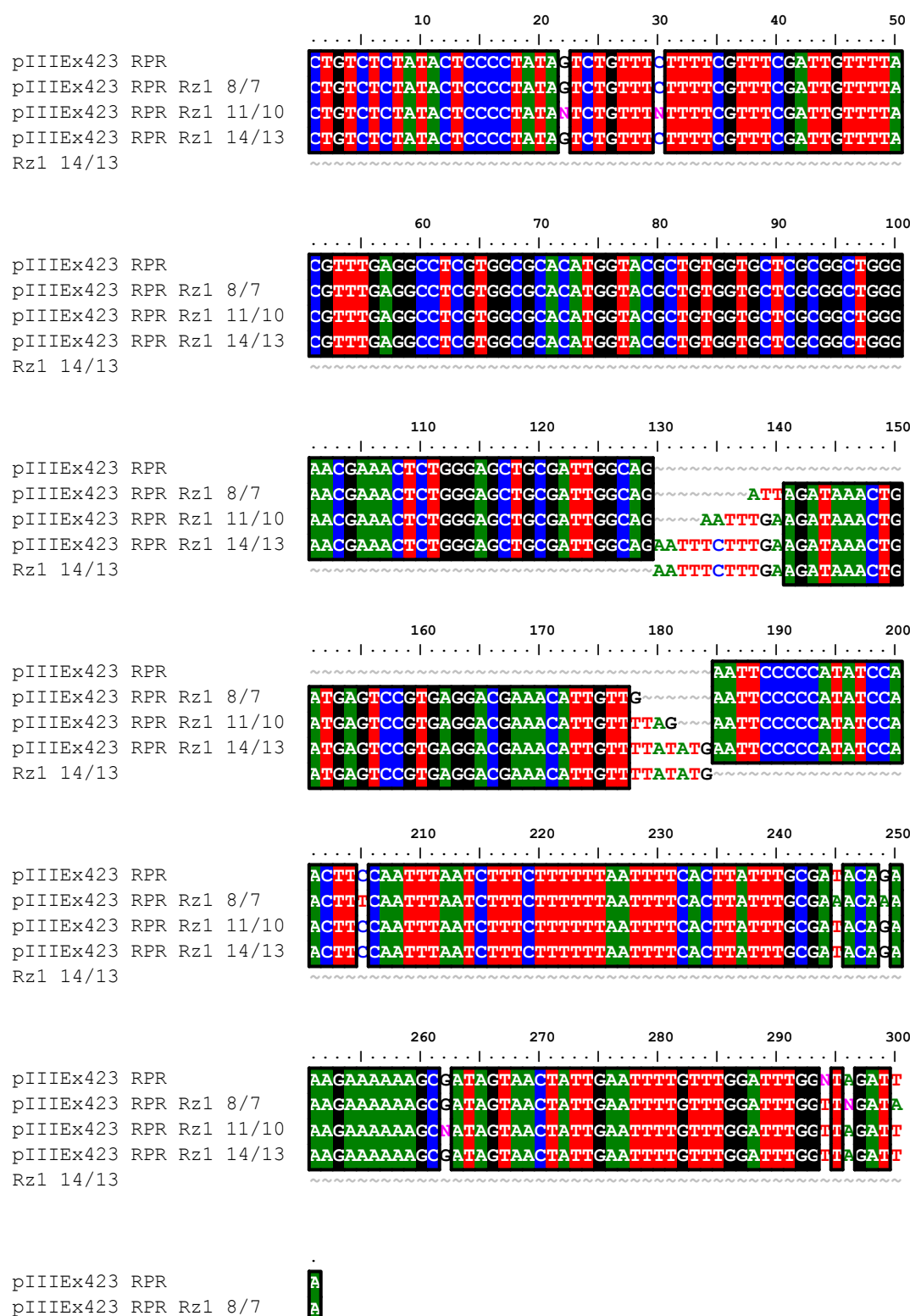


Figure A 6: Sequences of pIIIEEx423 RPR plasmids used for ribozyme delivering containing sequences coding for Rz1 (located at 130 to 180 nt), these sequences were compared with RZ114/13 sequence used for cloning.



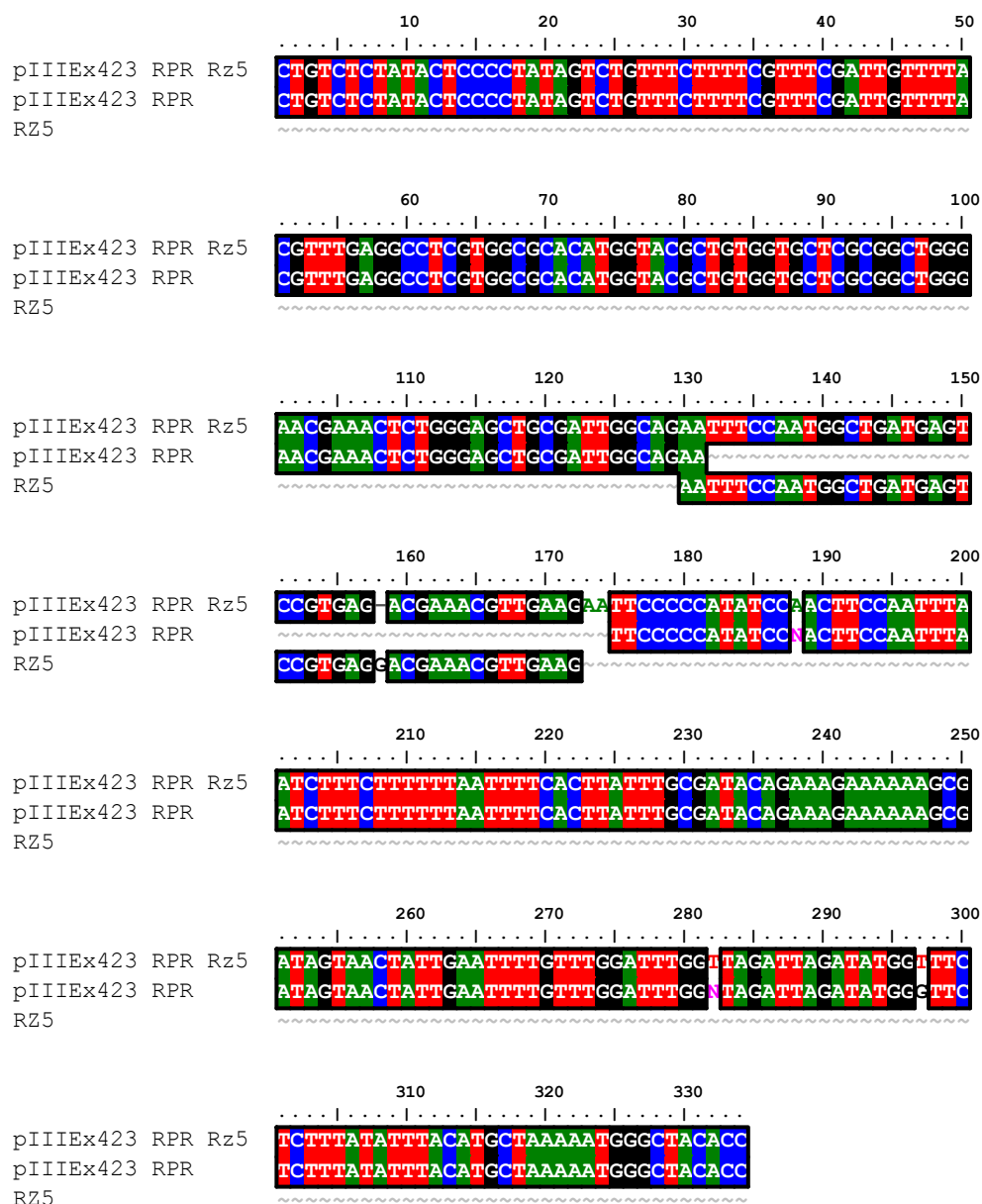


Figure A 8: Sequence comparison of pIIIEx423 RPR carrying Rz5 coding sequence, without ribozyme, and Rz5 sequence used. A punctual deletion, G, is observed at the catalytic core sequence located at 158 nt.

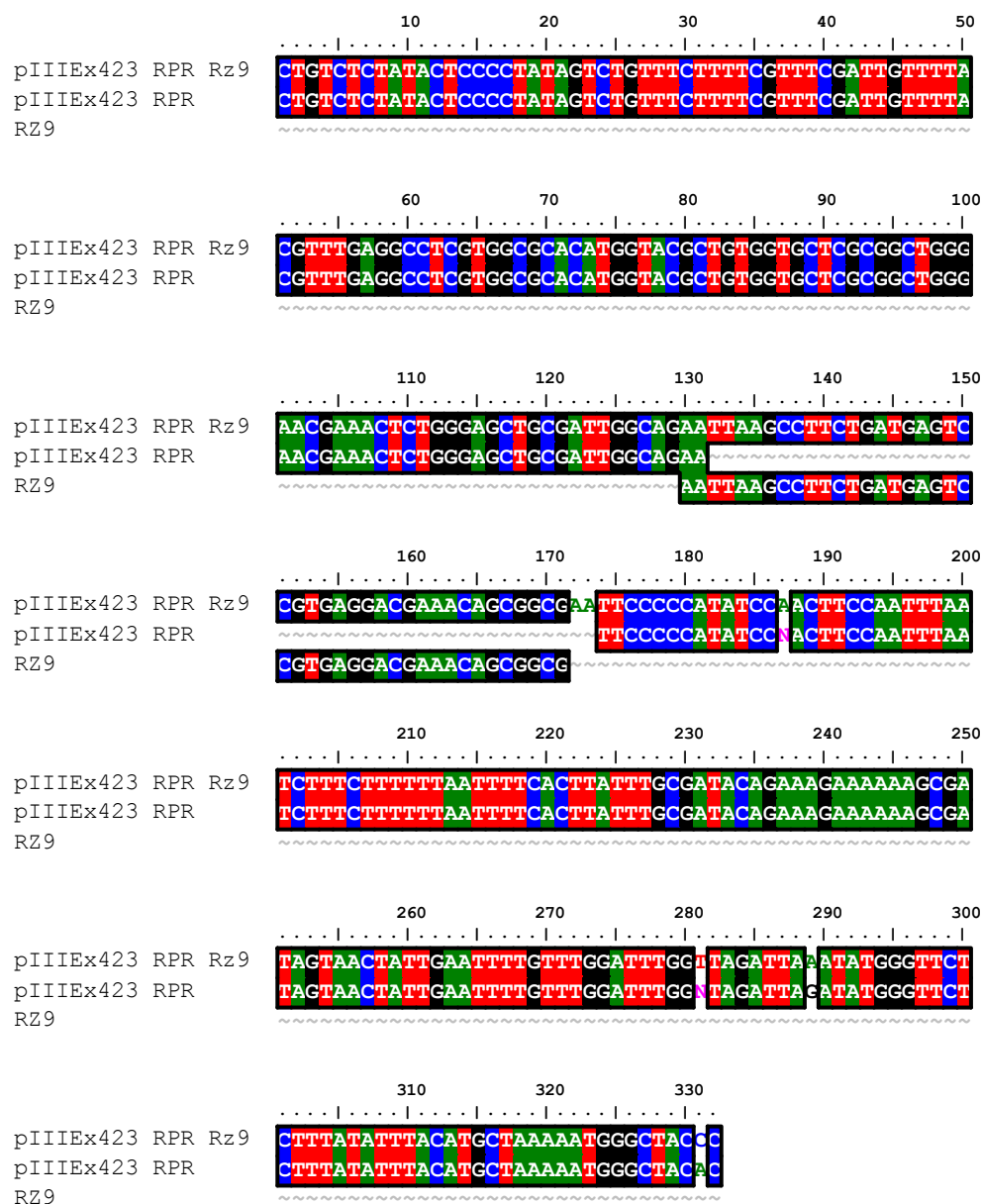


Figure A 9: Sequence comparison of pIIIEx423 RPR carrying Rz9 coding sequence with vector without ribozyme, and the expected Rz9 sequence used.

## **Curriculum vitae**

### **Persönliche Daten:**

Name: Vilches González  
Vorname: Sonia Carolina  
Geburtsdatum: 18.07.72  
Geburtsort: Santiago de Chile, Chile

### **Schulische Ausbildung:**

1977-1985 Grundschole "Nuestra Señora del Pilar. Madres Dominicas"  
1986-1989 Gymnasium " Colegio Carmela Carvajal de Prat"

### **Wissenschaftlicher Werdegang:**

1990-1997 Biochemiestudium an der Fakultät für Chemie und Biologie, Universidad Santiago de Chile.  
1998 Stipendiatin des Doktorandenprogramms für Zellular- und Molekularbiologie an der Fakultät für biologische Wissenschaften der Universidad católica de Chile.  
seit 12/1999 Stipendiatin des Doktorandenprogrammms für Biotechnologie an der Fakultät für Mikrobiologie und Genetik der Technischen Universität Berlin.